



# SCIENTIFIC RESEARCH OF THE SCO COUNTRIES: SYNERGY AND INTEGRATION

上合组织国家的科学研究：协同和一体化

Proceedings of the  
International Conference

Date:  
April 20

Beijing, China 2022



上合组织国家的科学研究：协同和一体化  
国际会议

参与者的英文报告

International Conference  
“Scientific research of the SCO  
countries: synergy and integration”

Part 2: Participants' reports in English

2022年4月20日，中国北京  
April 20, 2022. Beijing, PRC

Proceedings of the International Conference  
**“Scientific research of the SCO countries: synergy  
and integration”**. Part 2 - Reports in English

(April 20, 2022. Beijing, PRC)

ISBN 978-5-905695-82-7

这些会议文集结合了会议的材料 – 研究论文和科学工作者的论文报告。它考察了职业化人格的技术和社会学问题。一些文章涉及人格职业化研究问题的理论和方法论方法和原则。

作者对所引用的出版物，事实，数字，引用，统计数据，专有名称和其他信息的准确性负责

These Conference Proceedings combine materials of the conference – research papers and thesis reports of scientific workers. They examines technical and sociological issues of research issues. Some articles deal with theoretical and methodological approaches and principles of research questions of personality professionalization.

Authors are responsible for the accuracy of cited publications, facts, figures, quotations, statistics, proper names and other information.

# CONTENTS

## HISTORICAL SCIENCES

- 敖德萨汉学的形成和发展 (XIX<sup>th</sup> – XX<sup>st</sup>世纪的开始): 历史, 人物和特征  
The formation and development of sinology in Odessa (the XIX<sup>th</sup> – the beginning of the XX<sup>st</sup> centuries): history, personalities and features  
*Levchenko Valery Valerievich, Levchenko Galina Sergeevna, Levchenko Anastasia Valerievna*.....8

## MEDICAL SCIENCES

- 3岁以下儿童严重合并颅脑损伤急性期体温昼夜节律  
Circadian rhythm of body temperature in the acute period of severe concomitant traumatic brain injury in children under 3 years of age  
*Muhitdinova Hura Nuritdinovna*.....16
- 患者, 去试管婴儿, 发生了什么变化?  
Patients, going for IVF, what has changed?  
*Vosnesenskaya Nadezda Vadimovna, Volkova Natalya Alexandrovna, Klinysheva Svetlana Yuryevna*.....24
- 使用可编程真空技术对糖尿病足化脓性坏死伤口愈合动力学的细胞学研究  
Cytological study of the dynamics of healing of purulent-necrotic wounds in diabetic foot using programmable vacuum technologies  
*Sergeev Vladimir Anatolyevich, Glukhov Alexander Anatolyevich, Morozov Yuri Mikhailovich*.....31

## BIOLOGICAL SCIENCES

- 森林种植和木材利用对地球大气中二氧化碳平衡的影响  
On the influence of forest cultivation and wood use on the balance of CO<sub>2</sub> in the Earth's atmosphere  
*Bulatkin Gennady Alekcandrovich*.....47
- Fe(III) 还原和甲烷产生: 北极土壤中的两个主要厌氧微生物过程  
Fe(III) reduction and methane production: two major anaerobic microbial processes in Arctic soils  
*Zakharyuk Anastasiya Gennadevna, Zinoveva Olga Victorovna, Shcherbakova Viktoriya Arturovna*.....55

## VETERINARY SCIENCES

牛饲料混合物

Feed mixture for cattle

*Sainova Gaukhar Askerovna, Yessenbayeva Zhanar Zhenisovna,*

*Akbasova Amankul Dzhakanovna.....62*

## TECHNICAL SCIENCE

确保电光器件散热表面的热状态

Ensuring the thermal regime of the heat-releasing surface of an electro-optic device

*Rabzhirov Bazarzhab Punsukovich, Minkin Dmitrii Alekseevich.....69*

电力机车车辆集电器的主要故障及诊断方法

The main malfunctions of current collectors of electric rolling stock and methods for diagnosing them

*Fu Peisong, Tsaplin Aleksey Evgen'evich.....77*

磁悬浮的特点和工作原理

The characteristics and working principle of magnetic levitation

*Shen Jieyi, Tsaplin Aleksey Evgen'evich.....81*

高铁牵引供电系统

High-speed rail traction power supply system

*Li Yiyuan, Volodin Anatoly Alexandrovich.....87*

HXD2型电力机车单相牵引变流器的电能可以更好地返回牵引网

The electrical energy of HXD2 electric locomotive single-phase traction converter can be better returned to the traction network

*Gao Qi, Vikulov Ilya Pavlovich.....92*

混合动力机车和再生制动系统提高了机车的能源效率

Hybrid locomotives and regenerative braking systems increase the energy efficiency of locomotives

*Xu Jiale, Wu Yansong, Volodin Anatoly Alexandrovich.....99*

混合动力机车 HXN6 和 CKD6E6000

Hybrid locomotives HXN6 and CKD6E6000

*Wu Yansong, Xu Jiale, Volodin Anatoly Alexandrovich.....105*

交流机车电气设备

AC locomotive electrical equipment

*Jing Chao.....110*

无刷牵引电机在牵引机车车辆上的应用前景 Prospects for the use of brushless traction motors on traction rolling stock <i>Huang Jingxuan, Izvarin Mikhail Yulievich</i> .....	118
铁路车辆车钩缓冲装置磨损分析 Analysis of the wear of the buffer device of the railway vehicle coupler <i>Zhang Chunyang, Xu Yiming, Chudokov Alexander Ivanovich</i> .....	126
SS7e型电力机车电气设备电磁兼容研究 Research of electromagnetic compatibility of electric equipment of SS7e electric locomotive <i>Du Peidong, Volodin Anatoly Alexandrovich</i> .....	131
提高电力牵引系统的能源效率 Improving the energy efficiency of electric traction systems <i>Xi Faxiang, Rolle Igor Alexandrovich</i> .....	136
为直流电动火车的机械部分开发诊断支持 Development of diagnostic support for the mechanical part of a DC electric train <i>Li Kexin, Zelenchenko Alexey Petrovich</i> .....	140
用于电力机车和电力列车牵引制动控制系统设计的初始数据 Initial data for the design of traction-braking control systems for electric locomotives and electric trains <i>Chu Mingjing, Rolle Igor Alexandrovich</i> .....	148
电动巴士电池的选择 Selection of a battery for an electric bus <i>Vorobyov Alexander Alfeevich, Sychugov Anton Nikolaevich, Wang Meilun, Wang Peng</i> .....	153
永磁同步电机技术研究 Study of permanent magnet synchronous motor technology <i>Wang Helin, Vikulov I.P.</i> .....	159

## **EARTH SCIENCES**

南乌拉尔硫化物岩溶 Sulfide karst of the Southern Urals <i>Smirnov Alexandr Il'ich</i> .....	168
标准光学机械重力仪的自动化结果 Results of automation of a standard optical-mechanical gravimeter <i>Dubovskoi Vladimir Borisovich, Leontyev Vladimir Ivanovich, Boev Ivan Alekseevich</i> .....	175

敖德萨汉学的形成和发展 (XIXth – XXst 世纪的开始): 历史, 人物和特征

**THE FORMATION AND DEVELOPMENT OF SINOLOGY IN  
ODESSA (THE XIXth – THE BEGINNING OF THE XXst CENTURIES):  
HISTORY, PERSONALITIES AND FEATURES**

**Levchenko Valery Valerievich**

*Candidate of Historical Sciences, Associate Professor  
Odessa National Maritime University*

**Levchenko Galina Sergeevna**

*Candidate of Historical Sciences, Associate Professor  
Odessa National University named after I. I. Mechnikov*

**Levchenko Anastasia Valerievna**

*Odessa National University named after I. I. Mechnikov*

注解。这篇文章是由于十九世纪至二十世纪初敖德萨汉学的形成和发展的历史, 这是欧洲学派的句法研究的一部分。介绍了敖德萨 Synology 研究的发展过程以及该行业的敖德萨科学家的知识遗产, 其中涉及存储在乌克兰图书馆和档案馆中的科学文献和历史档案资源。在汉学(中国研究)领域突出了敖德萨科学家的科学研究阶段和特点。代表了敖德萨科学家以前不为人知的作品, 他们的科学重点、传统、特征、动机和研究方向。

关键词: 中国、汉学、敖德萨、历史、人物、知识遗产。

**Annotation.** *The article is due to the history of the formation by and development of Sinology in Odessa in the XIXth – early XXst centuries, which is part of the synological studies of European schools. The process of development of synological research in Odessa and the intellectual heritage of Odessa scientists in this industry with the involvement of scientific literature and historical archival sources stored in the collections of libraries and archives of Ukraine are presented. The stages and features of scientific research of Odessa scientists are highlighted in the field of sinology (Chinese studies). The previously unknown works of Odessa scientists, their scientific priorities, traditions, features, motivations and research directions are represented.*

**Keywords:** *China, Sinology, Odessa, history, personalities, intellectual heritage.*

At the end of the XVIth century. In Europe, an independent scientific direction

arose – Sinology, which was the result of the missionary activity of Europeans in China. There were formed national synological schools and research centers (British, with the centers in Oxford and Cambridge; Russian with the centers in Moscow and St. Petersburg, etc.) whose representatives focused on studying the history, culture and ethnography of the peoples of China in the second half of the XIXth century in Europe.

At the same time, interest in the research of various aspects of the history and culture of China in Odessa was started, where in the second third of the XIXth century a scientific and educational center began to take shape, whose representatives showed interest in studying Oriental studies in general and China in particular. The Institute of Oriental Languages was opened in 1838 at the Richelieu Lyceum. The training of orientologists in a leading educational institution in Odessa at that time was associated with an active development of international relations between the Russian Empire and the countries of the Near and Far East. This, in turn, separately, was reflected in an even greater rise in the importance of Odessa as a trade and port point through which the second sea route passed from the East in general and China.

The first among Odessa scientists who drew attention to the countries of the Far East, including China, was the graduate of St. Petersburg University, professor of the Institute of Oriental Languages in Odessa Vasily Grigoryev (1816–1881), as he emphasized in his report which was named «On the attitude of Russia to the East» [1]. He returned to alma mater after a short stay in Odessa from 1838 to 1844, and the first attempt at the origin of scientific interests in the field of sinology in the Black Sea city was neutralized.

In the middle of the second half of the XIXth century there was a second attempt at the birth of sinology as an independent scientific field in Odessa. It was due to the appearance in the Black Sea city of a graduate of the Moscow Theological Academy Alexander Kudryavtsev (1840–1888). On the 8th December 1873 he was approved as acting professor of theology of the Imperial Novorossiysk University. At the university, Kudryavtsev read church and canon law and was one of the major and prominent figures of his time. In Odessa, he was known as a preacher. His sermons were usually accusatory and were distinguished by energy and passion. Among the manuscript heritage of Kudryavtsev, identified in the scientist's personal fund in the State Archives of Odessa Region, the work entitled «On the causes of stagnation of mental and civil life in China» was discovered [2]. The negative context of the title doesn't reflect a complete picture of the content of the work. Kudryavtsev called China «a wonderful country of the east» [2, p. 1] through the prism of the views of the Orthodox priest, considering various aspects of the culture of the Chinese people, concludes that «...the Chinese will only recover from their mental euthanasia, when they overcome natural and

artificial barriers and eliminate eternal pride to unite together with the European peoples in order to borrow more convenient means from them for supporting both physical life and spiritual life, and most importantly when they turn to the one that is the path of truth and belly. ...the victorious power of the Cross of Christ has long reigned over the simple-minded inhabitants of this great nation» [2, p. 39]. A detailed acquaintance with the contents of the manuscript heritage of Kudryavtsev allows us to present the scientific and political face of the scientist, to determine his role in the study of the history of Sinology [3]. Thus, to show the philosophy of the history of European science about China in the XIXth century, which the system and society of the eastern countries perceived as a construct, a polar universal western civilization. The second attempt at the origin of sinology in Odessa was also unsuccessful.

While retaining the role of the main «southern» gate of the Russian Empire, an important port and transport point through which the thousands of people sent to different regions of the world, including the Far East, in Odessa, there was a constant interest in the emergence of popular information about such an exotic country like China. This explains the fact that in the second half of the XIX — at the beginning of the twentieth centuries. the authors of the works devoted to China were not sinology specialists, but the representatives of various professions — military, medical, geographers, economists, and simply travelers who, for various reasons, visited the Middle Kingdom [4, p. 76–77]. The proof of this thesis is a collection of articles previously published in local newspapers, «Odessa and Russian-Indo-Chinese Trade» [5], published in 1876 in Odessa, which succinctly describes the main priority in acquainting Odessa residents with China. Another confirmation of the above thesis was published in 1910, a collection of essays, stories and memoirs of military topographers «In the slums of Manchuria and our eastern outskirts», which contained rich illustrative material (208 illustrations in the text and 20 autotypes on separate sheets of chrome paper) [6]. The collection attempted to illuminate the conditions under which cartographic, geographical, and other materials were collected in sparsely populated places and wilds. Illustrations were placed depicting the nature and way of life of the population, where topographic surveys were conducted, as well as illustrating the everyday side of the work of topographers. Some illustrations were reproduced from very rare photographs of the wilderness of Manchuria, in connection with which the collection was given the corresponding name. In general, a characteristic feature of the development of Sinology in Odessa at the turn of the nineteenth and twentieth centuries. there was a predominant familiarization and description of contemporary events in China by non-professional researchers. The consequence of this was the publication in Odessa of a significant number of works on Sinology [7]. In these publications, the main emphasis was placed on the political, economic, cultural

and geographical aspects, which was aimed at determining the possibilities for further development of political, economic and cultural relations between the Russian Empire and China [4, p. 81].

At the end of the XIXth century studies on the Chinese language are beginning in Odessa, which indicates a transition from a purely pragmatic interest in Chinese culture to the formation of academic research in the direction of Sinology. The specialist who spoke Chinese at the academic level was A. Starkov, the author of a review of the Chinese-Russian dictionary [8]. After 10 years, another book of philological subject was published in Odessa — «Words and phrases of the Japanese and Chinese languages in Russian» [9], which gained wide popularity. Against this background, the appearance of two works by I. Zamotailo [10], devoted to issues of Chinese philosophy [4, p. 82]. Based on this, we can argue that at the beginning of the twentieth century. Odessa has become a leading center in the popularization and study of Sinology, which gave impetus to the formation and development of sinology studios. This was primarily due to the Imperial Novorossiysk University (1865–1920), within the walls of which there was no active research in this area, but the first glimpses of interest in sinology at the academic level only began to appear. For example, in 1885–1896. Professor of Comparative Linguistics was V. Shertsl (1843–1906). Being a Czech by origin, he received a philological education at the best universities in Europe (Prague, London, St. Petersburg), then taught at Kharkov University (1869–1884). He was an outstanding polyglot (owned 45 languages), among them - Sanskrit and Chinese, which he studied in London [11]. Without leaving practical research in the field of Sinology, he nevertheless certainly brought to the scientific community of Odessa certain knowledge and popularization in this direction.

The largest scientific development in the field of oriental studies in general, and in particular Sinology, in Odessa at the beginning of the twentieth century. belongs to the church historian, professor, dean (1913–1920) of the Faculty of History and Philology of the Imperial Novorossiysk University A. Dobroklonsky (1856–1937) [12]. In the «Personal Archive of A. Dobroklonsky» the manuscript «Buddha and Buddhism» [13] is stored, which consists of three parts (the second part is not in the archive) and, according to the number of sheets indicated in the inventory, totals 306 sheets. The manuscript belongs to of A. Dobroklonsky (identified by the author), the texts of all parts contain a huge number of edits, changes, additions, clarifications, etc., and despite the fact that there is no direct evidence confirming his authorship, we allow ourselves to refer this work is to the intellectual heritage of the historian. The exact dating of the manuscript has not yet been established. But on the first sheet at the top there is a second-person record: «No. 2269 January 10, 1907», which gives grounds to approximately date its writing in 1905–1907. The logical thesis is relatively unusual for A. Dobroklonsky

subjects of this work is also subject to a logical refutation (ideally, if there were direct confirmations), which is reflected in the first sentences of this text: «At present, there are a lot of admirers of Buddha ... How many of these admirers, no one knows for sure» [fourteen]. The topic of analyzing the history and content of Buddhism as a new scientific direction was chosen by A. Dobroklonsky not by chance. At the beginning of the twentieth century. Under the influence of the complex of events of domestic and foreign policy, the crisis of the state, society, the Orthodox Church and faith in the Russian Empire intensified. The crisis of the church was manifested in the fact that the number of parishioners showing indifference to faith was constantly increasing every year; petitions about the transition from Orthodoxy to another religion (including Buddhism) began to be received in large numbers, the renovationist movement in Russian Orthodoxy and other similar phenomena arose. Being a believer, apolitical, gentle and conservative in moral and Christian qualities, in the face of growing radical sentiments in society against the background of growing interest in the religions of eastern countries, she could hypothetically lead A. Dobroklonsky to study one of the oldest world religions recognized by various peoples with completely different traditions as a philosophical and religious doctrine of spiritual awakening. In the Chinese religion and philosophy, Buddhism, introduced to China from the outside and focused on the development of the spiritual principle, has traditionally been intertwined with Confucianism and Taoism and acted as an alternative to Chinese pragmatism.

Thus, in Odessa, during its stay as part of the Russian Empire, a center of scientific Sinology, as well as of Oriental studies as a whole, was not created. All scientific studies that were carried out in this area were individual in nature.

The revolutionary events of 1917, the transformation of the geopolitical situation in the world after the First World War and the appearance of the first socialist state (the USSR, formed on December 30, 1922) in the world entailed the continuation of scientific research in the field of Sinology, the formation and institutionalization of the scientific discipline — sinology. The activity of Soviet scientists in conducting research in this direction, unfortunately, was not provoked by academic interest, but by the political position of China, the leader of the socialist movement in the East. The transformation of all spheres of life in Odessa, as well as in the whole in the Ukrainian SSR (proclaimed March 10, 1919) led to changes in the scientific space. The establishment of Soviet power on 7 February 1920 in Odessa led to a radical reorganization of the network of higher educational institutions and scientific institutions. The closure of the Imperial Novorossiysk University in May 1920, for more than half a century the leading university in the south of the Russian Empire, did not interrupt oriental traditions in Odessa, as Skripnik points out [15, p. eleven]. On the contrary, they received new forms and methods [16] and were continued at two universities — the successors of the Imperial

Novorossiysk University — Odessa Institute of Public Education [17] and the Odessa Institute of National Economy, as well as at two academic institutions — the Odessa branch of the All-Ukrainian Scientific Association of Oriental Studies and Odessa local history commission at the All-Ukrainian Academy of Sciences. The introduced changes and innovations in the study of sinology acquired the features of a certain institutionalization. All the above-mentioned universities and scientific institutions were closely related by their personnel, because mainly all scientists combined teaching and research activities in several organizations at the same time. The leading academic center in Odessa in the field of oriental studies in the 1920s. became the Odessa branch of the All-Ukrainian Scientific Association of Oriental Studies. In the Soviet scientific literature on the history and role of this academic organization in the study of sinology, little attention was paid [18]. Only at the present stage, scientists began to show interest both in the academic unit itself and in the scientific heritage of its researchers [4, p. 109–110; 19–24].

### References

1. Григорьев В. *Об отношении России к Востоку: Речь, произнесенная исправляющим должность профессора В. Григорьевым. Одесса, 1840.*
2. *The State Archive of Odessa Region. F. 631. Op. 1. D. 2. 39 l.*
3. Левченко В. В., Левченко Г. С. *Китаеведение в научном наследии А. Н. Кудрявцева // III Міжнародна наукова конференція «Соціальний розвиток країн "Одного поясу та одного шляху»,: Розвиток Нового Шовкового шляху в Україні»: Тези доповідей / Відповідальна за випуск С. М. Гловацька. Одеса: ОНМУ, 2017. С. 57–58.*
4. Кіктенко В. О. *Нарис з історії українського китаєзнавства. XVIII – перша половина XX ст.: дослідження, матеріали, документи. К., 2002. 194 с.*
5. Рудич А. *Одесса и русско-индо-китайская торговля. Одесса, 1876. 15 с.*
6. *В трущобах Маньчжурии и наших восточных окраин. Сборник очерков, рассказов и воспоминаний военных топографов / Под ред. М. Н. Левитского. Одесса, 1910. VII, 520 с.*
7. Захарин Д. *Маньчжурия и Корея. Очерк природы, истории и населения этих стран. Одесса, 1904. 24 с.; Маракуев В. Н. Наши азиатские соседи китайцы (сост. по Р. Дугласу, Симону, Э. Реклю, Леггу и др.). Одесса, 1896. 190 с.; Мускатблит Ф. Россия и Япония на Дальнем Востоке: историко-политический этюд. Одесса, 1904. 63 с.; Синозерский М. Япония, Корея, Квандунская область и их обитатели: (Физико-географический и этнографический очерк). Одесса, 1904. 39 с. и др.*
8. Старков А. [Рецензия] Палладий [Кафаров] архимандрит и Попов П. С. *Китайско-русский словарь. В 2-х т. Пекин, 1888 // Одесские новости. 1890.*

9. Ю-в Е. Слова и фразы японского и китайского языка на русском языке. Одесса, 1900.

10. Замотайло И. Конфуцианство и даосизм // Известия Одесского библиографического общества. 1915. Т. 4. Вып. 3–4. С. 150–201; Замотайло И. Неопубликованный перевод Дао-дэ-цзина архимандрита Данила (Сивиллова) // Известия Одесского библиографического общества. 1915. Т. 4. Вып. 5–6. С. 209–245.

11. О нем см.: Карский Е. Викентий Шерцль — профессор в Харькове и Одессе. Умер 21/XI 1906 // Русский филологический вестник. Варшава, 1907. Т. 57, вып. 1. С. 205–206; Чуєпило А. А., Чуєпило Л. А. Из истории востоковедения в Харьковском университете: В. И. Шерцль // Харківський історіографічний збірник. 2015. Вип. 14. С. 110–125 и др.

12. О нем см.: Троицкий С. В. А. П. Доброклонский как историк Церкви // Записки Русского научного института в Белграде. 1938. Вып. 15. С. IX–XXII; Фармаковский В. В. А. П. Доброклонский (По личным воспоминаниям) // Записки Русского научного института в Белграде. 1938. Вып. 15. С. XXIII–XXV; Струве П. Б. Труды А. П. Доброклонского по русской истории // Записки Русского научного института в Белграде. 1938. Вып. 15. С. XXVII–XXXII; У. Др. Александар Павловић Доброклонски // Богословье: Орган православного богословского факультета у Београду (Београд). 1938. № 1. С. 80–87; Афанасьев Н. Памяти А. П. Доброклонского // Вестник: орган церковно-общественной жизни (Париж). 1938. № 1. С. 16–17; Боярченков В., Толстов В. Историк церкви А. П. Доброклонский // Рязанские ведомости. 1998. 25 декабря; Мирошниченко В. О. Доброклонський Олександр Павлович // Професори Одеського (Новоросійського) університету. Біографічний словник. Вид. 2-е, доп. Т. 1. Одеса, 2005. С. 60–65; Левченко В. В. На пути к венцу славы: этюды интеллектуальной биографии одесского периода историка А. П. Доброклонского // Рязанская старина. 2009–2018. № 7–16. С. 15–92 и др.

13. GAOO. F. 157. Op. 1. D. 154. 102 p. ; D. 155. 133 p. ; D. 156. 71 p.

14. GAOO. F. 157. Op. 1. D. 154. L. 1.

15. Скрипник В. В. Вчені-сходознавці в науковому та громадському житті Одеси (XIX – початок XX ст.): Автор. дис. ... канд. іст. наук. Миколаїв, 2011. 18 с.

16. Подробнее см.: Водотика С. Г. Наукове життя Одеси 1920-х рр. (структура та взаємодія дослідних установ гуманітарного профілю) // Одесі–200. Ч. II. Одеса, 1994. С. 112; Его же. Исторична наука УСРР 1920-х років: соціополітичні, організаційні та концептуальні основи функціонування: Монографія. Херсон: ХЮІ ХНУВС, 2006. 336 с.

17. *Подробнее см.: Левченко В. В. Історія Одеського інституту народної освіти (1920–1930 рр.): позитивний досвід невдалого експерименту / Відп. ред. В. М. Хмарський; наук. ред. Т. М. Попова. Одеса: ТЕС, 2010. 428 с.*

18. *Кузнецова Н. А., Кулагина Л. М. Из истории советского востоковедения. 1917–1967. М.: «Наука», 1970. С. 27; Востоковедные центры в СССР. Вып. I (Азербайджан, Армения, Грузия, Украина). М.: «Наука», 1988. С. 92 и др.*

19. *Урсу Д. П. З історії сходознавства на півдні України // Східний світ. 1994. № 1–2. С. 135–150.*

20. *Циганкова Е. Сходознавчі установи в Україні (радянській період). К.: Критика, 2007. С. 184–200.*

21. *Урсу Д. П., Музичко О. Є. Етапи та особливості розвитку сходознавства в Одесі у середині XIX–XX століттях // Східний світ. 2013. № 2–3. С. 92–118.*

22. *Левченко В. В. Китаєзнавство в інтелектуальному доробку одеських дослідників (XIX – початок XXI століття) // Соціальні трансформації: сім'я, шлюб, молодь, середній клас та інноваційний менеджмент у країнах Нового Шовкового шляху: монографія / [авт. кол.: Руденко С.В., Чен Гуангжун та ін.]. Одеса: КУПРІСНКО СВ, 2016. С. 203–206, 229.*

23. *Левченко В. В. Одеська філія Всеукраїнської наукової асоціації сходознавства – академічний осередок китаєзнавчих досліджень в Одесі у 1920-х рр. // II Міжнародна конференція «Соціальні трансформації: сім'я, шлюб, молодь, транспорт та інноваційний менеджмент у країнах нового шовкового шляху»: тези доповідей / Відп. за випуск С. М. Гловацька. Одеса: ОНМУ, 2017. С. 129–132.*

24. *Левченко В. В. Становление и развитие китаеведения в Одессе в XIX – в начале XXI веков: история, этапы, особенности // Россия – Китай: история и культура: Сборник статей и докладов участников X международной научно-практической конференции. Казань: Академия наук Республики Татарстан, 2017. С. 359–367.*

3岁以下儿童严重合并颅脑损伤急性期体温昼夜节律  
**CIRCADIAN RHYTHM OF BODY TEMPERATURE IN THE ACUTE  
PERIOD OF SEVERE CONCOMITANT TRAUMATIC BRAIN INJURY  
IN CHILDREN UNDER 3 YEARS OF AGE**

**Muhitdinova Hura Nuritdinovna**

*Doctor of Medical Sciences, Full Professor*

*Center for the Development of Professional Qualifications of Medical  
Workers*

抽象的。第一天,所有伤者的体温昼夜节律均与正常值无差异。在第1组 SCTBI 急性期(在 ICU 进行了  $5.9 \pm 1.3$  天的重症监护),该指标实际上没有变化,在第2组( $14 \pm 1.7$ 天)伤后第3.4.5天, a 体温昼夜节律中值显著增加  $0.5-0.4^{\circ}\text{C}$ 。第1组在第3天观察到体温降至标准值,第2组仅在第8天观察到。第2组的显著差异是由于更显著的应激反应,即对更显著组织损伤的全身炎症反应 OTBI (66%)、SCE (50%) 发生率较高、顶颞骨骨折伴颅底过渡 (48%)、创伤性休克严重程度 (82%) 高于1组。

关键词: 体温昼夜节律, 严重合并颅脑损伤, 儿童。

**Abstract.** *On the first day, the mesor of the circadian rhythm of body temperature did not differ from the norm in all the injured. In the acute period of SCTBI in group 1 (intensive care in the ICU was carried out for  $5.9 \pm 1.3$  days), the indicator practically did not change, in group 2 ( $14 \pm 1.7$  days) on days 3.4.5 after injury, a significant increase in the mesor of the circadian rhythm of body temperature by  $0.5-0.4^{\circ}\text{C}$ . A decrease in body temperature to the standard value was observed in group 1 on day 3, in group 2 only on day 8. The revealed differences in group 2 are due to a more significant stress response, a systemic inflammatory response to more significant tissue damage OTBI (66%), a higher frequency of SCE (50%), a fracture of the parietotemporal bone with a transition to the base of the skull (48%), severity of traumatic shock (82%) than in 1 group.*

**Keywords:** *circadian rhythm of body temperature, severe concomitant traumatic brain injury, children.*

### **Relevance**

Concomitant traumatic brain injury (CTBI) accounts for 43-68% in the structure of combined injuries and is observed in 23-63% of patients with severe trauma.

matic brain injury (TBI). The authors' analysis of lethal outcomes during CTBI showed that in almost half of the victims the injury was incompatible with life: severe, extensive bruises of the brain stem, massive crushing of the brain tissue, ruptures of large vessels, parenchymal and hollow organs. Patients died in the first hours after the injury. In other cases, the causes of death were traumatic shock and blood loss, dislocation and infringement of the brain stem, fat embolism, purulent-septic complications in the lungs, brain and its membranes, and trophic disorders. Extracranial risk factors for the development of an unfavorable outcome in patients with CTBI can be: the severity of the concomitant injury, the presence of multiple extracranial injuries, vertebral-spinal injury or trauma of the abdominal organs, the age of the victims over 70 years of age, the presence of episodes of hypoxia and arterial hypotension, the development of complications in the postoperative period. Intracranial risk factors are: depression of the level of wakefulness to stupor and coma, the presence of pathological motor reactions in response to a painful stimulus or diffuse muscle hypotension, the stage of development of the dislocation syndrome at the level of the midbrain and bridge. Postoperative mortality in patients with CTBI is 46.8% according to the authors. Unlike adults, babies do not have obvious symptoms of neurological disorders a few hours after injury. This is due to the physiological characteristics of a growing organism: the mobility of non-united cranial bones; immaturity of the brain, there is a mass division of cells, new neural connections are formed; vascular lability, flexibility and density of blood walls. During TBI in children, the shock wave spreads more evenly throughout the skull than in adults. Less risk of damage to the bones of the skull, but there are multiple injuries of brain tissue. The destruction of neural connections is manifested by loss of consciousness. But during a mild injury, diagnosing brain disorders in young children is difficult. With light strokes, vascular spasms that occur during TBI resolve quickly. In severe cases, the effect of hyperemia occurs, blood pressure decreases. Features of the clinical picture, diagnosis and surgical tactics. **Group I** - severe traumatic brain injury (medium and severe brain contusion, brain compression, diffuse axonal damage) and severe extracranial injuries (fractures of the hip, pelvis, shoulder, both bones of the lower leg, spine, multiple fractures of the ribs, jaws, injuries of the organs of the chest and abdominal cavities, multiple extracranial injuries). **Group II** - severe traumatic brain injury and non-severe extracranial injuries (fractures of the bones of the hand, foot, nose, one of the bones of the forearm). **Group III** - mild traumatic brain injury (concussion, mild brain contusion) and severe extracranial injuries. **Group IV** - mild traumatic brain injury and non-severe extracranial injuries [1-3]. The lack of data on changes in the structural characteristics of the circadian rhythm of body temperature in infancy prompted us to this study.

**Purpose of the work**

To study and evaluate changes in the circadian rhythm of body temperature after SCTBI in infancy.

**Material and research methods**

Of the 13 children (tab. 1) with severe concomitant traumatic brain injury (SCTBI) admitted to the Republican Center for Emergency Medical Care in infancy, 7 patients were in intensive care in the ICU for  $5.9 \pm 1.3$  days (group 1), 6 patients  $14 \pm 1.7$  days (group 2), which served as the basis for the creation of randomized groups according to the severity of traumatic injury, condition.

**Results and discussion**

*Table 1.*

*Characteristics of SCTBI patients admitted before the age of 3 years*

Groups	nd in ICU	Number of patients	gender male	age, months	RTA	catatrauma	Number of days in hospital.
1	$5.9 \pm 1.3$	7	4.	$20.8 \pm 7.8$	71% (5)	29% (2)	$15.2 \pm 7$
2	$14 \pm 1.7^*$	6	4	$23.1 \pm 4.7$	50% (3)	50% (3)	$20 \pm 4$

\*-the difference is significant

There were no significant differences in anthropometric data, age, gender, number of days spent in hospital treatment. Draws attention to the more severe nature of the combined injury due to catatrauma in group 2 (50%). In group 1 (tab. 2), the frequency of CITBI (71%), concussion (28%), and the number of operations on the first day after injury (71%) prevailed.

In group 1, out of  $5.9 \pm 1.3$  days spent in the ICU, only 1 patient out of 7 was on mechanical ventilation for 3 days in CMV mode, followed by extubation upon restoration of spontaneous breathing. In group 2, all patients were transferred to mechanical ventilation according to indications. Subsequently, out of  $14.6 \pm 1.7$  days spent in the ICU, the average ventilator rate in the CMV mode was carried out for  $6.8 \pm 2.2$  days, SIMV  $1.75 \pm 0.8$ , CPAP in 1 patient - 1 day, duration of spontaneous breathing was  $7 \pm 1.6$  days.

**Table 2.***The severity of the condition upon admission is due to*

<b>Diagnosis</b>	<b>Group 1</b>	<b>Group 2</b>
Closed traumatic brain injury (CITBI)	71% (5)	33% (2)
Open traumatic brain injury (OTBI)	28% (2)	66% (4)
Severe cerebral contusion (SCE)	14% (1)	50% (3)
Moderate brain injury	14% (1)	16% (1)
Mild brain injury	14% (1)	16% (1)
Brain concussion	28% (2)	16% (1)
Subarachnoid hemorrhage (SAH)	28% (2)	16% (1)
Fracture of the parietotemporal bone with the transition to the base of the skull	14% (1)	48% (3)
Rib fracture with ruptured lung	28% (2)	16% (1)
Rupture of the left lobe of the liver	28% (2)	32% (2)
Rupture of the right lobe of the liver	0	16% (1)
Liver contusion	14% (1)	16% (1)
Clavicle fracture	14% (1)	16% (1)
Fracture of the femur with displacement	28% (2)	16% (1)
Fracture of both femurs	28% (2)	0
Closed ischium fracture	14% (1)	16% (1)
Traumatic shock 2 degrees	71% (5)	66% (4)
Traumatic shock grade 3	0	16% (1)
Operated on the day of admission	71% (5)	66% (4)

In the 2nd more severe group, the number of OTBI (66%), the frequency of SCE (50%), the fracture of the parietotemporal bone with the transition to the base of the skull (48%), the severity of traumatic shock prevailed. All patients were discharged with improvement or transferred to a rehabilitation center.

The phase structure of the circadian rhythm of body temperature in connection with SCTBI in infancy was studied and assessed. On the first day, the mesor of the circadian rhythm of body temperature did not differ from the norm in all injured. However, in the following days, if in group 1 the indicator practically did not change, then in group 2, on days 3.4.5 after the injury (fig. 1), a significantly significant increase in the mesor of the circadian rhythm of body temperature by 0.5-0.4°C ( $p < 0.05$ , respectively). A decrease in body temperature to normal values was observed in group 1 on day 3, in group 2 only on day 8.

Apparently, the revealed differences in group 2 are due to a more pronounced stress response, a systemic inflammatory response to more significant tissue damage during OTBI (66%), a higher incidence of SCE (50%), a fracture of the parietotemporal bone with a transition to the base of the skull (48%), the severity of traumatic shock (82%) than in group 1.

**Table 3.**  
*Dynamics of the mesor of the circadian rhythm of temperature*

Days	1	2	3	4	5	6	7	8	9	10	11	12	13	14	15
Group 1	37.2±0.4	37.3±0.2	37.0±0.1	37.1±0.1	37.0±0.1	37.0±0.2	37.0±0.2								
Group 2	37.0±0.5	37.4±0.2	37.5±0.1*	37.6±0.1*	37.4±0.1*	37.3±0.1	37.2±0.1	37.0±0.1	37.1±0.1	36.9±0.1	36.9±0.02	36.9±0.02	36.8±0.1	36.8±0.01	36.7±0.1

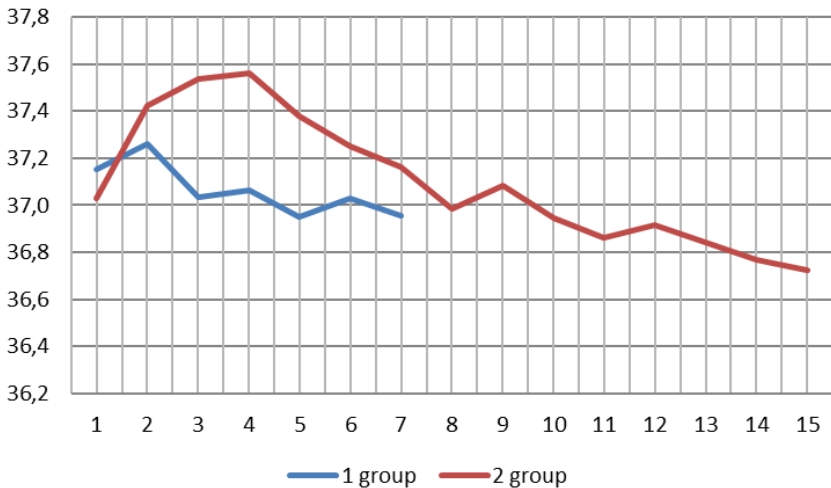


**Figure 1.** *Dynamics of the temperature circadian rhythm with SCTBI up to 3 years*

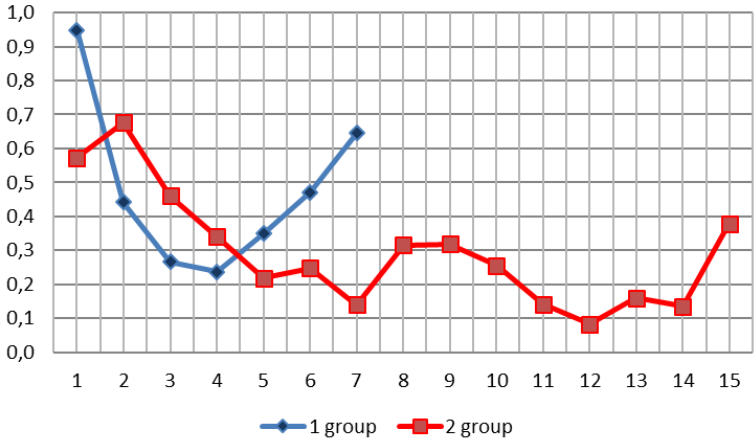


**Figure 2.** The amplitude of the circadian rhythm of body temperature at SCTBI up to 3 years

As shown in fig. 2, in group 1, the maximum increase in the amplitude of daily fluctuations was observed on day 1. The dynamics of the amplitude of the circadian rhythm of body temperature represents the period of the weekly biorhythm of body temperature. While in group 2, the relatively lower values of the amplitude of the temperature reaction, apparently, are due, along with more severe brain damage, but also more massive stress-protective, sedative, hypnotic therapy.

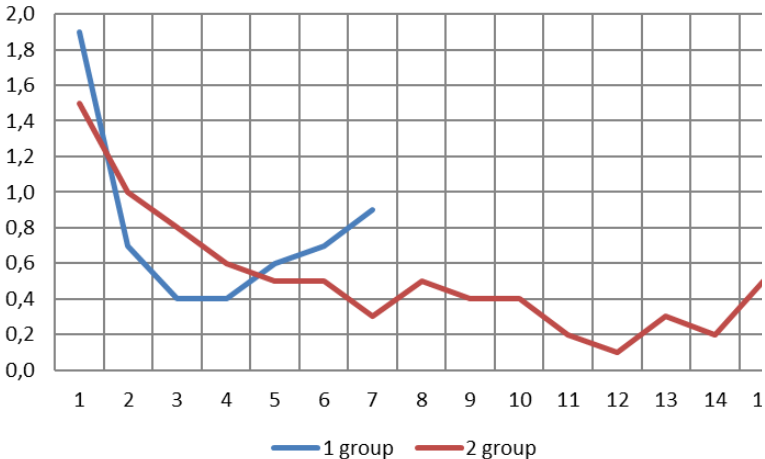


**Figure 3.** The range of daily fluctuations in body temperature up to 3 years

The range of fluctuations in body temperature was maximum on day 1 in both groups (fig. 3). In the following days, daily temperature drops decreased most significantly in group 1 on days 3-4, in group 2 on days 7.12. Thus, the revealed trend towards a decrease in the mesor of the circadian rhythm of body temperature on days 3-4 was accompanied by a decrease in the amplitude and range of daily fluctuations of the indicator in group 1, characterizing the tendency of gradual normalization of the phase structure of the circadian rhythm of the indicator. In more severe patients in group 2 on days 3,4,5,6,7, an increase in the level of the mesor of the circadian rhythm of body temperature was also accompanied by a tendency to decrease in the amplitude and range of daily fluctuations of the studied indicator, which, perhaps, firstly, characterizes the compensatory mechanism, aimed at an energy-saving mode of temperature regulation in the process of adaptation or is the result of more severe damage to the mesencephalic structures of the brain, given that in group 2 the amount of SCE prevailed - 50%, fracture of the parieto-temporal bone with the transition to the base of the skull - 48%, traumatic shock 2-3 degrees -82%.

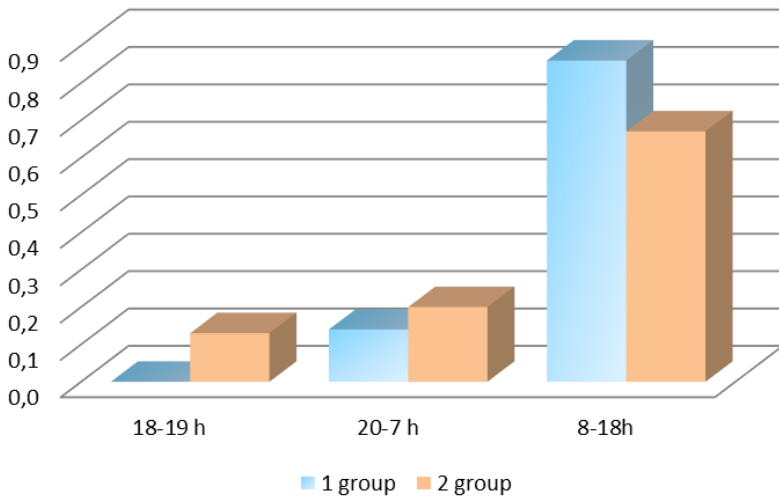


**Figure 4.** Duration and extent of acrophase shift

In both groups of traumatized infants during the acute period of SCTBI, the shift of the acrophase peak to the daytime prevailed. The absence of deeper changes, apparently, is a consequence of corrective, anti-inflammatory therapy in patients under 3 years of age.

## Conclusion

On the first day, the mesor of the circadian rhythm of body temperature did not differ from the norm in all injured. In the acute period of SCTBI in group 1, the indicator practically did not change, in group 2, a significantly significant increase in the mesor of the circadian rhythm of body temperature by 0.5-0.4°C was found on days 3.4.5 after the injury. A decrease in body temperature to the standard value was observed in group 1 on day 3, in group 2 only on day 8. The revealed differences in group 2 are due to a more significant stress response, a systemic inflammatory response to more significant tissue damage OTBI (66%), a higher frequency of SCE (50%), a fracture of the parietotemporal bone with a transition to the base of the skull (48%), severity traumatic shock (82%) than in group 1.

## References

1. <https://vbgi.ru/cough/sochetannaya-cherepno-mozgovaya-travma-sochetannaya-cherepno-mozgovaya-i/>
2. <https://golovaibolit.ru/chmt/chmt-u-detej>
3. <https://ymkababy.ru/good-to-know/sochetannaya-cherepno-mozgovaya-travma-sochetannaya-cherepno-mozgovaya.html>

患者, 去试管婴儿, 发生了什么变化?  
**PATIENTS, GOING FOR IVF, WHAT HAS CHANGED?**

**Vosnesenskaya Nadezda Vadimovna**

*Candidate of Medical Sciences, Associate Professor*

*Ulyanovsk State University*

**Volkova Natalya Alexandrovna**

*Obstetrician-Gynecologist*

*Ulyanovsk Oblast Children's Clinical Hospital Named After a Political and Public Figure Yu.F. Goryachev*

**Klinyшева Svetlana Yuryevna**

*Ulyanovsk State University*

抽象的。作者分析了过去三年体外受精 (IVF) 的结果。显示体外受精后怀孕病例数减少了近两倍。这一事实促使本研究旨在确定导致 IVF 有效性下降的可能因素。对94名进入该项目的患者的门诊卡进行了分析。研究了不孕症原因的结构、既往病史的特征、躯体状态、来自客观和临床和实验室检查的数据。结果表明, 不孕症的原因结构在三年内没有显著变化。转诊至 IVF 的最常见原因是输卵管-腹膜不孕症。大多数女性年龄在 35-39 岁 (26%), 即她们属于生育后期。40-45岁的老年组患者有所增加。半数患者体重指数升高: 30%的患者体重超重, 20%有不同程度的肥胖, 其中7%为重度肥胖。最常见的合并症是伴有甲状腺功能减退的自身免疫性甲状腺炎 (AIT), 在三年内这种疾病的发病率显著增加。发现碳水化合物代谢紊乱的发生率增加: 胰岛素抵抗和 2 型糖尿病 (DM 2), 在糖尿病和肥胖症的频率之间建立了相关性。

关键词: 体外受精, 体重指数, 自身免疫性甲状腺炎, 胰岛素抵抗, 糖尿病

**Abstract.** *The authors analyzed the outcomes of in vitro fertilization (IVF) over the past three years. Revealed a decrease in the number of cases of pregnancy after IVF by almost two times. This fact prompted the present study, which aimed to identify possible factors leading to a decrease in the effectiveness of IVF. 94 outpatient cards of patients who entered the program were analyzed. The structure of the causes of infertility, the features of the anamnesis, somatic status, data from an objective and clinical and laboratory examination were studied. It was revealed that the structure of the causes of infertility did not change significantly over a three-year period. The most common reason for referral to IVF was tubal-peritoneal infertility. Most of the women were aged 35-39 years (26%), i.e. they*

*belonged to the late reproductive period. There is an increase in patients of the older age group of 40-45 years. Half of the patients had an increased body mass index: in 30% of patients, body weight was overweight, and 20% had varying degrees of obesity, of which 7% had severe obesity. The most common comorbidity was autoimmune thyroiditis (AIT) with hypothyroidism, with a significant increase in this disease over the course of three years. An increase in the incidence of carbohydrate metabolism disorders was revealed: insulin resistance and type 2 diabetes mellitus (DM 2), a correlation was established between the frequency of diabetes and obesity.*

**Keywords:** *in vitro fertilization, body mass index, autoimmune thyroiditis, insulin resistance, diabetes mellitus*

Assisted reproductive technologies (ART) methods are the most popular and effective for the treatment of all forms of infertility. Since 1978, in vitro fertilization has been used in world practice. Previously, infertile couples with tubal-peritoneal infertility under the age of 35 were referred for IVF. Now the range of indications has been significantly expanded, and the main contraindications are only severe somatic diseases in the stage of decompensation and severe mental disorders. This, of course, gives hope and great chances for the birth of a child to many infertile couples. [1,2,3]

According to official world statistics, the incidence of infertility is up to 15% of the world population, and this figure continues to grow [2,3]. Every couple in that percentage who resort to IVF treatment aims for a positive outcome, which is a progressive uterine pregnancy ending in a live birth.

Overcoming infertility is not only a medical but also a social problem, since infertility is one of the main causes of the demographic crisis. IVF is included in the list of services paid for by compulsory health insurance, and the effectiveness of financial costs reflects the outcomes of the programs carried out.

Thus, there are many stakeholders involved in completing IVF with a successful pregnancy and childbirth. But to this day, the problem of non-pregnancy and childbirth remains in more than half of the couples who entered the IVF protocol. It is possible to obtain a developing uterine pregnancy using IVF and PE, according to the RAHR registry (2019), in 37.4% of cases. According to the same source, the pregnancy rate over the past 5 years has remained virtually unchanged in all ART programs [3,4]. According to the consultative and diagnostic department of the Perinatal Center of the Ulyanovsk Regional Clinical Hospital in Ulyanovsk, over the past two years, the percentage of positive outcomes after IVF has decreased by almost 2 times. This was the reason for conducting the present study.

### **Purpose of the study**

To identify changes in the structure of the causes of infertility in women referred for IVF over the past 3 years, changes in their somatic status (age, BMI, presence of somatic diseases). Determine the frequency of pregnancy among the examined women for 2019-2021.

### **Materials and research methods**

The study was conducted in the consultative and diagnostic department of the Perinatal Center of the Ulyanovsk Regional Clinical Hospital in Ulyanovsk in 2019-2021. 94 outpatient records of patients referred for IVF were analyzed. The anamnesis, data of objective and clinical and laboratory examination were studied. In the process of statistical data processing, methods of descriptive statistics, correlation and graphical data analysis were used based on the Microsoft Excel and Statistica for Windows, Realease 10 application packages. The significance of differences was determined at a confidence level of 95% or higher.

### **Results and discussion**

The pregnancy rate in the IVF program was: 2019 - 32.4%, 2020 - 14.7%, 2021 - 15.4%. As a result of the study, it was found that the outcome of induced pregnancy is associated with such factors as the patient's age, body mass index, parity and causative factors of infertility, as well as the presence of somatic pathology: autoimmune thyroiditis with hypothyroidism, diabetes mellitus and insulin resistance. For 2019-2021. The Center for Reproductive Health at the Consultative and Diagnostic Department of the Perinatal Center SHI UOCH sent 94 couples to IVF. The structure of the causes of infertility was presented as follows: 40% tubal-peritoneal infertility, 10% lack of ovulation, 9% male factor, 6% infertility of unknown origin, 35% other causes (of which 28% of combined genesis). Thus, the leading cause of infertility among this contingent of women over the entire period of observation was tubal-peritoneal infertility. Over a three-year period (fig. 1), we found a gradual increase in the incidence of tubal-peritoneal infertility (from 35% to 46%) and a gradual decrease in the incidence of other causes of female infertility (from 44% to 23%). This trend may be associated with an annual increase in inflammatory diseases of the pelvic organs in women, an increase in the frequency of surgical interventions, in particular, to remove endometriotic lesions.

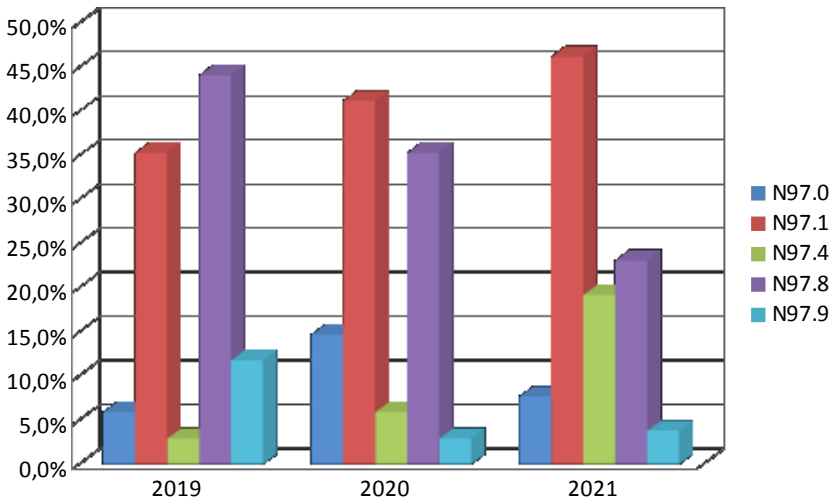


*Figure 1* Distribution of causes of infertility for the period 2019-2021

For 2019-2021, the majority of women referred for IVF were aged 35-39 years (26%), i.e., were in the late reproductive period. At this age, patients more often decide in favor of assisted reproductive technologies. There is an increase in patients of the older age group of 40-45 years. At the age of 18-24 years, the lowest percentage of infertility is 4%. Perhaps this is due to the trend towards a shift in the average age of childbearing to 30 years, as well as the low incidence of gynecological diseases in this group, leading to infertility, which is confirmed by Rosstat data. The average age of women with primary infertility was 31.9 (28-35.8), secondary - 35.8 (32 - 39). The difference is statistically significant (U - Mann-Whitney test  $p < 0.001$ ).

Less than half of the women with infertility (47%) had normal body weight, 30% of patients were overweight, and 20% had varying degrees of obesity, of which 7% had severe obesity.

In our study, women with infertility were identified, against the background of existing endocrine disorders (fig. 2). The most common disease was autoimmune thyroiditis (AIT) with hypothyroidism. There is an increase in the number of women with AIT from 2.9% to 15.4% ( $p < 0.05$ ), with insulin resistance from 2.9% to 11.5% ( $p < 0.05$ ). BMI was found to correlate with the presence of DM in women: 25.4 (21.2-28.2) in the group without DM and 32.2 (28.2-36.3) with diabetes mellitus, respectively. This fact is confirmed by numerous studies in which it is noted that with an increase in BMI, the risk of developing DM increases. The relative risk of DM increases by 72% with a BMI increase of 5 units [1].

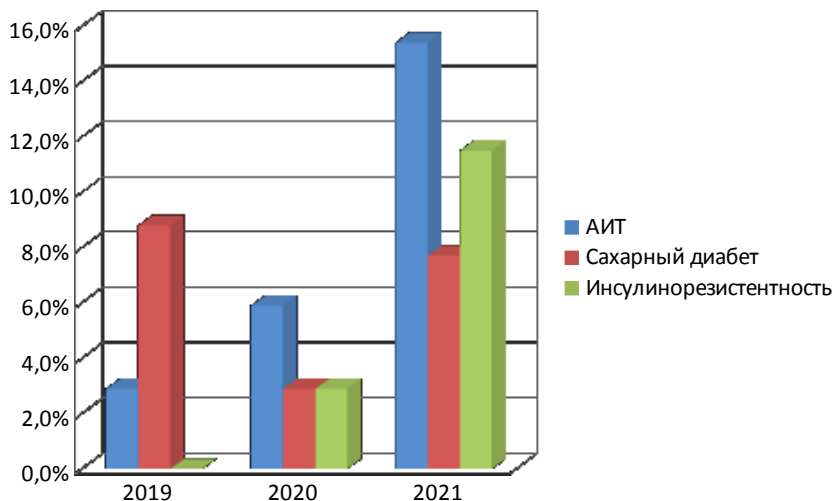


**Figure 2.** Observed endocrine disorders and their frequency in women with infertility

According to the data of FSBI "V.I. Kulakov RC OGaP" when examining women with infertility, thyroid pathology was detected in 47.9%, which is 3.8 times higher compared to fertile women (12.5%). The structure of thyroid pathology is dominated by the carriage of AT-TPO in combination with echo signs of AIT, noted 2.8 times more often in the group of infertile women compared to fertile women (24% and 8.7%;  $p < 0.05$ ), hypothyroidism in the outcome of AIT (9.4% and 2.5%;  $p < 0.05$ ) [6]. The growth of patients with autoimmune thyroiditis may be associated with the prevalence of acute respiratory viral infections, which women get sick more than once a year; with foci of chronic infections in the upper respiratory tract; with prolonged uncontrolled use of iodine preparations, hormonal agents; with excessive insolation; radiation; psychological overstrain [5]. Insulin resistance is most often associated with malnutrition in the form of excessive consumption of sugar and fat, which can also lead to obesity.

During the observation period, pregnancy in the IVF program was noted only in 11% of women with autoimmune thyroiditis. Patients with insulin resistance and DM did not have positive IVF results. (fig.3)

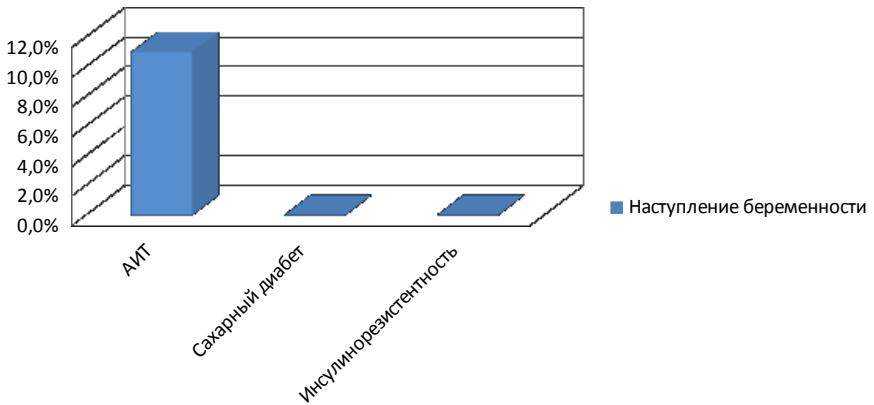


**Figure 3.** The frequency of pregnancy in women with endocrinopathies

Thus, as a result of the study, it was found that women of late reproductive age with primary and secondary infertility are more often referred for IVF. Poor outcomes occur in patients with metabolic disorders such as obesity and varying degrees of carbohydrate metabolism disorder. Timely and rational correction of these disorders at the stage of pregravid preparation can increase the percentage of positive outcomes after IVF.

## References

1. *IVF in gynecological and endocrine diseases* / ed. T. A. Nazarenko. — M.: GEOTAR-Media, 2016. — 176 P
2. *Barren marriage: versions and contraversions* / [Radzinsky V. E., Orazov M. R., Lokshin V. N. and others]; under the editorship of Corresponding Member of the RAS, Professor V. E. Radzinsky. 2nd edition, revised and enlarged – Moscow: GEOTAR-Media, 2020. - 432 P
3. *Infertility: diagnostics, modern methods of treatment* / N. M. Podzolkova, N. L. Shamugiya, Yu. A. Koloda, M. Yu. Skvortsova. - Moscow: GEOTAR-Media, 2018. - 141 P.: ill., tab.; 19 cm. - (For a practicing gynecologist)
4. "Russian Association of Human Reproduction" – ART register. Report for 2019.– 54 P.
5. Nikonova L.V., Davydchik E.V., Tishkovsky S.V., Gadomskaya V.I. Thyroid disease and pregnancy. Part I. Autoimmune thyroiditis, hypothyroidism, thyrotoxicosis during pregnancy: modern principles of diagnosis and treatment // *Journal of Grodno State Medical University*. 2016.

6. *Perminova S.G. Female infertility and dysfunction of the thyroid gland // Barren marriage. Modern approaches to diagnosis and treatment. Ed. G.I. Sukhikh, T.A. Nazarenko 2-nd ed. rev. and add. - M.,:GEOTAR-MEDIA.- 2010. – P. 237-272.*

7. *Ahmad Jayedi, Sepideh Soltani, Sheida Zeraat-talab Motlagh, et al. Anthropometric and adiposity indicators and risk of type 2 diabetes: systematic review and dose-response meta-analysis of cohort studies. BMJ 2022*

DOI 10.34660/INF.2022.94.64.141

使用可编程真空技术对糖尿病足化脓性坏死伤口愈合动力学的细胞学研究  
**CYTOLOGICAL STUDY OF THE DYNAMICS OF HEALING OF  
PURULENT-NECROTIC WOUNDS IN DIABETIC FOOT USING  
PROGRAMMABLE VACUUM TECHNOLOGIES**

**Sergeev Vladimir Anatolyevich**

*candidate of Medical Sciences, Associate Professor*

*Orel State University named after I.S. Turgenev, Orel, Russia*

**Glukhov Alexander Anatolyevich**

*Doctor of Medical Sciences, Full Professor*

*Voronezh State Medical University named after N. N. Burdenko,  
Voronezh, Russia*

**Morozov Yuri Mikhailovich**

*Doctor of Medical Sciences, Full Professor*

*Orel State University named after I.S. Turgenev, Orel, Russia*

研究目的：使用可编程真空技术检查糖尿病足化脓性坏死伤口患者愈合过程的细胞学特征。

方法：该研究涉及 110 名糖尿病足综合征 (DFS) 化脓性病変患者，根据 F.W. Wagner (1979) II-IV 度无严重缺血。患者被随机分为两组。在对照组 (n=52) 中，术后患者接受传统的局部治疗。在主要组 (n=58) 中，使用 AMP-01 设备在术后期间进行可编程真空消毒。同时，用管状引流管引流脓腔，通过单独的切口将其取出，并对伤口进行盲缝。该设备在离线模式下以循环原理运行，允许您选择卫生参数（速度、注射量或抽吸）并针对每个特定病例采取单独的治疗方法。化脓性伤口修复过程的动力学通过表面或穿刺活检方法获取的材料的细胞学照片进行评估。

结果：在主要患者组中，注意到化脓性伤口的细胞反应率较高。到术后第 9 天，细胞学图片与再生型细胞图相对应。中性粒细胞的退行性形式的减少在统计学上显著加快，刺伤和分段中性粒细胞的重新分布以及再生-退行性指数的高值 ( $p < 0.001$ )，表明炎症过程的缓解加速。同样在主要组中，以纤维细胞、成纤维细胞、纤维纤维的形式出现的巨噬细胞和年轻结缔组织细胞 ( $p < 0.001$ ) 在统计学上显著较早地观察到，这表明伤口中有活跃的再生过程。在对照组中，伤口中的细胞反应强度较低，炎症阶段延长，再生阶段持续时间较长，疤痕重组阶段开始较晚。

结论：进行的细胞学研究证明了使用可编程真空技术的有效性，有助于减少炎

症阶段, 加速糖尿病足化脓性坏死伤口患者的修复过程。

关键词: 糖尿病足, 化脓性坏死伤口, 可编程真空技术, 细胞学检查, 愈合过程。

**Purpose of the study:** *to examine the cytological features of healing processes in patients with purulent-necrotic wounds in diabetic foot using programmable vacuum technologies.*

**Methods:** *The study involved 110 patients with purulent lesions of the diabetic foot syndrome (DFS) according to F.W. Wagner (1979) II-IV degree without critical ischemia. The patients were randomized into two groups. In the comparison group (n=52), after surgery, patients received traditional local treatment. In the main group (n=58), programmable vacuum sanitation was performed in the postoperative period using the AMP-01 device. At the same time, the purulent cavity was drained with tubular drains, they were removed through separate incisions, and a blind suture was applied to the wound. The device operates on a cyclic principle in an offline mode, allows you to select the sanitation parameters (speed, volume of injection or aspiration) and carry out an individual approach to the treatment of each specific case. The dynamics of reparative processes in purulent wounds was assessed by the cytological picture of the material taken by the method of surface or puncture biopsy.*

**Results:** *In the main group of patients, a higher rate of cellular reactions in purulent wounds was noted. By day 9 after the operation, the cytological picture corresponded to the regenerative type of cytograms. There was a statistically significant faster decrease in degenerative forms of neutrophils, a positive redistribution of stab and segmented neutrophils in combination with high values of the regenerative-degenerative index ( $p < 0.001$ ), indicating an acceleration in the relief of the inflammatory process. Also in the main group, the appearance of macrophages and cells of young connective tissue in the form of fibrocytes, fibroblasts, fibrous fibers ( $p < 0.001$ ) was statistically significantly earlier observed, which indicated active regenerative processes in the wound. In the comparison group, a lower intensity of cellular reactions in the wound, a lengthening of the inflammation phase, a significant duration of the regeneration phase, and later onset of the scar reorganization phase were revealed.*

**Conclusion:** *The conducted cytological study proved the effectiveness of the use of programmable vacuum technologies that help reduce the inflammation phase, accelerate reparative processes in patients with purulent-necrotic wounds in diabetic foot.*

**Keywords:** *Diabetic foot, purulent-necrotic wounds, programmable vacuum technologies, cytological examination, healing process.*

## Introduction

At the present stage, the problem of diabetes mellitus (DM) is gaining medical and social significance, which is explained by the high progressive prevalence, significant disability and increasing mortality in patients with diabetes [1,2,3,4]. According to the World Health Organization (WHO), DM currently affects approximately 285 million people, and by 2035 experts predict an increase in the number of DM patients to 600 million people [1,2,5]. In Russia, the mortality rate from type 2 DM is 60.3 per 100,000 population [1]. In the US, DM affects approximately 9.4% of the population over the age of 18 [6]. Approximately 25% of diabetics are at risk of developing purulent-necrotic complications, which is the main reason for their hospitalization, which costs US\$ 40,000 per event [7,8,9]. It is possible to achieve healing of a diabetic ulcer by conservative measures only in 63-81% of cases, amputation of various levels of the limb is required in 14-24% of patients, while mortality rates reach 13%. These figures emphasize the need to find innovative approaches to the problem of treating purulent-necrotic complications of DM [10,11].

In recent years, fundamental scientific research in molecular cell biology has made it possible to better understand the underlying mechanisms of wound healing. It has been proven that the healing process in any wound is genetically determined; at first, the inflammation phase always begins, which is replaced by the regeneration phase and the phase of scar reorganization and epithelialization [12-15]. At the present stage, the solution of the problems of predicting the course of reparative processes underlying the structural and functional restoration of altered tissues becomes more and more relevant. In this regard, the interest in the development of both new approaches to treatment and methods for assessing the dynamics of healing of wound defects is of current interest [16-19]. To obtain quick and objective information about the course of reparative processes in wounds of various origins, the use of the cytological method remains preferable [12,20-23]. A cytological study allows one to characterize various types of the course of the wound process, to reliably assess the effectiveness of the treatment [12,24-27]. There are 6 types of cytological picture according to V.F. Kamaev (1954), corresponding to different stages of the wound process: degenerative-necrotic type, degenerative-inflammatory type, inflammatory type, inflammatory-regenerative type, regenerative-inflammatory type, regenerative type [12,29]. For a complete assessment of the picture of wound healing, the regenerative-degenerative index (RDI) is calculated using the formula [30]. An RDI value less than one indicates a pronounced inflammatory process in the wound, and if the value of this indicator becomes greater than one, this means the transition of the wound process to the regeneration phase. Evaluation of the reparative reaction in the wound based on cytological verification is one of the objective methods for studying the features of the course of the wound process, which allows optimizing the treatment tactics.

**Purpose:** to study the results of a cytological study of healing processes in purulent diseases of soft tissues using programmable sanitation technologies.

**Material and methods**

For the period 2012-2020, we observed 110 patients with purulent-necrotic complications of diabetic foot aged 38 to 76 years.

Criteria for inclusion in this study: the age of patients over 18 years of age, the presence of purulent lesions of the foot according to F.W. Wagner (1979) II-IV degree without critical ischemia, the presence of informed voluntary consent. Exclusion criteria for the study: the presence of extensive skin defects in the area of surgical treatment, signs of anaerobic infection, the presence of pregnancy, oncological pathology, insufficiency of the circulatory organs and insufficiency of the respiratory organs of the III degree. The neuropathic form of DFS was observed in 65.5% of cases, neuroischemic - in 34.5% of cases.

Depending on the methods of sanitation of purulent foci in the postoperative period, all patients were randomized into two groups. In the comparison group, after surgical treatment, patients received traditional local treatment, the wound was treated openly using iodophor solutions, polyethylene glycol-based ointments. In the main group, after surgical treatment, the wound was drained with tubular drains, they were removed through separate incisions, and the wound was then sutured tightly. The drains were connected to the original device AMP-01 (patent for invention №176572 dated 23.01.2018), which was used to carry out programmable vacuum sanitation in the postoperative period. On the control unit of the device, an individually selected program of cyclically occurring processes of irrigation, antiseptic aspiration and constant vacuuming, carried out offline, was installed. The specified level of vacuum in the purulent cavity (60-80 mmHg) was maintained using a built-in pressure sensor. Basic therapy was the same in both groups of patients.

In the main group, the mean age of patients ( $M \pm \sigma$ ) was  $59 \pm 13$  years, in the comparison group it was  $60 \pm 11$  years. In the main group, there were 24 men, 34 women, in the comparison group 19 and 33, respectively. Thus, there are no statistically significant differences between the study groups by sex and age, which made it possible to judge the homogeneity of the groups ( $p = 0.854$  and  $p = 0.875$ , respectively).

The distribution of patients in the study groups depending on the nosological form of purulent complications of DFS and the extent of the lesion in accordance with the classification of F.W. Wagner (1979) are presented in table 1.

**Table 1.**

*Distribution of patients in the study groups depending on the nosological form of purulent-necrotic complications of DFS and the extent of the lesion in accordance with the classification of F.W. Wagner (1979)*

Nosological form of purulent-necrotic process on the foot	Damage volume according to F.W.Wagner classification (1979)	Main group (n=58)		Comparison group (n=52)		Total
		n	%	n	%	
Deep ulcer	2	5	8.6	4	7.7	9
Deep ulcer + Chronic osteomyelitis of the finger	3	3	5.8	3	5.8	6
Finger phlegmon + foot phlegmon	2	8	13.8	7	13.5	15
Osteomyelitis of the finger + phlegmon of the foot	3	8	13.8	9	17.3	17
Purulent wound after amputation of fingers or resection of the foot, previously performed in other medical institutions	3	14	24.1	13	25	27
Dry gangrene of one or more fingers	4	12	20.7	9	17.3	21
Wet gangrene of the finger + phlegmon of the foot	4	8	13.8	7	13.5	15
Total:		58	100	52	100	110

According to the independent criterion  $\chi^2$ -Pearson ( $p = 0.953$ ), the dependence of the distribution of patients according to the nosological form in the study groups was not found.

To assess the healing of purulent foci, a cytological method was used. We used the technique of surface biopsy according to M.P. Pokrovskaya and M.S. Makarov (1942) modified by M.F. Kamaeva (1954). In the comparison group, material was taken by lightly scraping the surface layer of the wound with the handle of a surgical scalpel. The resulting material was applied to glass, fixed and stained according to the May-Grunwald-Romanovsky-Giemsa method. In the main study group, cell and tissue elements were taken using the "puncture biopsy" method (Kaem R.I., Karlov V.A., 1977; Sergel O.S., Goncharova Z.N., 1990). 4-5 smears were sequentially taken from the same area of the wound. Cytological examination of smears from the surface of the wounds was carried out on the first day, and then on the 3rd, 5th, 7th, 9th days. The smears were examined under microscopy with

a  $\times 40$  lens, while the formed elements were counted and the average value was calculated over 10 fields of view. The value obtained was expressed as a percentage per 100 counted cells. We used an Axio A1 light microscope (Zeiss, Germany) with a set of accessories.

At the time of randomization in both groups of the study in patients with purulent lesions of DFS, the cytological picture was characteristic of a degenerative-necrotic type of cellular reaction. Among the cellular elements, degenerative neutrophils (DN) predominated ( $64.5 \pm 9.2\%$ ), there were very few preserved forms of leukocytes. The regenerative-degenerative index (RDI) was significantly below one ( $0.2 \pm 0.1$ ). The microflora was in large quantities, predominantly extracellular. In the preparations, accumulations of necrotic masses and amorphous gelatinous interstitial substance were observed. Figure 1 shows a fragment of a cytological smear from the wound surface in patients with purulent lesions of the diabetic foot at the time of randomization on the 1st day of the study.

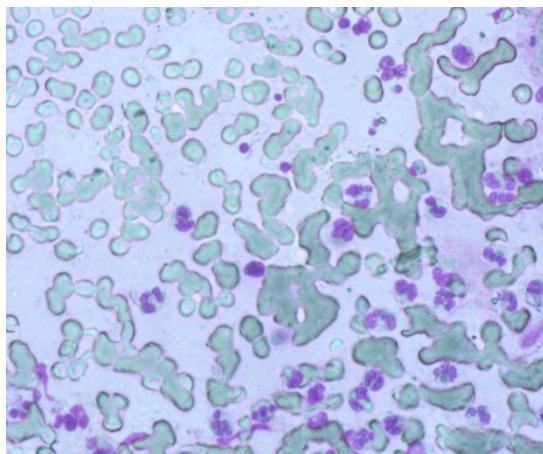


**Figure 1.** A fragment of a cytogram of a smear from the wound surface in patients with purulent lesions of the diabetic foot on the 1st day. Degeneratively altered polymorphonuclear leukocytes predominate, the microflora is in large numbers, mainly extracellular, there is an accumulation of necrotic masses and an amorphous gelatinous intermediate substance. Coloring according to Romanovsky-Giemsa. Lens  $\times 40$

The cellular composition of cytological smears in patients with purulent lesions of the diabetic foot in the study groups at the time of randomization is presented in table 2.

**Table 2.**

*Cellular composition of cytological smears in patients with purulent lesions of the diabetic foot in the study groups at the time of randomization, in % per 100 cells*

Cell types	Main group		Comparison group		p-value t-criterion
	M±σ, in % per 100 cells	Me[Q1;Q3]	M±σ, in % per 100 cells	Me[Q1;Q3]	
STN	1.8±0.2	1.82 [1.77;1.87]	1.7±0.2	1.74 [1.64;1.81]	0,682
SEN	15.2±0.6	15.19[15.07;15.32]	16.2±0.4	16.16[16.07;16.25]	0,647
DN	64.5±9.2	65.89[63.65;68.13]	62.2±6.2	68.84[67.57;70.09]	0,022
RDI	0.2±0.1	0.18 [0.16;0.21]	0.2±0.1	0.18 [0.16;0.21]	0,976
L	0.4±0.2	0.39 [0.35;0.43]	0.2±0.1	0.17 [0.15;0.19]	0,000

**Note:** STN - stab neutrophils, SEN - segmented neutrophils, DN - degenerative neutrophils, RDI - regenerative-degenerative index, L - lymphocytes

Most of the parameters of the statistical evaluation of the cellular composition of cytological smears on the first day of observation in both groups of the study were similar in values ( $p > 0.05$ ), which made it possible to judge the homogeneity of the groups. However, homogeneity was not statistically proven for DN and L, which can be explained by the small sample of the study.

The work was carried out in the design of a simple randomized comparative controlled study in parallel groups. SPSS Statistics 25 (IBM) software was used for statistical processing of the obtained data. To study the relationship between qualitative features, contingency tables were built and the  $\chi^2$ -Pearson test or Fisher's exact test was calculated. To assess the change in the dynamics of quantitative indicators, we used analysis of variance with repeated measurements with a time factor and a group. Differences were considered statistically significant at a probability value less than 0.05 for a two-sided critical region.

### Results

The cytological picture of smears in the main group on the 5th day from the moment of randomization corresponded to the inflammatory or inflammatory-regenerative type of cellular reaction. There was a statistically significant decrease in the number of degenerative neutrophils (DN) (16.7±2.2%), a statistically significant increase in RDI - 2.9±0.4 ( $p < 0.001$ ). Plasma cells and histiocytes appeared. A statistically significant increase in the number of active macrophages was observed - 4.6±0.6%, lymphocytes - 5.8±0.6%, fibroblasts - 4.2±0.5% ( $p < 0.001$ ). Groups of cells of young connective tissue in the form of fibrocytes, fibroblasts, fibrous fibers were found. The microflora was determined in a small amount at the stage of completed phagocytosis.

In the comparison group on the 5th day of treatment, the cytological picture in smears corresponded to the inflammatory type of cellular reaction and was characterized by a neutrophilic reaction - the number of preserved forms of neutrophils increased: SEN -  $42.6 \pm 3.8\%$ , STN -  $6.2 \pm 0.8\%$ , the number of degenerative forms became less -  $56.7 \pm 2.2\%$ . RDI was close to unity -  $0.9 \pm 0.2$ . The microflora was determined intra- and extracellularly, but cases of completed phagocytosis were more common. There were single actively phagocytic leukocytes, macrophages, lymphocytes. Elements of granulation tissue are single. Figures 2 and 3 show fragments of cytological smears from the wound surface on the 5th day in the studied groups.

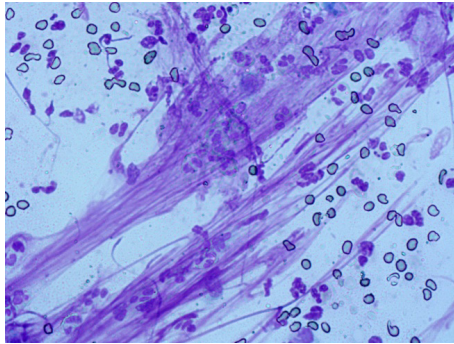


**Figure 2.** A fragment of a cytogram of a smear from the surface of the wound on the 5th day, the main group. Fibrocytes, fibroblasts, fibrous fibers were found among neutrophils and polyblasts. Coloring according to Romanovsky-Giemsa. Lens  $\times 40$

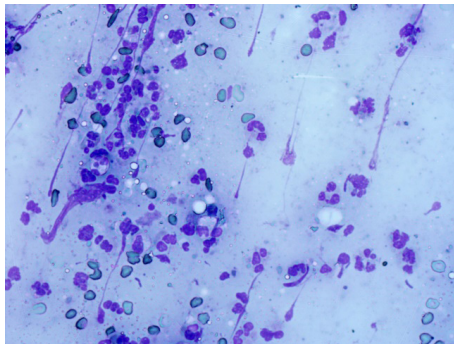


**Figure 3.** A fragment of a cytogram of a smear from the surface of the wound on the 5th day, the comparison group. Single actively phagocytic leukocytes, macrophages, lymphocytes are observed. Elements of granulation tissue are single. Coloring according to Romanovsky-Giemsa. Lens  $\times 40$

On the 9th day of the postoperative period in the main group, the cytological picture corresponded to the regenerative-inflammatory or regenerative type of cellular reactions. Figures 4 and 5 show fragments of cytological smears from the wound surface on the 9th day in the studied groups.

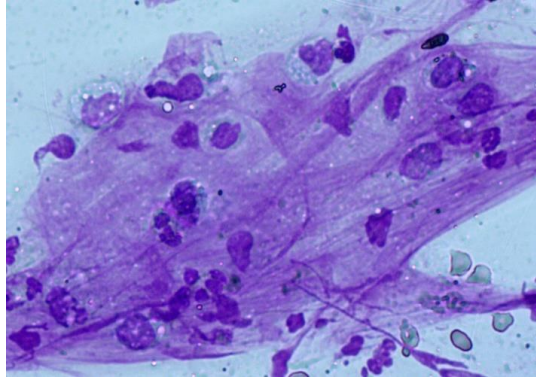


**Figure 4.** A fragment of a cytogram of a smear from the wound surface on the 9th day, the main group. Young elements of connective tissue, fibroblasts, polyblasts, macrophages are located among the fibrous structures of the intermediate substance. The epithelium is presented in the form of layers of cells. Coloring according to Romanovsky-Giemsa. Lens  $\times 40$

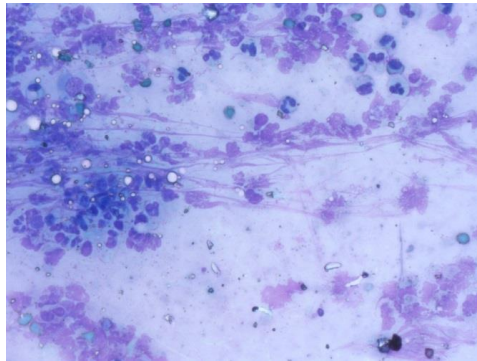


**Figure 5.** A fragment of a cytogram of a smear from the surface of the wound on the 9th day, the comparison group. The number of mononuclear cells decreased, the number of polyblasts, fibroblasts, macrophages increased. Delicate fibrous structures of the intermediate were observed. Coloring according to Romanovsky-Giemsa. Lens  $\times 40$

According to the results of the analysis of variance with repeated measurements for both groups, statistically significant changes in the cellular composition in cytograms on the 1st and 9th days of the postoperative period were proved. The number of DN in the main group significantly decreased from  $64.5 \pm 9.2\%$  to  $3.8 \pm 0.3\%$ , in the comparison group from  $68.8 \pm 6.2\%$  to  $12.5 \pm 0.4\%$ ; RDI values in the main group increased significantly from  $0.2 \pm 0.1\%$  to  $8.2 \pm 0.1\%$ , in the comparison group from  $0.2 \pm 0.1\%$  to  $2.4 \pm 0.1\%$ . Statistically significant differences between the groups as a whole were proved for the entire observation period from the first to the 9th day, therefore, we reject the hypothesis of the equality of the means between the groups without taking into account time ( $p < 0.001$ ). There was also a significant interaction between the time factor and the group ( $p < 0.001$ ). In the main group in the postoperative period, a more rapid decrease in the number of DN was observed, which on the 9th day was  $3.8 \pm 0.3\%$ , in contrast to the comparison group -  $12.5 \pm 0.4\%$ . A more rapid increase in RDI values was also observed in the main group, which increased to  $8.2 \pm 0.1$  on the 9th day, in contrast to the comparison group ( $2.4 \pm 0.1$ ). This indicated more active phagocytosis, more intensive cleansing of the purulent cavity of purulent foci in patients of the main group. Dynamics of average values of degenerative neutrophils and RDI values in cytological smears in patients with purulent complications of diabetic foot in both study groups are presented in figures 6 and 7.

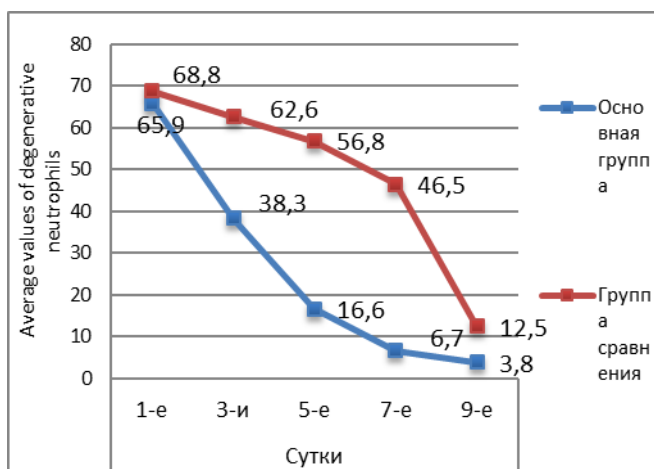


**Figure 6.** Dynamics of mean values of degenerative neutrophils in cytograms of both study groups in patients with purulent complications of diabetic foot

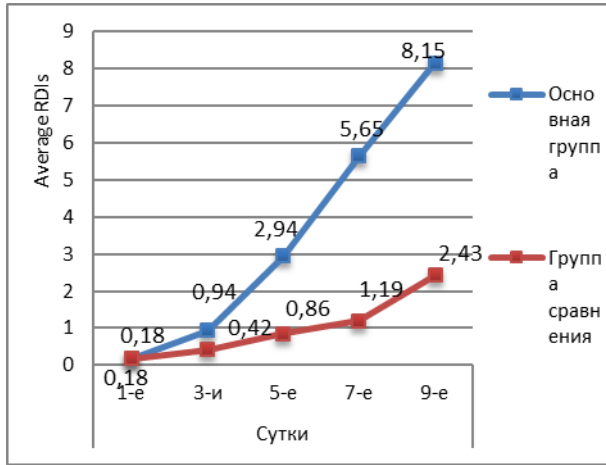


**Figure 7.** Dynamics of the average values of the regenerative-degenerative index in the cytograms of both study groups in patients with purulent complications of diabetic foot

To assess the reparative potential of purulent wounds, a cytological assessment of the quantitative composition of lymphocytes, macrophages and fibroblasts was carried out in the study groups on the 1st and 9th days of the postoperative period. The results of the calculation of the analysis of variance with repeated measurements showed that for these variables we reject all three null hypotheses, for all three hypotheses  $p < 0.05$ . The difference between groups for these variables is statistically significant overall over the entire observation period. In the main group, where programmable vacuum technologies were used, the number of lymphocytes, macrophages and fibroblasts was always higher. Also, for these variables, a significant interaction between the time factor and the group was found. This indicated active regenerative processes in the wound in the main group of patients, and the structure of cytograms in cytological smears in the main group was characterized by a regenerative type. Dynamics of average values of degenerative neutrophils and RDI values in cytological smears in patients with purulent complications of diabetic foot in both study groups are presented in figures 8.9.

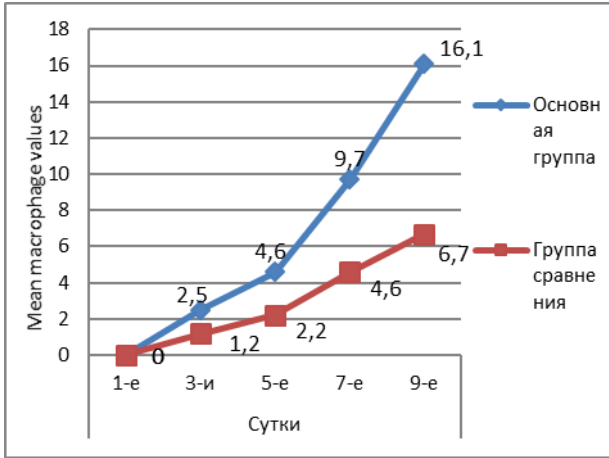


*Figure 8. Dynamics of mean values of macrophages in cytograms in study groups in patients with purulent complications of diabetic foot*

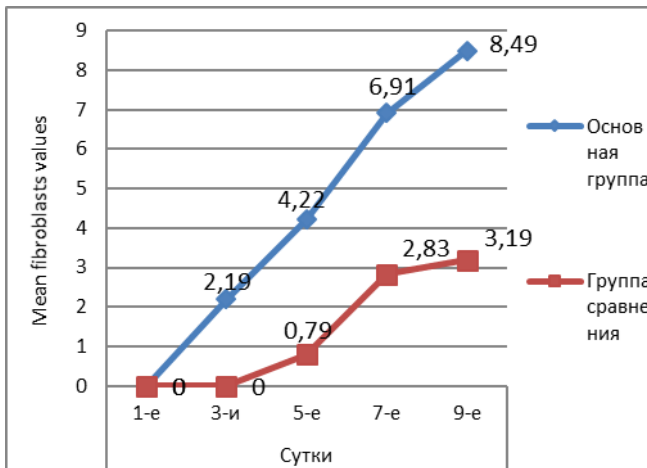


*Figure 9. Dynamics of mean values of fibroblasts in cytograms in study groups in patients with purulent complications of diabetic foot*

**Discussion**

Analyzing the dynamics of the cytological picture in patients with purulent complications of the diabetic foot, it was noted that in the comparison group with traditional treatment, a low intensity of cellular reactions in the wound was revealed, an prolongation of the inflammation phase, and the inflammatory type of

cytograms was noted only by 9 days after surgery. Also, in the comparison group, the lethargy of reparative processes in the wound was observed, causing a significant duration of the regeneration phase, later onset of the scar reorganization phase. This led to a lengthening of the healing time.

The use of programmable vacuum technologies made it possible to create conditions for a better sanitation of the purulent focus, and led to a reduction in all phases of the wound process. Surgical treatment of the purulent focus, prolonged washing of the wound cavity in the postoperative period, software for the process of active drainage with evacuation of the wound cavity made it possible to quickly clean the wound from non-viable tissues, toxins and proteolytic enzymes, reducing microbial contamination in the wound. As a result, the stage of rejection of necrotic tissues was extremely reduced. Early closure of the wound with sutures using active drainage with vacuum under conditions of a minimally pronounced inflammatory reaction in the wound significantly accelerated reparative processes, creating conditions for the development and completion of the regeneration phase.

### Conclusion

Cytological examination of smears in patients with purulent-necrotic complications of diabetic foot using programmable vacuum technologies revealed a higher rate of cellular reactions in the wound. At the same time, a statistically significant faster decrease in degenerative forms of neutrophils was noted, a positive redistribution of stab and segmented neutrophils, combined with an increase in the regenerative-degenerative index, indicating a more rapid relief of the inflammatory process. The appearance of macrophages and cells of young connective tissue in the form of fibrocytes, fibroblasts, fibrous fibers was also reliably observed at an earlier date, which indicated active regenerative processes in the wound.

### References

1. Galstyan G.R., Vikulova O.K., Isakov M.A. et al. *Epidemiology of diabetic foot syndrome and lower limb amputations in the Russian Federation according to the Federal register of diabetes patients (2013–2016). Diabetes mellitus. 2018;21(3):170–177.*
2. Dedov I.I., Shestakova M.V., Vikulova O.K. *Epidemiology of diabetes mellitus in the Russian Federation: clinical and statistical analysis according to the Federal register of Diabetes Mellitus. Diabetes mellitus. 2017;20(1):13–41.*
3. Mitish V.A., Paskhalova, Y.S., Eroshkin I.A. et al. *Purulent necrotic lesions in the neuroischemic form of diabetic foot syndrome. Surgery. Magazine them. N.I. Pirogov. 2014;(1):48–53.*

4. Bakker K., Apelqvist, J. Lipsky, B.A., Van Netten J.J. *International Working Group on the Diabetic Foot. The 2015 IWGDF guidance documents on prevention and management of foot problems in diabetes: development of an evidence-based global consensus. Diabetes Metab. Res. Rev.* 2016;(32):2–6.

5. Stupin V.A., Silina E.V., Koreyba K.A., Goryunov S.V. *Diabetic foot syndrome (epidemiology, pathophysiology, diagnosis and treatment). M.: Litterra;* 2019.

6. Centers for Disease Control and Prevention (2014) *National Diabetes Statistics Report: Estimates of Diabetes and Its Burden in the United States, 2014. US Department of Health and Human Services, Atlanta.*

7. Ray JA, Valentine WJ, Secnik K, Oglesby AK, Cordony A, Gordois A, et al. *Review of the cost of diabetes complications in Australia, Canada, France, Germany, Italy and Spain. Curr Med Res Opin.* 2005;21(10):1617–29. <https://doi.org/10.1185/030079905X65349>.

8. Armstrong DG, Boulton AJM, Bus SA. *Diabetic foot ulcers and their recurrence. N Engl J Med.* 2017;376(24):2367–75. <https://doi.org/10.1056/NEJMr1615439>.

9. Jang M.Y., Hong J.P., Bordianu A. et al. *Using a contradictory approach to treat a wound induced by hematoma in a patient with antiphospholipid antibody syndrome using negative pressure wound therapy. Low Extrem. Wounds.* 2015;14(3):303–306.

10. Nickerson D.S. *Improving outcomes in recurrent and other new foot ulcers after healed plantar forefoot diabetic ulcer. Wound Repair and Regeneration.* 2018;26(1):108–109.

11. Ivanov D.P. Serebryakova O.V., Ivanov P.A. *Diabetic foot syndrome: classification and diagnosis of ischemic form, current state of the issue. Trans-Baikal Medical Bulletin.* 2018;4:111–122.

12. Kuzin MI, Kostyuchenok BM. *Wounds and wound infections: A guide for physicians. Moscow: Medicine.* 1990; 592 p. Available at: <http://med-books.by/hirurgiya/2948-rany-i-ranevaya-infekciya-kuzin-mikostyuchenok-bm-1990-god-592-s.html>.

13. Stadelmann, W.K. *Physiology and healing dynamics of chronic cutaneous wounds / W.K.Stadelmann // American Journal of Surgery. - 1998. - Vol. 176. – N 2. - P. 26S–38S.*

14. Midwood, K.S. *Tissue repair and the dynamics of the extracellular matrix / K.S.Midwood // The International Journal of Biochemistry & Cell Biology. -2004. - Vol. 36. - N 2. –P. 1031-1037.*

15. Deodhar, A.K. *Surgical physiology of wound healing: a review / A.K. Deodhar // Journal of Postgraduate Medicine. - 1997. – N 43. – P. 52-56.*

16. Eskes AM, Gerbens LA, van der Horst CM, Vermeulen H, Ubbink DT. *Is the red-yellow-black scheme suitable to classify site wounds? An inter-observer analysis.* *Burns.* 2011;37(5):822-826. doi: 10.1016/j.burns.2010.12.019. [PubMed: 21345594].
17. Zemskov MA, Chorochilov AA, Iljina EM, Domnich OA. *Peculiarities of changes of immune status in chronic inflammatory diseases.* *Journal of experimental. and clinical surgery.* 2011; 4(3):468-72. doi: 10.18499/2070-478X-2011-4-3-468-472
18. Lacci K, Dardik A. *Platelet-rich plasma: support for its use in wound healing.* *Yale J Biol Med.* 2010;83(1):1-9. [PubMed: 20351977].
19. Han T, Wang H, Zang YQ. *Combining platelet-rich plasma and extracellular matrix-derived peptides promote impaired cutaneous wound healing in vivo.* *J Craniofac Surg.* 2012;23(2):439-47. doi: 10.1371 / journal.pone.0032146. [PubMed: 22384158].
20. Larichev AB, Shishlo VK, Lisovsky AV, Chistyakov AL, Vasiliev AA. *Wound infection prevention and morphological aspects of aseptic wound healing.* *J of Exp and Clin Surg.* 2011;4(4):728-33. doi.org/10.18499/2070-478X-2011-4-4-728-733.
21. Titova MI, Svetukhin AM, Kurochkina AI, Astasheva NG, Doroshina TI, Krylova NN, Agofonov VA. *Current methods of morphological and hemostasiological analysis of reparative process in wounds making use of information programs.* *Klin Lab Diagn.* 2000;7(24-36). [PubMed: 10981393].
22. Kocjan Gabrijela. *Cytopathology of the Head and Neck: Ultrasound Guided FNAC.* 2nd ed. -Wiley-Blackwell. 2017;212 p.
23. Field Andrew S. (ed.) *Practical Cytopathology. A Diagnostic Approach to Fine Needle Aspiration Biopsy.* Elsevier. 2017;563 p.
24. Ivanusa SY, Risman BV, Ivanov GG. *Modern ideas about methods of assessment the course of the wound process in patients with purulo-necrotic complications of the diabetic foot syndrome.* *Herald of the Russian Military Medical Academy.* 2016;54(2):190–194. Internet address: <http://elibrary.ru/item.asp?id=26280216>
25. Larichev AB, Chistyakov AL, Komlev VL. *Comparative assessment of wound healing by using a local flap and full-thickness skin graft in reconstructive head and neck surgery.* *Wounds and wound infections. The prof. B.M. Kostyuchenok journal.* 2016;3(2):37-46. <https://doi.org/10.17650/2408-9613-2016-3-2-37-46>
26. Sergeev VA, Glukhov AA. *Results of operative therapy of diabetic foot purulent complications using programmed sanitation technologies.* *Zeitschrift für Gefäßmedizin.* 2020; 17 (3): 13-17

27. Sergeev VA, Glukhov AA, Sorokin AS. *Cytological study of the dynamics of the wound process in purulent lesions of the diabetic foot syndrome with the use of programmable rehabilitation technologies. Periódico Tchê Quimica. 2021; 18(37): 212-227.*

28. Sergeev VA, Glukhov AA, Sorokin AS, Zhuchkov SA, Gorokhov AV, Troshkina EN. *Clinical-functional and morphological parameters of purulonecrotic foci healing in diabetic foot syndrome using programmable sanitation technologies. International Journal of Health Sciences. 2021;5(3), 260-275.*

29. Kamaev MF. *Types of cytograms in a superficial biopsy of the wound. Collection of works of the Odessa medical Institute named after N. I. Pirogov. Kiev. 1954;267-276.*

30. Davydov IA, Larichev AB, Abramov AI. *Substantiation of Using Forced Early Secondary Suture in the Treatment of Suppurative Wounds by the Method of Vacuum Therapy. Vestn Khir Im I I Grek. 1990;144(3):126-8. [PubMed: 2169094].*

DOI 10.34660/INF.2022.21.82.142

森林种植和木材利用对地球大气中二氧化碳平衡的影响  
**ON THE INFLUENCE OF FOREST CULTIVATION AND WOOD USE  
ON THE BALANCE OF CO<sub>2</sub> IN THE EARTH'S ATMOSPHERE**

**Bulatkin Gennady Alekcandrovich**

*Doctor of Biological Sciences, Lead Research Officer*

*Institute of Basic Biological Problems RAS*

抽象的。制定了原始方法，并开发了一种新的三阶段评估植物群落二氧化碳平衡的方法。在“管理”的森林中，在计算碳平衡时，不仅要考虑直接排放的二氧化碳，还要考虑铺设人工林、照料种植和最终使用砍伐的技术能源的间接成本。

作为一个模型，计算了用于种植白杨的天然和转基因形式的技术能源成本 *Populus tremula L.*。显示了技术能源间接成本在人工林中 C-CO<sub>2</sub> 平衡中的重要作用。大气中二氧化碳径流的最终量仅取决于森林面积及其生产力，还取决于木材的使用方式。

关键词：管理森林、可再生能源、巴黎气候协定、技术能源成本、*Populus tremula L.*、评估森林和木材使用对大气中二氧化碳平衡影响的方法。

**Abstract.** *An original methodology was formulated and a new three-stage method for assessing the CO<sub>2</sub> balance in plant communities was developed. In "managed" forests, when calculating the carbon balance, it is necessary to take into account the release of CO<sub>2</sub> not only at direct, but also at indirect costs of technical energy for laying plantations, caring for plantings, and felling for final use.*

*As a model, the costs of technical energy for the cultivation of natural and genetically modified forms of aspen *Populus tremula L.* are calculated. The large role of indirect costs of technical energy in the balance of C-CO<sub>2</sub> in forest plantations is shown. The final amount of CO<sub>2</sub> runoff from the atmosphere depends only on the area of forests and their productivity, but also on the way the wood is used.*

**Keywords:** *managed forests, renewable energy sources, Paris climate agreement, technical energy costs, *Populus tremula L.*, methodology for assessing the impact of forests and wood use on CO<sub>2</sub> balance in the atmosphere.*

According to the FAO (Global Assessment..., 2021), the world's forests store 662 billion tons of carbon, of which 44.5% is biomass, 10.3% is dead wood and litter, and 45.2% is in the soil. In the Paris Climate Agreement, forests play a major role in reducing CO<sub>2</sub> levels in the atmosphere. During the growing season,

managed forest stands absorb a huge amount of CO<sub>2</sub>, ten times greater than emissions due to direct and indirect costs of technical energy (Bulatkin, 2021). The generally accepted calculation of C-CO<sub>2</sub> fluxes in forests leads to the conclusion that with an increase in planting area and their productivity, the runoff of carbon dioxide from the atmosphere increases sharply. Based on this approach, country-by-country carbon balances are compiled and emissions trading is proposed. However, further, deeper consideration of the fate of wood in time leads to a different conclusion. The objective results of assessing the impact of tree plantations on CO<sub>2</sub> fluxes in the atmosphere largely depend on the duration of the analysis of natural and anthropogenic transformations of wood.

To calculate the CO<sub>2</sub> balance in the atmosphere during forest cultivation, we used the results of a model experiment on the creation of forest plantations based on aspen (*Populus tremula L.*), its natural and modified forms (Komarov et al., 2015). To assess the cost of technical energy in the experiment and the value of C-CO<sub>2</sub> flows, we analyzed all technological operations for growing, starting with the production of aspen seedlings in the nursery. The calculation of technical energy costs was made using the methods (Mindrin, 1997, Bulatkin, 2008).

The transgenic clone was created in the forest biotechnology laboratory of the Institute of Bioorganic Chemistry of the Russian Academy of Sciences and contains the sp-Xeg1b recombinant xyloglucanase gene from the fungus *Penicillium canescens*. According to experimental data, this clone is characterized by a complex modification of the plant phenotype: accelerated growth, changes in the ratio of leaf and root biomass to stem wood biomass (Schestibratov et al, 2011).

The model experiment was carried out by the authors on the example of the soil and climatic conditions of the north-west of the Leningrad Oblast. The growth of plantations with a short turnover of felling (30 years), established on the site of cut down spruce forests, was modeled.

In order to accelerate the growth of the forest stand and reduce the loss of soil fertility, nitrogen mineral fertilizers were applied in the experiment at a dose of 150 kg of active substance per 1 ha at planting, 10 years after planting and 5 years before the main felling.

The results of simulation experiments show that the use of 2 thinnings leads to an increase in the formation of economically valuable biomass up to 100–120 t/ha, compared to 70 t/ha in the scenario without thinnings. (Komarov et al., 2015). At the same time, on genetically modified plantations, an additional 16.3–22.6 t/ha of dry matter of woody biomass is obtained due to thinning on average for 2 plantation rotations.

Fertilizers proved to be a significant factor in increasing the productivity of all types of forest stands. Thus, the productivity with the application of nitrogen fertilizers for planting unmodified forms of aspen was 5% higher during the first

rotation of the plantation and 18% higher during the second rotation compared to the variants without fertilizers.

The use of a genetically modified clone of aspen with the introduction of nitrogen fertilizer significantly increases the productivity of plantations compared to its natural form. At the same time, the C-CO<sub>2</sub> sink in stem wood increased by 24.8%. The total runoff of C-CO<sub>2</sub> in the synthesized woody biomass in the fast-growing form of aspen increased by 14.2 t/ha or by 23.9%.

However, large direct and indirect investments of technical energy are associated with the use of nitrogen fertilizers. The total cost of technical energy in the variant with a transgenic clone and the introduction of ammonium nitrate amounted to 46.8 GJ/ha, including indirect energy costs due to fertilizers (for the production of fertilizers, delivery to the farm warehouse and application) - 45.2 GJ/ha, which is 85% of the total energy investment. Emissions of CO<sub>2</sub> into the atmosphere due to indirect costs of technical energy amounted to 3.4 t/ha of CO<sub>2</sub> and are estimated at 1.4% of the runoff with wood.

The table presents the results of the analysis of the influence of growing various forms of aspen on the emission and sink of CO<sub>2</sub> in plantations.

**Table.**

*C-CO<sub>2</sub> balance in plantations of natural and genetically modified forms of aspen Populus tremula L. (2nd rotation of the plantation)*

Unit of measurement	Aspen shapes		
	natural	natural with N fertilizers	genetically modified with N fertilizers
stem wood			
t/ha*	75,7	89,4	91,0
technical energy costs in wood production			
GJ/ha	9,4	55,2	55,2
C-CO <sub>2</sub> emissions from wood production			
t/ha from technical energy	0,22	1,2	1,2
t/ha from loss of soil humus	9,0	9,0	10,0
C-CO <sub>2</sub> sink in stem biomass			
t/ha	37,9	44,7	45,5
thinning wood			
t/ha*	12,3	14,4	19,3
C-CO <sub>2</sub> runoff in the wood of thinnings			

t/ha	6,2	7,2	9,7
total C-CO <sub>2</sub> emissions from wood production			
t/ha	9,22	10,2	11,2
stem wood and thinnings			
t/ha*	88,0	103,8	110,3
total C-CO <sub>2</sub> sink in woody biomass			
t/ha	44,1	51,9	55,2

\*according to Komarov et al. (2015)

After the establishment of model plantations, soil carbon reserves are significantly reduced (from 9 to 7 kg/m<sup>2</sup>). Such a sharp drop is observed mainly in the first 5-7 years. This is due to the intensive decomposition of forest litter accumulated in previous spruce plantings. During the second rotation of the plantation, the intensity of depletion of forest litter and the reduction of carbon stocks in soils decrease and the losses amount to about 1 kg/m<sup>2</sup> C for 30 years. Due to the loss of soil carbon, C-CO<sub>2</sub> is emitted into the atmosphere at the level of 10 t/ha.

Logging residues are an important source of carbon dioxide runoff from the atmosphere. However, the final effect largely depends on the further use of logging residues. Under production conditions, logging residues usually remain on the forest plot in heaps, in a short period of time they rot or are burned on the spot and carbon dioxide is completely returned to the atmosphere. However, it is energetically and environmentally expedient to use the entire biomass of logging residues for the production of fuel pellets, briquettes, etc. In this case, solar energy stored in biomass replaces fossil non-renewable energy and thus reduces the release of CO<sub>2</sub> into the atmosphere.

Aspen tree plantations with a short felling rotation (up to 30 years), taking into account the total (direct and indirect) costs of technical energy, are large net absorbers of atmospheric carbon dioxide. The content of C-CO<sub>2</sub> in commercial aspen wood fluctuated from 47.7 to 62.5 t/ha in the first rotation of the plantation and from 37.9 to 45.5 t/ha in the second. The total emissions of C-CO<sub>2</sub> from the use of technical energy in the cultivation of aspen amounted to no more than 1.2 t/ha.

Such calculations and conclusions drawn from them usually inspire great hope in researchers and international organizations for the decisive positive role of forests in the sink of carbon dioxide from the Earth's atmosphere and in reducing the greenhouse effect. However, if we trace the further fate of wood and its transformation during the time of use, the conclusions will not be so optimistic.

***A new three-stage methodology for assessing the impact of forests on the balance of CO<sub>2</sub> in the atmosphere.*** The objective results of assessing the impact of tree plantations on the CO<sub>2</sub> balance in the atmosphere largely depend on the

duration of the analysis of the natural and anthropogenic transformation of wood. We have developed a methodology and proposed a new three-stage method for calculating the C-CO<sub>2</sub> balance when growing forests and using wood. 1) Bio-ecenotic balance (for a period of 30–120 years of cultivation, depending on the forest-forming species and the period of felling for the main use), 2) natural and economic balance (for 170–200 years from the moment of forest renewal to the completion of the service of wooden structures), 3) biogeochemical C-CO<sub>2</sub> balance (associated with the cultivation of tree plantations and the use of wood and culminating in the entry of residual organic matter into the earth's crust, accumulative landscapes).

The mode of use of industrial wood is essential in the release of carbon dioxide into the atmosphere. The service life of buildings made of wood fluctuates slightly and averages about 50 years. After this period of time, buildings are usually dismantled, the remains of wood are either burned or partially used for a short time on the farm (figure). Thus, the positive impact of forest planting on reducing the concentration of carbon dioxide in the atmosphere when wood is used only in construction will not be significant due to the short period of operation of structures.

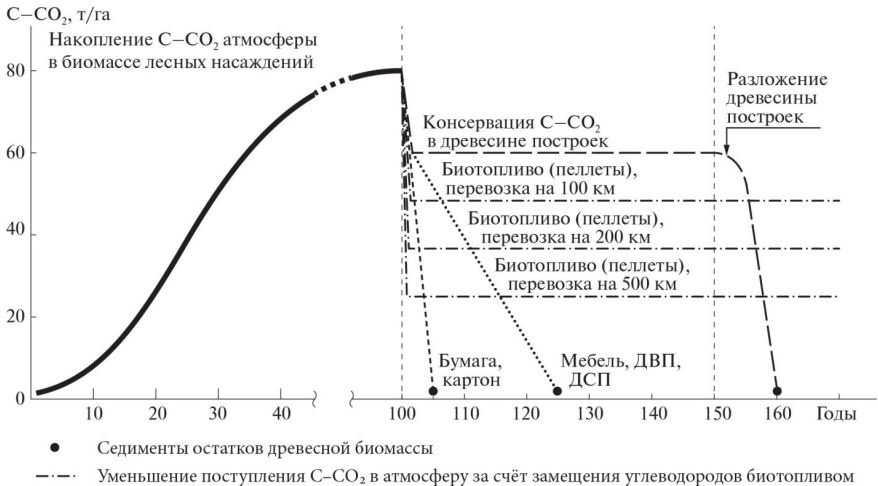


**Figure.** Scheme of a three-stage method for calculating the balance of C-CO<sub>2</sub> in the atmosphere when growing forests and using wood

Eventually, the former timber will rot and turn back into CO<sub>2</sub>. Part of the wood is used to make paper, cardboard, plywood, and furniture. However, these materials and products have a short life span. First of all, paper and cardboard are consumed. Furniture usually lasts no more than 25 years (figure).

Thus, the initial large carbon sink with industrial wood leads to a temporary (up to 150 years) removal of CO<sub>2</sub> from the atmosphere. During this period, various wood products are gradually destroyed, decomposed by microorganisms, and carbon dioxide absorbed by green plants re-enters the atmosphere.

The long-term cycle of C-CO<sub>2</sub> in the system atmosphere - green plants - industrial wood - man-made buildings - the atmosphere ends only with a small positive balance. It is known that only a small part - 0.8–1.0% of the organic matter synthesized by plants enters the large geological cycle, transforms and is preserved for millions of years (Kovda, 1973, Alpatiev, 1983).

The bulk of the buried dispersed organic matter is concentrated in the sediments of the continents and the oceanic vector (Bazilevich, 1979). Concentrated organic reserves of ancient biospheres are found in deposits of coal, hydrocarbon gases and oil. Their intensive extraction and use in the modern period leads to a sharp release of carbon dioxide into the atmosphere. However, *there is a highly effective way of using forest plantations to regulate the content of carbon dioxide in the atmosphere*, which is currently little paid attention.

This path is the use of part of the wood for energy production and the replacement of fossil hydrocarbons used by mankind.

Indeed, when wood is used for energy, biomass carbon burns out and also enters the atmosphere in the form of CO<sub>2</sub>. In this case, carbon dioxide does not replenish the pollutant pool. C-CO<sub>2</sub> simply recirculates in the atmosphere-green plants-wood-atmosphere system.

When processing plant biomass into a commercial energy carrier (for example, pellets), about 6.5 kg of CO<sub>2</sub> is emitted into the atmosphere per 1000 MJ of energy contained in the fuel (Bulatkin, 2018).

At the same time, it is important to take into account that the transportation of biofuel from wood over long distances significantly reduces its efficiency and increases C-CO<sub>2</sub> emissions into the atmosphere. Thus, the transportation of pellets by road for 200 km reduces the overall energy efficiency from 6 to 3, and carbon dioxide emissions increase by 10.8 kg per 1000 MJ of energy content in biofuels. When transporting 500 km, the energy efficiency drops to 1.7. The release of CO<sub>2</sub> into the atmosphere from transport reaches 17.6 kg per 1000 MJ (Bulatkin, 2018).

Thus, from the point of view of ecology, biofuels should be considered as a local source of energy, since transportation over considerable distances almost "none" its effect in the sink of CO<sub>2</sub> from the atmosphere.

The use of wood for the production of heat and electricity is currently growing at a rapid pace.

The work of M. Sidorova et al. (2019) shows that the global consumption of wood pellets by 2028 can reach 93 million tons, which in terms of calorific value corresponds to 10.7 million tons of oil equivalent. In Russia every year 9/10 of wood

waste remains in the forest and in landfills. Our country can increase the volume of wood biofuel production by 10 times if woodworking waste is included in the trade turnover, as well as logging residues, which are often simply left in the forest and burned at logging sites. According to analysts, Russia produces about 1.5 million tons of pellets per year (this figure has grown 2.5 times since 2013). At the same time, the volume of the domestic biofuel market is only 100–200 thousand tons.

In Russia, there are currently about 70-80 million hectares of unproductive and overgrown agricultural land suitable for forestry. Part of the area can also be used for growing such a new energy crop for Russia as Chinese miscanthus (*Miscanthus sinensis* Anders.). Areas not occupied by crops make up about one tenth of the total forest area of the country. If even on half of these areas a forest with a short felling rotation (about 30 years) is grown using fast-growing tree species, then with a total bioproductivity (trunks + thinning wood) of about 100 t/ha, 3500-4000 million tons of biomass can be obtained. In terms of 1 year, the productivity will be about 115-130 million tons. This amount of biomass corresponds to 2070-2340 million GJ per year of renewable energy. Taking into account the costs of growing forests, logging and production of biofuel in the form of pellets, the amount of *additional energy* will be 1656-1926 million GJ per year, which can replace about 38.8-45.1 million tons of hydrocarbon fuel in oil equivalent per year, or about 22- 26% of the annual oil consumption in the Russian Federation. As a result of replacing hydrocarbons with biofuels, CO<sub>2</sub> emissions into the atmosphere will be reduced by 122-142 million tons per year. The total emission of CO<sub>2</sub> equivalent is currently 1.6 billion tons per year (Strategy of social and economic development..., 2021).

In Russia, artificial reforestation is beginning to increasingly prevail over natural. The number of forest nurseries producing planting material with a closed root system is increasing every year. However, there are a number of problems. No nursery produces planting material for fast-growing softwoods. Forest development projects at the leased bases of timber industry enterprises provide for the restoration of clearings only with coniferous, in rare cases, hardwood species, even if softwood trees were harvested in this clearing (Grigoriev et al., 2019). The planting of energy forests in Russia is associated with the development of a nursery system, and the production of fuel pellets is associated with the construction of processing plants. But, most importantly, there is a need for comprehensive propaganda among the population, industrialists and entrepreneurs of the idea of widespread use of a type of fuel that is practically new for our country. It also requires the development, discussion by region and approval of the Federal Program for the cultivation of energy forests, as a new and highly efficient source of renewable energy and the most important mechanism for the sink of CO<sub>2</sub> from the Earth's atmosphere by replacing hydrocarbon fuels.

## References

1. Alpatiev A.M. *Development, transformation and protection of the natural environment*. L.: Science. 1983. 239 P.
2. Bulatkin G.A. *Ecological and energy bases for optimizing the productivity of agroecosystems*. Moscow: NIA-Science. 2008. 366 P.
3. Bulatkin G.A. *Study of the effectiveness of energy crops on the example of miscanthus sinensis (Miscanthus sinensis Anderss.)*. Ecological and economic problems // *Ecological Bulletin of Russia*. 2018. №10. P. 36-41.
4. Bulatkin G.A. *Assessment of the impact of managed forests on the balance of carbon dioxide in the Earth's atmosphere* // *Life of the Earth*. 2021. №1. V. 43. P. 54-66.
5. *Global Forest Resources Assessment 2020. Main report*. FAO: Rome, Italy. 2021. 184 P.
6. Grigoriev I., Kunitskaya O., Davtyan A. *Energy forest plantations* // *Forest industry*. №9 (137). 2019. P. 24-29.
7. Kovda V.A. *Fundamentals of the doctrine of soils. Book I*. M.: Science. 1973. 447 P.
8. Komarov A.S., Chertov O.G., Bykhovets S.S., Pripulina I.V., Shanin V.N., Vidyagina E.O., Lebedev V.G., Shestibratov K.A. *Influence of aspen plantations with a short turnover felling on the biological cycle of carbon and nitrogen in the forests of the boreal zone: a model experiment* // *Mathematical biology and bioinformatics*. 2015. № 10. P. 398–415.
9. Mindrin A.S. *Energy-economic evaluation of agricultural products*. Diss. dr. econ. sci. M., 1997. 291 P.
10. Sidorova M., Gorchilina K. *Demand for pellets will grow three times* // *Forest Industry*. 2019. № 9 (137). P. 17-23.
11. *Strategy for socio-economic development of the Russian Federation with low greenhouse gas emissions until 2050* <http://static.government.ru/media/files/Shestibratov R., Lebedev V., Podrezkov A, Salmova M. Transgenic aspen and birch trees for Russian plantation forests // BMC. Proceedings. 2011. V. 5. Suppl. 7. P. 124>.

DOI 10.34660/INF.2022.17.46.143

Fe(III) 还原和甲烷产生：北极土壤中的两个主要厌氧微生物过程  
**FE(III) REDUCTION AND METHANE PRODUCTION: TWO MAJOR  
ANAEROBIC MICROBIAL PROCESSES IN ARCTIC SOILS**

**Zakharyuk Anastasiya Gennadevna**

*Candidate of Biological Sciences, Research Officer*

**Zinoveva Olga Victorovna**

*Undergraduate*

**Shcherbakova Viktoriya Arturovna**

*Doctor of Biological Sciences, Laboratory Head,*

*Pushchino Scientific Center for Biological Research RAS*

抽象的。从距离拉普捷夫海南部不远的西西伯利亚低地地区采集的土壤样本中，首次获得了嗜冷和耐冷细菌的富集培养物，在 6–15 °C 的温度下还原三价铁。在获得的铁还原细菌 (IRB) 的富集培养物中，有 60% 记录了甲烷的形成。已确定还原铁的量、含铁矿物的形式和所研究的富集培养物中形成的生物甲烷浓度之间的关系。结果表明，培养温度对铁还原和产甲烷过程的活性没有显著影响。

关键词：苔原土壤，铁还原，产甲烷，北极。

**Abstract.** *From soil samples taken in the region of the West Siberian Lowland, not far from the southern part of the Laptev Sea, enrichment cultures of psychrophilic and psychrotolerant bacteria were obtained for the first time, reducing ferric iron at temperatures of 6–15 °C. In 60% of the obtained enrichment cultures of iron-reducing bacteria (IRB), the formation of methane was recorded. A relationship has been established between the amount of reduced iron, the form of the iron-containing mineral, and the concentration of biogenic methane formed in the studied enrichment cultures. It was shown that the incubation temperature had no significant effect on the activity of iron reduction and methanogenesis processes.*

**Keywords:** *tundra soil, iron reduction, methanogenesis, Arctic.*

Temperature is one of the most important environmental factors affecting microorganisms. Constantly cold ecosystems are quite widespread on Earth. In addition to the cold, many of these ecosystems are characterized by little or no oxygen. Low-temperature ecosystems have a great influence on the formation of the Earth's climate and are an indicator of its state.

Iron(III) is a common and one of the main electron acceptors in anaerobic ecosystems [1, 2]. According to the literature data, from 40 to 90% of bacteria and archaea in anaerobic microbial communities are able to oxidize organic matter, while reducing various Fe(III) minerals [3]. A number of works have been published showing that the reduction of Fe(III) in the Arctic deposits plays the main role at the terminal stages of organic carbon oxidation under anaerobic conditions [4, 5]. It has been established that microbial processes of iron reduction can create favorable redox conditions for the development of the methanogenic archaea community, thereby stimulating the biogenic process of methane formation [6–8]. Methane, as one of the greenhouse gases, plays an important climate-forming role. The intensity of many natural sources of methane, such as degradation of bottom permafrost [9] or methane hydrates [10], depends on temperature [11]. The temperature of the air and the underlying surface in the Arctic is growing over the years twice as fast as the average for the globe [12]. The role of methane positive feedback in the anomalous warming of the Arctic cannot be ruled out either in the present or even in the future.

The aim of this work was to determine the processes of microbial iron reduction and methanogenesis in enrichment cultures obtained from soil samples taken in various parts of the Russian Arctic.

**Materials and methods of research**

**Sampling and description of samples.** We used samples of tundra soil from two sections provided by the Soil Cryology Laboratory of the Institute of Physico-chemical and Biological Problems of Soil Science, Russian Academy of Sciences (IPCaBP RAS). Samples were taken in the areas of Mamontova Khayata (horizons: BG; above/permafrost; in/permafrost) and Ivashkina Lagoon (horizons: TG; G2; GC<sub>3</sub>m), located on Buor-Khaya Bay, in the southern part of the Laptev Sea, to the southeast from the delta of the Lena River (tab. 1).

*Table 1.  
Description of soil samples*

District	Section name	Horizon
Mammoth Hyatt	p. 139-19	BG
		above/permafrost
		in/permafrost (2-4 cm)
Ivashkina lagoon	p. 149-19	TG
		G2
		GC <sub>3</sub> m

**Conditions for the cultivation of microorganisms.** To obtain IRB enrichment cultures and their further study, 1 g of soil was added to 60 ml of the medium. The modified medium of composition (g/l) was used: NaCl – 1;  $MgCl_2 \times 6H_2O$  – 0,2;  $NaHCO_3$  – 2,5;  $KH_2PO_4$  – 0,68;  $CaCl_2 \times 2H_2O$  – 0,1;  $NH_4Cl$  – 1; yeast extract (Difco) – 0.002; microelement solution [13] – 1.0 ml; vitamin solution [14] – 10.0 ml. A mixture of sodium formate and sodium acetate at a final concentration of 20 mM was used as a carbon source and electron donors. The following (mM) Fe(III) citrate and insoluble iron oxide (analogous to natural ferrihydrite) in the form of amorphous iron oxide hydroxide (AIOH) – 10 were introduced as terminal electron acceptors (mM). The preparation of the mineral medium and the cultivation of microorganisms were carried out under strictly anaerobic conditions under  $N_2$  (100% in the gas phase). Medium pH 7.0-7.2. Incubated in the dark at 6 °C and 15 °C for 30 days. Mineral medium without inoculation was used as a chemical control.

To assess the content of methanogenic archaea in the microbial community, IRB enrichment cultures were subcultured into the above mineral medium without the addition of ferric iron. Methanol was added as a substrate (final concentration 20 mM), and cysteine-HCl +  $Na_2S$  (0.25 g/l) was used as a reducing agent. All inoculations were sterilely blown with a mixture of  $H_2/CO_2$  (4:1) to a pressure of 1 atm and CoM was added at a rate of 0.7 g/l and vancomycin at a rate of 150 mg/l. medium pH 6.8. Incubated in the dark at temperatures of 6 and 15 °C for 30 days.

### **Morphology**

Living cells were examined using an Axiostar PLUS light microscope ("Carl Zeiss", Germany) with phase contrast at a magnification of 1000x.

### **Analytical methods**

The reduction of Fe(III) was evaluated by the colorimetric method by the formation of a stable colored complex of ferrous iron with ferrozine (Viollier et al., 2000). The methane content in the gas phase was measured on a Pye Unicam 304 gas chromatograph (Great Britain) with a flame ionization detector. A glass column (length 1 m, inner diameter 2 mm) filled with Parapak Q, 80-100 mesh (Fluka, Germany) was used for the determination. The temperatures of the column, injector, and detector were 90, 150, and 180 °C, respectively. The carrier gas was nitrogen at a flow rate of 20 ml/min.

### **Results and discussion**

From different horizons of tundra soils, we obtained twenty-four enrichment cultures of bacteria capable of reducing soluble and insoluble Fe(III) compounds with formate and acetate as a carbon source and electron donor at cultivation temperatures of 6 and 15 °C. After 30 days at an incubation temperature of 15 °C, the content of Fe(II) ions in enrichment cultures varied from 0.2 to 15 mM. The maximum amount of Fe(II) was recorded in the **r/m** enrichment culture obtained

from a sample taken in the permafrost of section 139-19 and grown with AIOH as an electron acceptor (fig. 1, 2). The amount of reduced iron at 6 °C in enrichment cultures ranged from 0.3 to 10 mM. The maximum value of Fe(II) was observed in the TG enrichment culture obtained from a sample from the upper horizon of section 149-19 in the area of Ivashkina Lagoon grown with Fe(III) citrate (fig. 1, 2).

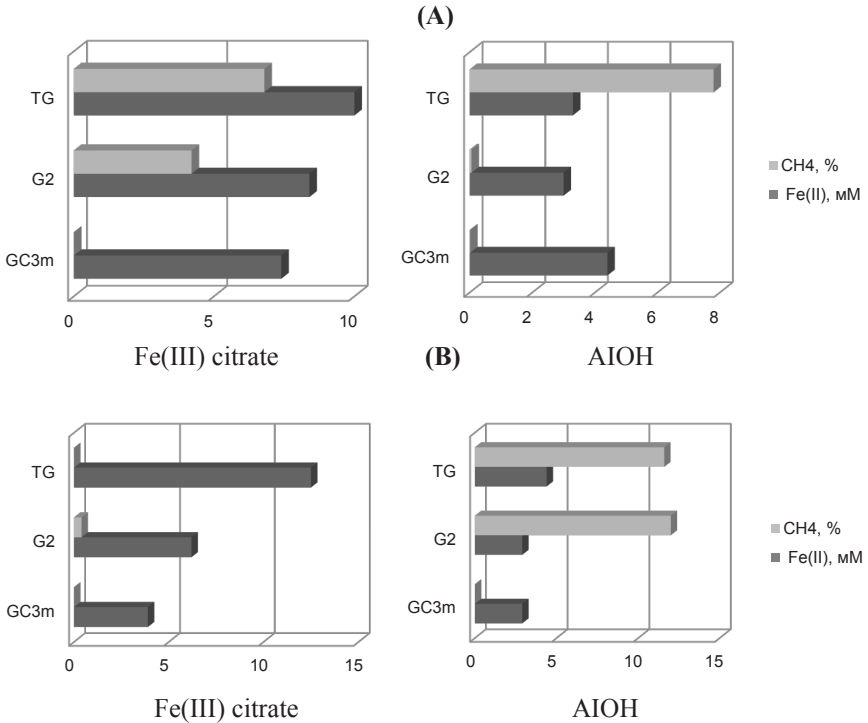


**Figure 1.** Formation of Fe(II) and methane in enrichment cultures obtained from samples of section 149-19 in the area of Ivashkina Lagoon (section 149-19) A) 6 °C; B) 15 °C

In all IRB enrichment cultures, the process of methane formation was studied. On the thirtieth day of cultivation, the maximum amounts of methane (11.6–12% CH<sub>4</sub>) were found in enrichment cultures obtained from the upper soil horizons of section 149–19 in the area of the Ivashkina lagoon. Fe(III) in the form of an insoluble oxide was used as an electron acceptor. Analysis of enrichment crops, which were obtained from soil samples of Mammoth Hayat, showed a weak process of methane formation. The largest amount of methane (10% CH<sub>4</sub>) was found

in the **n/m** enrichment culture taken from the subsurface horizon. In enrichment cultures, which were obtained from samples taken in permafrost (2–4 cm), at all temperature options and with different forms of Fe(III), the process of formation of biogenic methane was not recorded (fig. 2).

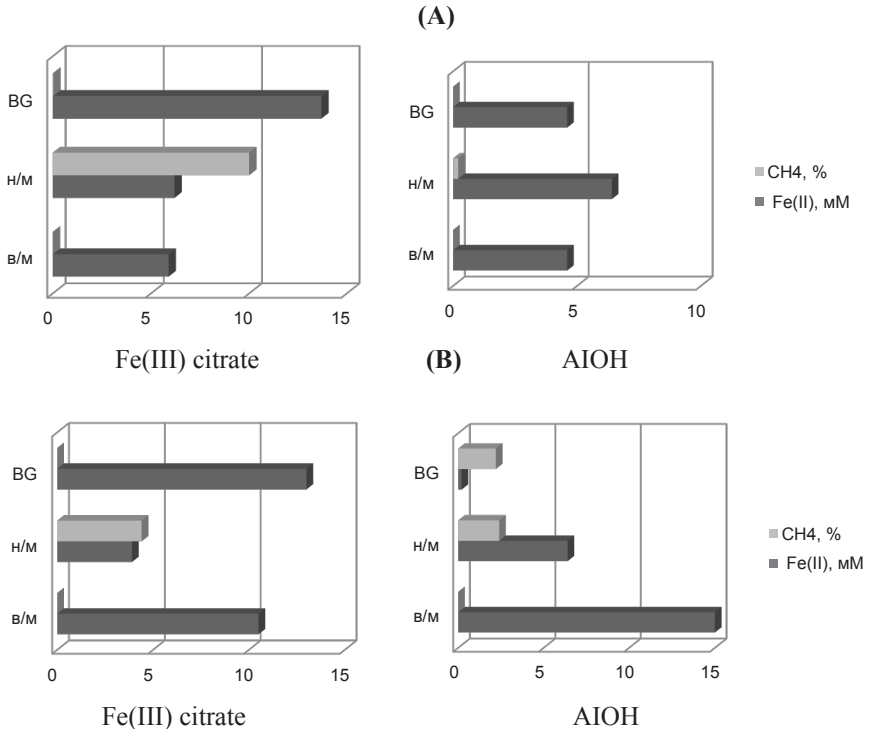


**Figure 2.** Formation of Fe(II) and methane in enrichment cultures obtained from samples of section 139-19 in the area of Mamontova Khayata (section 139-19) A) 6 °C; B) 15 °C

As a result of microscopic studies of the obtained IRB enrichment cultures, several morphotypes of bacterial cells were found. In each of the examined samples, there were movable and immobile rods of different sizes. Microscopy of **TG**, **BG**, and **r/m** enrichment cultures revealed cells with spores.

Thus, the data obtained indicate that in extremely cold habitats with a constantly low temperature, the microbial community is actively functioning, which carries out two key terminal anaerobic processes — Fe(III) reduction and methane formation. In the course of the work, enrichment cultures of psychrophilic and psychrotolerant microorganisms were obtained, in which, in addition to iron

reduction, there was a process of methanogenesis. At the same time, both competition and cooperation of different groups of prokaryotes were possible. In enrichment crops obtained from soils that were formed under the influence of the sea (section 149-19), the process of methane formation was actively going on. A relationship was established between the amount of reduced iron, the form of the iron-bearing mineral, and the concentration of biogenic methane. The maximum amounts of CH<sub>4</sub> were found in IRB enrichment cultures, in which Fe(III) in the form of insoluble oxides was used as an electron acceptor. In nature, iron reducers, as a rule, often use soluble Fe(III) compounds as an electron acceptor. In enrichment cultures grown with Fe(III) citrate as an electron acceptor, microbial iron reduction inhibited methanogenesis. The studies performed showed that the incubation temperature had no significant effect on the activity of Fe(III) reduction processes and methane formation.

Further study and description of the processes associated with the reduction of ferric iron will make it possible to evaluate the contribution of IRB to the biogenic process of methane formation.

The work was supported by the RSF project № 22-24-00518.

### References

1. Lovley D.R. *Dissimilatory Fe(III) and Mn(IV) reduction* // *Microbiol. Rev.* 1991. V. 55. P. 259-287.
2. Thamdrup V. *Bacterial Manganese and Iron Reduction in Aquatic Sediments* // *Advances in microbial ecology.* 2000. V.16. P. 41-84.
3. Lovley D.R., Holmes D.E., Nevin K.P. *Dissimilatory Fe(III) and Mn(IV) reduction* // *Advances in Microbial Physiology.* 2004. P. 49. P. 219-286.
4. Kostka J.E., Thamdrup Bo, Glud R.N., Canfield D. *Rates and pathways of carbon oxidation in permanently cold Arctic sediments* // *Marine Ecology-Progress Series.* 1999. V. 180. P. 7-21.
5. Glud R.N., Risgaard-Petersen N., Thamdrup Bo, Fossing H., Risgaard S. *Benthic carbon mineralization in a high-Arctic sount (Young Sound, NE Greenland)* // *Marine Ecology- Progress Series.* 2000. V. 206. P. 59-71.
6. Rivkina E.M., Fedorov-Davydov D.G., Zakharyuk A.G., Shcherbakova V.A., Vishnivetskaya T.A. *Free iron and iron-reducing microorganisms in soils and permafrost deposits of northeastern Siberia* // *Soil Science.* 2020; N 10. P 1247-1261.

7. Nozhevnikova A.N., Russkova Yu.I., Litti Yu.V., Parshina S.N., Zhuravleva E.A., Nikitina A.A. *Syntrophy and interspecific electron transfer in methanogenic microbial communities* // *Microbiology* 2020; V.89, N 2. P131-151.

8. Barua S., Dhar B.R. *Advances towards understanding and engineering direct interspecies electron transfer in anaerobic digestion* // *Bioresour. Technol.* 2017; V. 244. P 698–707.

9. Kosmach D.A., Sergienko V.I., Dudarev O.V., Kurylenko A.V., Gustaffson O., Semiletov I.P., Shakhova N.E. *Methane in the surface waters of the marginal seas of Northern Eurasia* // *DAS*. 2015. V. 465. № 4. P. 441–445.

10. Obzhirov A.I. *Geology and methods of searching for gas hydrates* // *Bulletin of the Engineering School of the FEFU*. 2012. № 1 (10). 90–94.

11. Anisimov O.A., Lavrov S.A., Reneva S.A. *Emission of methane from permafrost bogs of Russia under conditions of climate change* // *Problemy ekologich. modeling and monitoring of ecosystems*. Ed. Yu.A. Israel. St. Petersburg: Gidrometeoizdat, 2005. P. 124–142.

12. Walsh J.E., Kattsov V.M., Chapman W.L., Govorkova V., Pavlova T. *Comparison of Arctic climate simulations by uncoupled and coupled global models* // *Journal of Climate*. 2002. Vol. 15. P. 1429–1446.

13. Slobodkin, A.I. and Wiegel, J., *Fe(III) as an electron acceptor for H<sub>2</sub> oxidation in thermophilic anaerobic enrichment cultures from geothermal areas, Extremophiles*, 1997, Vol. 1, P. 106–109.

14. Wolin, E.A., Wolin, M.J., and Wolfe R.S., *Formation of methane by bacterial extracts, J. Biol. Chem.*, 1963, Vol. 238, P. 2882–2886.

牛饲料混合物  
**FEED MIXTURE FOR CATTLE**

**Sainova Gaukhar Askerovna**

*Doctor of Technical Sciences, Biology PhD*

**Yessenbayeva Zhanar Zhenisovna**

*Doctoral Candidate PhD*

**Akbasova Amankul Dzhakanovna**

*Doctor of Technical Sciences, Full Professor*

*Akhmet Yassawi International Kazakh-Turkish University*

抽象的。本文讨论了获得和使用新饲料混合物的方法的实验研究结果，该混合物可用作独立饲料和传统动物饲料的添加剂。对小牛进行了研究，这些牛在摊位内容中。主要任务是用具有生物活性的饲料混合物代替用于预防和治疗动物的合成抗生素。开发的进料混合物具有以下以重量计的平均组成。 %：红加州蠕虫生物量 (3.0)、膨润土 (1.5)、谷物混合物 (49.5)、药用植物山羊芸香 (29.5)、腐植酸钙 (1.5)，其余为粗粉和饼的混合物 (质量1:1比) 棉籽油产量。

由于主要必需和非必需氨基酸、维生素和易消化碳水化合物化合物的含量，开发的饲料混合物具有很高的营养价值，改善了适口性，微量和大量元素，这使得增加自然抵抗力，提高动物生产力成为可能并降低每单位增长的成本。

关键词：饲料添加剂，牛，动物生产力。

**Abstract.** *The article discusses the results of experimental studies on methods for obtaining and using a new feed mixture, which can be used as an independent feed and as an additive to traditional animal feed. Studies were carried out with young cattle, which are in the stall content. The main task was to replace synthetic antibiotics used for the prevention and treatment of animals with a biologically active feed mixture. The developed feed mixture has the following average composition in wt. %: biomass of red California worms (3.0), bentonite (1.5), grain mixture (49.5), medicinal plant goat's rue (29.5), calcium humate (1.5), the rest is a mixture of meal and cake (mass 1:1 ratio) of cottonseed oil production.*

*The developed feed mixture has a high nutritional value due to the content of the main essential and non-essential amino acids, vitamins and easily digestible carbohydrates, improved palatability, micro- and macroelements, which make it possible to increase natural resistance, increase animal productivity and reduce costs per unit of growth.*

**Keywords:** *feed additive, cattle, animal productivity.*

### **Introduction**

In modern agricultural production, there is a need for the livestock industry to improve the quality of feed and increase the forage base. There is currently an emerging interest in finding new feed additives with a high nutrient content. Protein occupies a special place among feed nutrients [1–2]. Crude protein consists of protein and amides. The role of proteins in animal nutrition is to provide the body with a set of amino acids necessary to build body proteins, milk, wool and other products. Amino acids make it possible to increase the digestibility of feed and thereby achieve high weight gain [3-4]. In practice, to regulate the metabolic processes in their organisms, namely, to meet the needs for proteins, vitamins, minerals, to suppress the activity of certain groups of microbes, stimulate growth and development, feed additives of various nature and composition are introduced into the diets of natural animal feed [5- 6].

In defiance of existing prohibitions, many farms, in order to maintain livestock and stimulate animal growth, introduce certain amounts of antibiotics into feed or feed additives. As a result of the use of antibiotics in animal husbandry, there is a danger of the emergence of resistant forms of pathogenic microorganisms in the environment and a decrease in the therapeutic effect of many antibiotic substances in case of human disease [7-8]. In this regard, the use of feed additives without antibiotics and other synthetic substances is of particular interest.

By optimizing the structure of the diet of animals, it is possible to obtain high-quality, cost-effective, competitive and in-demand products. Domestic and foreign experience in the use of feed additives shows that the most rational for achieving high results is the use of non-traditional feed additives containing mixtures of organic and mineral substances of natural origin [9-10].

The purpose of this work is to develop a new feed additive composition for fattening young cattle, which allows optimizing the diet in terms of energy and protein, macro- and microelements, vitamins and biologically active substances.

### **Objects and methods of research.**

The choice of each component for the composition of the proposed feed additive (FA) is based on their known chemical and biological properties. For example, goat's rue is a valuable fodder crop containing a lot of protein, essential and essential amino acids, phosphorus, potassium, fiber, and an abundance of vitamins [11]. The biomass of red California worms contains about 18 amino acids, including aspartic acid, threonine, serine (alpha-amino-beta-hydroxypropionic acid), glutamic acid, pyrrolidine-alpha-carboxylic acid, glycine, alanine, cysteine, valine, methionine, isoleucine, leucine, tyrosine: tryptophan, lysine, gitidine. It consists of essential fatty acids - 5.9%, essential and non-essential amino acids - 59.8%,

enzymes, vitamins, carbohydrates, a wide range of macro- and microelements of the following composition (in terms of dry matter) in mg / kg: iodine –  $0.8 \pm 0.11$ ; calcium -  $1.4 \pm 0.2$ ; potassium -  $0.3 \pm 0.1$ ; phosphorus -  $0.5 \pm 0.2$ ; nitrogen -  $0.9 \pm 0.05$ ; selenium -  $0.1 \pm 0.02$ ; iron -  $1055 \pm 30.5$ ; zinc -  $227.6 \pm 13.3$ ; copper -  $12.9 \pm 1.8$ ; manganese -  $13.7 \pm 2.8$ , which contributes to an increase in carbohydrate, lipid, vitamin nutrition. The high-protein biomass of red Californian worms is characterized by a curative property against many diseases and it has a positive effect on all vital systems of the body [12-13].

Bentonite provides animals with macro- and microelements, just as the sorbent in the gastrointestinal tract absorbs pathogenic microorganisms and toxins, allowing better use of the nutrients and minerals of the main diet [14].

Meal and cake of oilseed production allows to lengthen the period of effective action of the drug. The meal has a strong and long-lasting aroma of sunflower seeds. It is a valuable high-protein feed product [15].

Calcium humate provides the body with calcium, to a certain extent replaces antibiotics, improves immunity.

The grain mixture has a high energy nutritional value (1.0-1.34 feed units per 1 kg of feed), extruded grain is characterized by high digestibility ( $\geq 95\%$ ), is characterized by a high content of phosphorus, vitamins B and E.

To conduct production tests from young animals (16-18 months), 4 groups (1 control and 3 experimental) were formed taking into account age, fatness and physiological state, 5 animals each, weighing 363-389 kg. The experiments were carried out against the background of balanced feeding of animals according to diets developed on the farm, taking into account the norms of feeding cattle. The main feed was supplemented with a feed additive of the following composition: 3.0% dry biomass of California red worms, 1.5% calcium humates, 1.5% bentonite, 49.5% grain mixture, 29.5% goat's rue medicinal plant, the rest is a mixture sunflower cake and meal (1:1). During the day, with three meals a day, young animals additionally received from 0.1 to 0.4 g of feed additive. Before feeding, they were regularly given 3 times clean water with a total volume of 40-45 liters. In general, fattening lasted 2 months (November-December) before the slaughter of animals. The absolute (kg/day) and relative (%) increase in live weight, the yield of meat products were determined using widely known calculation methods in practice [16]. Blood sampling was carried out before feeding from the jugular vein according to a method known in hematology [17].

### **Results and discussion**

When conducting research to control the physiological state of animals, the hematological composition of blood taken from young cattle of the experimental and control groups was studied. The content of hemoglobin, erythrocytes, leukocytes and platelets in the blood of animals was determined.

As a result of biochemical studies of the blood of young cattle from the experimental and control groups, an increase in hemoglobin content in the experimental groups by 10.5 g/l (group 1), 17.3 g/l (group 2) and 19.2 g/l (group 3), respectively, compared with the control.

Platelets take an active part in blood coagulation and non-specific protective reactions of the body. In our test, at the final stage, the formed elements vary from 600.1 to 493.0 x 10<sup>9</sup>/l, in percentage terms, the difference in the number of platelets is 4.9-7.1% in the experimental groups compared to the control group. This proves the predominant trend towards an increase in the assimilation of nutritional components in the experimental groups, especially micro-ingredients of inorganic form.

As can be seen from the results of hematological blood tests of the animals participating in the experiments, an increase in indicators was revealed - erythrocytes, hemoglobin, leukocytes, which indicates the activation of cellular immunity, indicates the correct metabolism as a result of receiving good nutrition.

Table 1 presents the results obtained in the study of the chemical composition and calorie content of the meat of the control and three experimental groups, in the diet of which additionally introduced feed additives (FA).

**Table 1.**  
*Chemical composition of beef meat, %*

Indicator	Groups			
	Control, %	Test with FA, %		
		0.1	0.2	0.4
Moisture	70.33±2.23	69.98±2.10	68.50±2.01	70.12±2.14
Protein	17.62±0.75	18.07±0.69	18.80±0.71	19.02±0.83
Fat	10.02±0.13	10.69±0.12	11.65±0.10	11.03±0.09
Ash	1.93±0.02	1.56±0.02	1.00±0.02	1.38±0.01
Energy per 100 g of meat, kilocal (loin + breast part = 1:1)	288.25	332.12	389.03	390.20

Tab. 1 shows an increase in protein and fat in the meat of the experimental groups compared to the control group, while the content of both protein and fat increases with an increase in the concentration of the feed additive in the feed.

From the results of studies on the effect of feed additives on animal body weight gain, it follows that the proposed ratio of components normalizes micro-biocenosis, increases feed digestibility by activating the gastrointestinal tract, and improves protein-carbohydrate metabolism (table 2).

Based on the analysis of the results of experimental studies, it can be noted that feeding the young animals of the experimental groups with a protein-vitamin-

mineral feed additive helps to improve the biochemical parameters of the blood and increase the gain in live weight.

**Table 2.**  
*Effect of feed additive on live weight gain of young cattle*

<b>The mass of young animals by the end of the experimental period (after 60 days)</b>				
<b>Indicator</b>	<b>Group I (FA – 0.1kg)</b>	<b>Group II (FA – 0.2kg)</b>	<b>Group III (FA – 0.4kg)</b>	<b>Control group</b>
Average live weight of young animals, kg: at the start of the test	363.7±2.99	376.0±3.31	367.5±3.02	388.5±4.10
at the end of the test	481.5±3.05	498.4±2.08	497.2±3.55	469.8±2.83
Absolute gain, kg	117.8±3.02	122.4±2.70	129.7±3.29	81.3±3.46
Average daily gain, g	1963±53	2040±45	2161±55	1355±58

The total average live weight of 1 animal of the experimental group, fattened with the use of a feed additive, was ~ 492 kg. The weight of the obtained meat after slaughter, including internal fat, liver, kidneys, heart and other entrails, weighed 305 kg, which corresponded to a slaughter yield of 62.0%. The slaughter yield for young cattle of the control group, which received feed without a feed additive, did not exceed 55.4%.

### **Conclusions**

On the basis of experimental studies, the effectiveness of including a feed additive in the basic diet of horses containing, along with a complex of vitamins and minerals, a goat's rue plant and biomass of red Californian worms, which are characterized by a number of medicinal properties, has been established. The biochemical parameters of the blood of all experimental animals were within the normative parameters.

The feed additive contributed to an increase in the average slaughter yield up to 62.0%. The meat of young cattle of all experimental groups had a very tasty, strongly pronounced aromatic smell, with a delicate texture and abundant juiciness.

The technical and economic advantages of the proposed feed additive for animal husbandry is to eliminate disturbances in the metabolic processes of the animal body and maintain the normal functioning of the digestive, musculoskeletal, immune systems of the body and increase the body's resistance to the adverse effects of anthropogenic and other factors.

The proposed mixture allows you to expand the range of feed additives that increase the live weight gain of farm animals.

## References

1. Krasnova O.A. *Increasing milk and meat productivity of cattle using biologically active substances: diss. ... dr. agr. sci.* – Izhevsk, 2017. – 212 P.
2. Vinogradov V.N., Duborezov V.M., Kirilov M.P. *Feeding and fodder production in dairy cattle breeding // Achievements of science and technology of the agro-industrial complex.* - 2009. - №8. – P.33-35.
3. Kislyuk S.M. *Classification of feed additives from the point of view of the manufacturer and consumer // Anniversary collection for the tenth anniversary of the "Vitargos-Rossovit" company.* - 2009. – P. 30-31.
4. Mukhina N.V. *Feed and biologically active feed additives for animals.* – M.: KolosS., 2008. – 271 P.
5. RF patent № 2467590, publ. 27.11.2012 Bull. № 33. *Feed additive for farm animals and birds.* /Kalinikhin V.V., Efimova L.V., Lopatina E.V., Kalinikhin E.V.
6. RF patents №2295253. *Feed mixture for farm animals and poultry.* /Authors: Kuznetsov B.B., Akseonov A.V., Kozintsev A.L., Ulanova R.V. Publ.: 20.03.2007.
7. Pervov N.G. *The use of antibiotics in the cultivation and fattening of young cattle: diss. ... dr. agr. sci.* - M., 1983. – 314 P.
8. Kalnitskaya O.I. *Veterinary and sanitary control of residual amounts of antibiotics in raw materials and products of animal origin: diss. ... dr. vet. sci.* – M., 2008. - 343 P.
9. Russian patent №2470521. *Method for the production of protein-vitamin fodder flour from a hybrid of red Californian worm and vermicomposted apple pomace.* /Authors: Irikov O.V. and Zabudsky Yu.I. Publ. 27.12.2012.
10. Russian patent for the invention № 2131677. *Feed additive "Biovitos"/* Loshkarev G.L., Spiridonov V.E., Troshin N.A.
11. Khaziakhmetov F.S., Gadiev R.R. *Oriental goat's rue in the diets of pigs: monograph.* Ufa, BSAU. 2008. -192 P.
12. Akbasova A.D., Isakov O.A., Sainova G.A. *Ecologization of agriculture through the rational use of vermi products and biological products based on:/ monograph/.* – Almaty: "Nurly Alem", 2015. – 176 P.
13. Sainova G., Akbasova A.Zh., Isakov O.A. *Vermitechnology onimderinin bolashagy: /monograph/ - Almaty: "Nurly Alem", 2017№ - 232 b.*
14. Yapparov A.Kh. *The use of natural bentonites of the Tarn-Var and Biklyan deposits of the Republic of Tatarstan for the correction of metabolism in replacement heifers / A.Kh. Yapparov, A.M. Ezhkova, R.N. Fayzrakhmanov // Coll. rep. All-Russian Scientific Conference of the Tatar SRI ACP.* – Kazan, 2008. – P. 155-160.
15. USSR patent №608518. *The method of obtaining feed from the waste of cotton ginning plants.* /Authors: Shadiev K.Sh., Sharasulov N.S., Popov B.N. Publ.: 30.05.1978.

16. Kim G.L., Adylkanova Sh.R., Sadykulov T.S. *Workshop on animal husbandry: textbook.* – Almaty: Kaz SAU, 2007. -154P.

17. Khazipov N.N., Garipov T.V. *Physiological characteristics and morphological composition of blood in beef cattle in the Republic of Tatarstan.* // Magazine: *Sci. notes of Kazan State Academy of Veterinary Medicine named after N.E. Bauman*, 2011. – iss. 2. - V. 206. – P.240-246.

DOI 10.34660/INF.2022.77.76.145

提供光电子器件表面的热态  
**ENSURING THE THERMAL REGIME OF THE HEAT-RELEASING  
SURFACE OF AN ELECTRO-OPTIC DEVICE**

**Rabzhirov Bazarzhab Punsukovich**

*Master's degree student*

**Minkin Dmitrii Alekseevich**

*Candidate of Technical Sciences, Associate Professor*

*Saint-Petersburg University of State Fire Service of EMERCOM of  
Russia*

抽象的。由于局部对流传热强度的变化，提出了一种确保散热表面等温条件的方法。

关键词：对流传热系数，温度场，传热强化，平面通道。

**Abstract.** *A method is proposed to ensure isothermal conditions on the heat-emitting surface due to the variable intensity of local convective heat transfer.*

**Keywords:** *coefficient of convective heat transfer, temperature field, heat transfer intensification, flat channel.*

### **Introduction**

Obtaining objective information about the number of natural fires and their areas, the dynamics of fire development, areas of smoke is important for managing the extinguishing process, determining evacuation routes for the population and providing assistance to the victims. In the practice of the fire service, satellite systems equipped with remote monitoring equipment are successfully used for these purposes. Such systems make it possible to assess the fire situation throughout Russia and register outbreaks already at the initial stage of ignition, which makes it possible to quickly suppress them.

Satellite systems in outer space are exposed to many factors, including extremely low temperatures and solar radiation, which can lead to unstable operation of key equipment elements or their failure. In this regard, to ensure the normal functioning of such systems, satellites are equipped with a thermal control system (TCS).

### **The design of the heat exchanger**

At the stage of designing and developing TCS, it is necessary to know the power of heat release on the satellite surfaces, where it is supposed to place the

TCS elements. Since the satellite is a multicomponent system consisting of heterogeneous elements, the estimation of the heat release rate is carried out experimentally in the course of ground tests. In this case, devices for measuring heat flows (DMHF) are used [1]. In this paper, we consider a device that implements a calorimetric method for measuring the heat flux from the surfaces of devices in a stationary thermal regime. In the process of operation, the DMHF should allow: from the heated surface area to measure the heat flux in a stationary mode; to ensure highly efficient heat removal on it; provide a uniform temperature field.

During measurements, a heat exchange device (radiator) is installed on a heat-releasing surface. Distilled water is pumped through it in the channels between the ribs (Fig. 1).

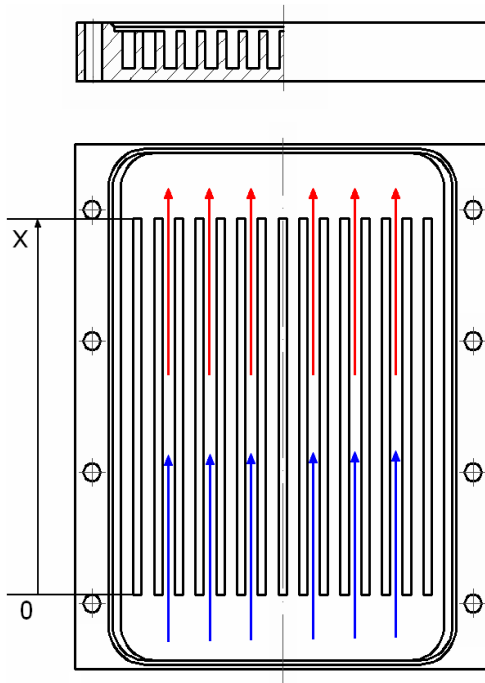


**Figure 1.** Heat exchange device (radiator)

The flow rate can be adjusted with a tap on the flow meter. By measuring the values of the temperature difference between the inlet and outlet sections of the radiator and the coolant flow rate, the heat flux  $P$  from the investigated surface is indirectly measured in the stationary mode:

$$P = c_p \rho G_v (t_{\text{obl}x} - t_{\text{ex}}), \quad (1)$$

where  $c_p$ , specific heat capacity J/kgK, and  $\rho$  is the density of distilled water, kg/m<sup>3</sup>;  $G_v$  is the volume flow, m<sup>3</sup>/s. The developed DMHF is installed at the site of the heat sink of the spacecraft, so the radiator, in terms of the efficiency of removing the heat flow in terrestrial conditions, should replace the heat pipe in space. The installation of the heat pipe itself is impractical, since its operation during the test will depend on the forces of gravity.

Intensive heat transfer can be achieved due to the high speed of pumping the coolant. However, along with an increase in the convective heat transfer coefficient, this will lead to a decrease in the accuracy of heat flow measurement: the coolant, passing through the radiator, will be heated weakly. As a result, small values of the temperature difference between the inlet and outlet sections of the heat exchanger will lead to significant (more than 30%) errors in heat flow measurement. For the normal operation of the device, it is necessary to find the optimal ratio of the pumping speed and the temperature difference of the coolant, given that the highest accuracy of heat flow measurement is achieved at low flow rates and maximum temperature differences.

#### Ensuring a uniform temperature field

One of the main reasons for the non-uniformity of the temperature field of the radiator base is the variable intensity of local values of convective heat transfer in the sections of the channels. This is due to a number of factors, among them: variable values of the local heat transfer coefficient at the boundary of the channel wall and the heat carrier, local values of the heat release power, conductivity of the channel walls, heating of the liquid when moving through the channels.

As a result, the temperature difference between the radiator wall and the liquid in the initial sections is greater than in the final sections, the heat exchange in the initial sections takes place with greater intensity, and, accordingly, their temperature is lower than in the final sections.

The distribution of the local heat transfer coefficient  $\alpha(x)$  in a flat channel with laminar flow can be found from the relations [2]:

$$Nu(x) = \frac{4 \sum_{n=0}^{\infty} B_n \exp\left(-\frac{8}{3} \varepsilon_n^2 \frac{1}{Pe} \cdot \frac{x}{a_K}\right)}{3 \sum_{n=0}^{\infty} \frac{B_n}{\varepsilon_n^2} \exp\left(-\frac{8}{3} \varepsilon_n^2 \frac{1}{Pe} \cdot \frac{x}{a_K}\right)}, \quad (2)$$

$$Nu(x) = \frac{\alpha(x) \cdot h}{\lambda_s}, \quad Pe = \frac{\nu \cdot h}{a}, \quad (3)$$

where  $\nu$  - kinematic viscosity of the liquid,  $m^2/s$ ;  $a_k$  - is the channel width,  $m$ ;  $h$  - characteristic dimension,  $m$  - for a flat channel  $h=2a_k$ ;  $a$  - thermal diffusivity,  $m^2/s$ ;  $B_n, \epsilon_n$  - are the coefficients from the solution of the equation for fluid motion in a flat channel [2]. As an example, Fig. 2 shows the result of calculating  $\alpha(x)$  along the length of the channel  $a_k = 5$  mm, with length  $l=150$  mm at a water velocity  $\nu = 1$  m/s. The decrease in the values of  $\alpha(x)$  along the length of the channel occurs by more than four times.

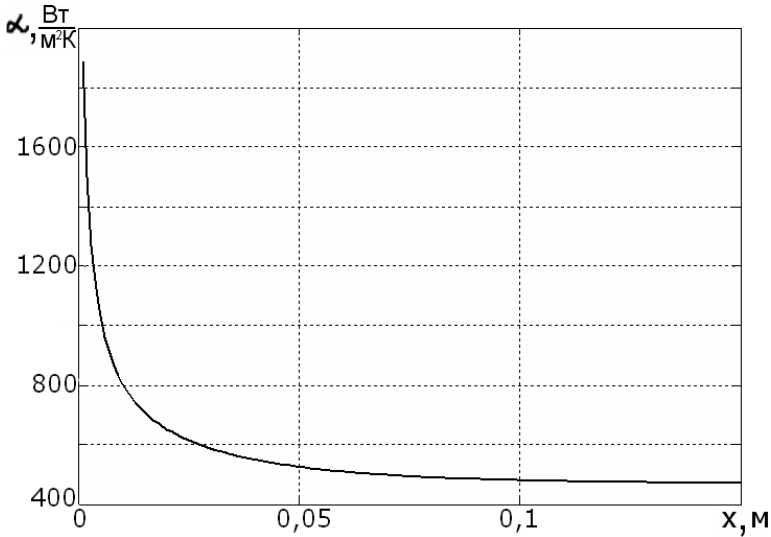


**Figure 2** Distribution of the convective heat transfer coefficient along the length of the channel, channel width  $a_k = 5$  mm

To form a uniform temperature field of the radiator base, a method for calculating and selecting parameters is proposed, which makes it possible to provide variable values of the heat transfer intensity in different parts of the heat exchanger base due to a local change in the heat transfer coefficient  $\alpha_{mp}(x)$ . We study the possibility of implementing this method by locally changing the height of the edges.

To form a uniform temperature field of the radiator base, it is necessary to calculate the required values of the local heat transfer coefficient  $\alpha_{tr}$  in its various sections. Let us find the distribution  $\alpha_{mp}(x)$  from the differential equation of the plate under the following conditions. on the one hand, a constant heat flux density  $q_s$  is maintained on the base of the heat exchanger. On the other hand, the heat flow is carried away by the flowing coolant; heat transfer from the ends is neglected; the change in the heat flux density due to thermal conductivity along the length of

the channels is negligible. The thermal regime is stationary, the reference point is the entrance to the channel:

$$\frac{d^2 t_c}{dx^2} - \frac{\alpha_{mp}(x) \Pi(t_c - \overline{t_{жс}}(x))}{\lambda \delta Y} + \frac{q_s}{\lambda \delta} = 0 \quad (4)$$

The proposed method makes it possible to form temperature fields of various types on the basis of the radiator. The solution of equation (4) for the case of a uniform temperature field of the base gives  $\frac{d^2 t_c}{dx^2} = 0$ . Then the heat transfer coefficient is expressed from equation (4):

$$\alpha_{mp}(x) = \frac{q_s Y}{\Pi(t_c - \overline{t_{жс}}(x))}, \quad (5)$$

where the temperature difference between the wall and the liquid is found from the solution of the heat conduction equation for the laminar flow of a liquid in a flat channel at a constant wall temperature [3]:

$$t_c - \overline{t_{жс}}(x) = (t_c - t_0) \cdot 3 \sum_{n=0}^{\infty} \frac{B_n}{\varepsilon_n^2} \exp\left(-\frac{8}{3} \varepsilon_n^2 \frac{1}{Pe} \cdot \frac{x}{a_K}\right) \quad (6)$$

The calculation result  $\alpha_{mp}(x)$  is shown in fig. 3.

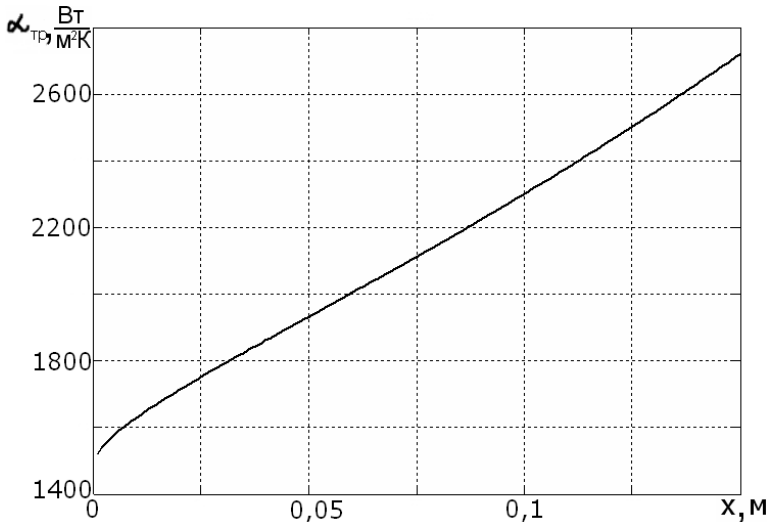


Figure 3. Distribution of the required values of the heat transfer coefficient

To implement this type of distribution, it is proposed to influence the intensity of local heat transfer by changing the height of the edges i.e. make them with a lower height in the initial section and in the final section, with a higher one, as shown in Fig.4.

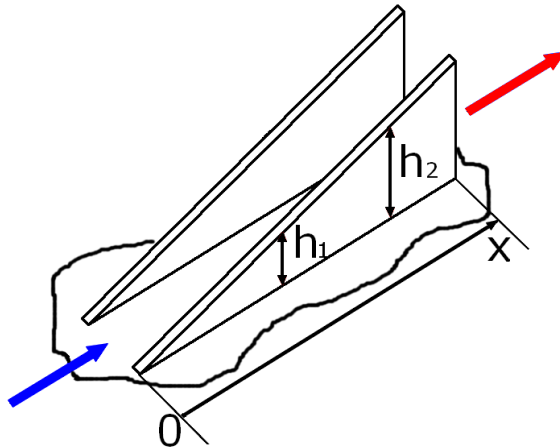


Figure 4. Variable edges height

To calculate the required height of the edges, it is convenient to use the effective heat transfer coefficient  $\alpha_{\text{эф}}(x)$  [4], which characterizes the intensity of heat transfer on the finned surface - the base of the radiator. The dependence  $\alpha_{\text{эф}}(x)$  on the edge height  $h(x)$  can be found from the relations [4]:

$$\alpha_{\text{эф}}(x) = \frac{\sigma(x)}{A}, \quad (7)$$

$$\sigma(x) = \alpha(x) \cdot S_{\text{сп}} + \lambda_p f \sqrt{\frac{\alpha(x)U}{\lambda_p f}} \operatorname{th} \left( \sqrt{\frac{\alpha(x)U}{\lambda_p f}} \cdot h(x) \right), \quad (8)$$

where  $\alpha(x)$  - the coefficient of convective heat transfer in a flat channel with isothermal walls is found from equations (5) and (6),  $\lambda_p$  - the thermal conductivity of the edge material, W/mK;  $f$  - sectional area of edge,  $\text{m}^2$ ,  $U$  - sectional perimeter of edge, m.

The necessary distribution of the height of the edges  $h(x)$  along the length of the heat exchanger can be found by solving a system of equations composed of expressions (2), (3), (5), (6), (7), (8):

$$\left\{ \begin{aligned} \alpha_{\kappa-mp}(x) &= \frac{q_s}{t_c - t_{\kappa c}(x)} \\ t_c - \overline{t_{\kappa c}}(x) &= (t_c - t_0) \cdot 3 \sum_{n=0}^{\infty} \frac{B_n}{\varepsilon_n^2} \exp\left(-\frac{8}{3} \varepsilon_n^2 \frac{1}{Pe} \cdot \frac{x}{a_K}\right) \\ \alpha_{mp}(x) &= \frac{\alpha(x) \cdot S_{np} + \lambda_p f \sqrt{\frac{\alpha(x)U}{\lambda_p f}} th\left(\sqrt{\frac{\alpha(x)U}{\lambda_p f}} \cdot h(x)\right)}{A} \\ \alpha(x) &= \frac{4\lambda \sum_{n=0}^{\infty} B_n \exp\left(-\frac{8}{3} \varepsilon_n^2 \frac{1}{Pe} \cdot \frac{x}{a_K}\right)}{3h(x) \sum_{n=0}^{\infty} \frac{B_n}{\varepsilon_n^2} \exp\left(-\frac{8}{3} \varepsilon_n^2 \frac{1}{Pe} \cdot \frac{x}{a_K}\right)} \end{aligned} \right. \quad (9)$$

The solution was carried out numerically at  $q_s=15 \frac{kW}{m^2}$ ,  $\lambda_p=390 \frac{Bm}{KM}$ ,  $a_K=3$  mm,  $b_K=2$  mm, coolant temperature at the inlet  $t_0=35$  °C, base temperature  $t_c=42$  °C, coolant flow rate  $G=3,44 \cdot 10^{-7} \frac{M^3}{c}$ . The result of calculating the distribution  $h(x)$  is shown in Fig.5.

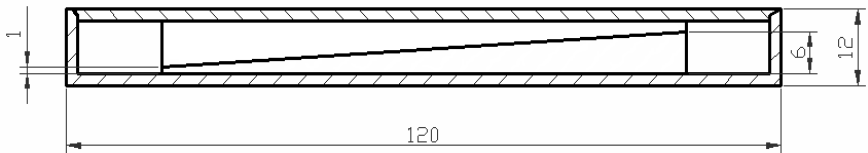


Figure 6. Heat exchanger with variable edges height

It can be seen that to ensure a uniform temperature field on the base of the radiator, it is necessary to make edges with a height varying from 1 mm to 6 mm. Experimental studies of the temperature field of the radiator base using thermocouples showed its high isothermality (no worse than  $\pm 0.2$  K).

Thus, the application of the method of forming a uniform temperature field, along with those proposed in [5], [6], made it possible to develop and create a device that allows you to provide the necessary thermal regime of the heat-releasing surface during measurements of heat fluxes. The device allows you to determine the heat fluxes in the range from 5 to 100 W with an error of no more than 10%.

### References

1. Korablev V.A., Minkin D.A., Sokolov A.N., Sharkov A.V. *A device for measuring heat flows from the surface of a fuel element // Scientific and technical bulletin of St. Petersburg State University ITMO. 2009. №3. p. 48-52.*
2. Zhukauskas A., Zhyugda I. *Heat transfer in a laminar fluid flow. - Vilnius: Mintis, 1969. - 266 p.*
3. Petukhov B.S. *Heat transfer and resistance in laminar fluid flow in pipes. - M.: Energy, 1967. - 411 p.*
4. Dulnev G.N. *Heat and mass transfer in electronic equipment: A textbook for universities on special. "Design. and production radio equipment." - M.: Higher. school, 1984. - 247 p., ill.*
5. Minkin D.A., Korablev V.A., Savintseva L.V., Sharkov A.V. *Creation of a uniform temperature field of radiating surfaces in a device for calibration devices. Izv. universities. Instrumentation. 2007. V. 50, No. 12 P. 52-55*
6. Sharkov A.V., Korablev V.A., Makarov D.S., Minkin D.A., Savintseva L.V., *A device for calibrating thermal imagers. Devices + Automation. 2008 No. 3 P. 44-46.*

DOI 10.34660/INF.2022.61.76.146

电力机车车辆集电器的主要故障及诊断方法  
**MAIN FAULTS OF ELECTRIC MOTIVE POWER COLLECTORS AND  
METHODS FOR THEIR DIAGNOSTICS**

**Fu Peisong**

*Master's degree Student*

**Tsaplin Aleksey Evgen'evich**

*Candidate of Technical Sciences, Associate Professor*

*Emperor Alexander I St. Petersburg State Transport University*

抽象的。文章分析了电动式集电器的工作原理，确定了其零部件的主要故障，考虑了集电器的目视控制法、激光法和超声波诊断法等方法。对电动机集电器的诊断方法，阐述了其优缺点。

关键词：集电器，电动动力，技术诊断。

**Abstract.** *The article analyzes the operation of electric motive power collectors, identifies the main malfunctions of their components and parts, considers such methods for diagnosing collectors as the visual control method, the laser method and the ultrasonic diagnostic method. For methods of diagnosing collectors of electric motive power, their advantages and disadvantages are formulated.*

**Keywords:** *collector, electric motive power, technical diagnostics.*

The purpose of technical diagnostics of electric motive power equipment is to quickly identify faults and restore the equipment, individual units and rolling stock as a whole, measure the necessary parameters and accumulate information about the technical condition of the equipment and subsequent troubleshooting. Technical diagnostics of electric rolling stock is an integral part of maintenance and repair and is performed to determine the need for repair work and predict equipment life, as well as to create a rational motive power repair system, taking into account its actual technical condition. The most promising are automatic systems of technical diagnostics, organized according to the principle of automated workstations (AWS) based on a personal computer. An automated diagnostic system is used, which is a set of instruments based on an aggregated system of electrical measuring instruments with automatic registration of measurement data. The system is combined by means of switching devices into a single set of measuring instruments used in accordance with the task. In manual systems, portable, digital

and analog instruments are used to measure the parameters of mechanical, electrical equipment, which carry out a tolerance assessment of the parameters of the technical condition of locomotives.

One of the most important elements of electrical equipment of electric motive power is the collector. It is a device used to provide movable current collection from a contact wire. The collector consists of a bow, a frame, a subframe and a transmission system. The geometric shape of the collector can change in accordance with the operating mode. The design of current collectors and their characteristics are determined by the power and speed of the electric motive power, the dimensions of the rolling stock and the proximity of buildings, the location of the contact wires in the plan and in height [1].

Let's consider the main malfunctions of the collector runner and ways to identify them.

The most important element of the current collector is the skid, which is a sprung upper node of the current collector that interacts with the contact wire and provides sliding contact along the contact wire. The pantograph skid is fixed on movable devices - carriages, which are fixed on the upper frames of the collector.

The material that provides the current collection from the contact wire is mainly solid carbon. As a constructive part of the current collector, it receives current through direct contact with the contact wire. The contact wire is made of copper alloy, and its hardness is higher than that of the carbon sliding plate.

The main cause of skid carbon plate failure is poor adjustment of the static contact force.

Also, the main faults of the carbon sliding plate of the current collector are: fatigue damage to the pantograph, plate cracks, partial wear of the carbon plate, abnormal pressure of the pantograph lifting. These malfunctions can occur as a result of poor organization of the maintenance process and insufficient professional skills of the maintenance personnel.

The main reason for collector failure during movement is that it may collide with foreign objects, causing the sliding carbon plate to deform and break, in some cases this may even cause the collector to fall. In addition, when the train is moving, the elements of the pantograph are affected by the aerodynamic force.

An important indicator of the contact network, which determines the nature of its interaction with the current collector, is the elasticity of the contact suspension. Due to the difference in the elasticity of the contact network itself, the presence of additional weights, skewed clamps and improper installation during movement, especially at high speeds, the collector may swing abnormally.

If the contact pressure is too low, the contact resistance at the point of interaction of the collector skid with the contact suspension increases, as a result of which the power loss also increases. In addition, in the process of movement, the

current collector can be detached from the contact wire, resulting in an arc and increased wear of the contact wires and sliding carbon plates of the current collector. Separation of the collector skid from the contact wire can also lead to the fact that the onboard electrical equipment will be subject to high-frequency electrical oscillatory processes and overvoltages, which is also highly undesirable and can lead to malfunctions.

Thus, the collector must provide the required relatively stable contact pressure within its operating range of heights, which is determined by the mechanical structure of the collector as a whole and the parameters of each of its parts. Proper static contact pressure can ensure normal contact between the pantograph skid and contact wire, reduce autonomy, overcome the influence of wind, high-speed air flow and mechanical vibration, and ensure good current collection performance.

The lifting of the collector is mainly controlled by the circuit and provided with compressed air. The main reason why malfunctions in the collector lifting system can occur is air leakage. When there is air leakage, even if all channels are working normally, the pressure value will not reach the working value necessary to lift the collector or keep it in the raised position. The second common cause is a faulty collector air control valve. By adjusting the valve, the time and static contact pressure of the collector can be adjusted. If the connection between the valves is loose or there is a compressed air leak, this may cause the collector to lift slowly or even fail to lift.

Also a common cause of collector failures is damage to the flexible cable, which can lead to poor current reception. The function of the flexible power cable is to conduct current to the bearing to prevent damage to the bearing by ionization.

An important element of the collector design is the pressure switch. The pressure switch generates a control signal to the electric control valve, compares the pressure value and controls the switching on and off of the compressed air supply circuit, controlling the electric control valve.

From the analysis of the above typical failures, it can be seen that collector failures can be detected in time through regular maintenance. Therefore, every time electric rolling stock enters the depot for maintenance, it is necessary to carry out a thorough inspection of the collector.

The main methods for detecting faults in current collectors of electric rolling stock are the visual inspection method, the laser diagnostic method, and the ultrasonic diagnostic method [2].

The method of visual control is as follows. After the train stops, it is necessary to lower the collector, turn off the power and make sure that the inspection is safe.

The repair personnel of the depot use a special hand-held measuring tool during inspection. This method of fault detection is not efficient enough, time consuming, and largely dependent on the experience of maintenance personnel in

assessing possible faults. It also does not allow real-time online monitoring, which contradicts the construction of modern control and diagnostic systems for electric move power of railways.

The principle of the laser fault detection method is to scan the sliding plate of the collector at high speed according to the laser sensor installed above the collector, and then obtain information about the thickness of the carbon plate and calculate the wear and external dimensions of the collector online through the processor of the automated diagnostic system. The system uses a laser generator and a high-speed dynamic camera for imaging at the same time. When the collector reaches the detection point, the laser generator emits laser light on the surface of the sliding plate, and the high-speed camera collects information to build a three-dimensional image of it. Based on this, wear, cracks and other malfunctions of the collector sliding plate are detected. The laser method can detect wear in real time, but it is expensive and can be highly dependent on light.

With the ultrasonic method of control, the ultrasonic sensor is installed at the top on the board of the receiving room. When the sliding plate reaches the observation point, an ultrasonic wave is emitted by the transducer and reflected from the contact plate of the current collector. In this case, the total time of transmission and reception of the ultrasonic wave during its propagation in the air is measured. The speed is calculated to obtain the measured thickness of the contact plate [3].

### References

1. Biryukov I.V., Savoskin A.N., Burchak G.P. *Mechanical part of traction rolling stock. M.: Transport, 1992 – 440 p.*
2. Zelenchenko A.P., Rolle I.A., Tsaplin A.E. *Technical diagnostics of electric rolling stock: textbook. - St. Petersburg: PGUPS, 2015 – 60 p.*
3. *Non-destructive testing and diagnostics. Handbook, ed. Klyuyeva V.V. – M.: Mashinostroenie, 2005 – 656 p.*

DOI 10.34660/INF.2022.77.68.147

磁悬浮的特点和工作原理  
**THE CHARACTERISTICS AND WORKING PRINCIPLE OF  
MAGNETIC LEVITATION**

**Shen Jieyi**

*Master's degree Student*

**Tsaplin Aleksey Evgen'evich**

*Candidate of Technical Sciences, Associate Professor*

*Emperor Alexander I St. Petersburg State Transport University*

注解。 文章讨论了磁悬浮铁路与常规铁路的区别,概述了磁悬浮铁路的运行原理及其供电系统,并确定了磁浮列车的优越性。

关键词: 磁悬浮铁路、供电系统。

**Abstract.** *The article discusses the difference between the maglev railway and the conventional railway, outlines the operation principle of the maglev railway and its power supply system, and determines the superiority of the maglev train.*

**Keywords:** *maglev railway, power supply system.*

In the entire range of speeds of movement of people, there are different types of transport. Road transport speed is generally 50 to 100 km/h, railway 100 to 300 km/h, air transport 500 to 1000 km/h. can not get rid of the limitation of earth friction resistance. Thus, there is a gap between railways and aviation. People have long been thinking about how to bridge the gap between railroads and airplanes. Magnetic rail is a high-speed land transportation system that is attracting a lot of attention and has great prospects in today's world.

Since the early 1960s of XX century, some developed countries have begun to explore ultra-fast maglev vehicles. The adhesion railway in Germany and Japan started operating earlier, but both countries adopted different standards. Germany uses normally directional adhesion levitation trains, while Japan uses superconducting magnetic repellant trains. Although the vehicle structure and line varies depending on suspension, steering and movement, the basic principle is the same.

**The basic standard and working principle of the magnetic railway**

Although electromagnetic force is used for levitation, according to the way

the electromagnet is used on the train, the basic standard can be divided into three categories.

1. On superconducting magnets (electrodynamic suspension, EDS).

Superconducting magnet - a solenoid or electromagnet with a winding made of a superconducting material. The winding in the state of superconductivity has zero ohmic resistance. If such a winding is short-circuited, then the electric current induced in it remains almost arbitrarily long.

The magnetic field of the undamped current circulating through the winding of a superconducting magnet is exceptionally stable and ripple-free, which is important for a number of applications in scientific research and engineering. The winding of a superconducting magnet loses the property of superconductivity when the temperature rises above the critical temperature  $T_k$  of the superconductor, when the critical current  $I_k$  or the critical magnetic field  $H_k$  is reached in the winding. With this in mind, materials with high values of  $T_k$ ,  $I_k$ , and  $H_k$  are used for windings of superconducting magnets.

2. On electromagnets (electromagnetic suspension, EMS).

3. On permanent magnets; it is the new and potentially most economical system.

### **The principle of operation of the magnetic railway**

1. On superconducting magnets (electrodynamic suspension, EDS).

(1) Suspended system.

EDS type superconducting magnetic repellent electric magnetic train is the principle of magnetic pole repulsion, so that the vehicle floats on the track, the bottom of the vehicle-mounted superconducting magnet (comes in a liquid helium tank) installed on both sides of the track, arranged by a certain aluminum ring coil when the superconducting coil is turned on to create a strong magnetic field. If the vehicle is moving forward at a certain speed (due to the linear motor) the magnetic field will induce an electric current in the aluminum ring. The magnetic flux generated by the induced current will be opposite to the magnetic flux of a superconducting magnet on a vehicle. Two magnetic fluxes will create a repulsive force. The greater the force, the greater the repulsion (at this time the speed is 80 km / h) and the train rises up to 100 millimeters. When the train is running at low speed or at rest, the induced current on the earth coil decreases, the buoyancy decreases and disappears, and the train rests on the rails with auxiliary wheels. This form is an electric suspension.

(2) Control system.

The traditional train is controlled by the interaction between the wheel rim and the rail. A magnetic train is the use of electromagnetic force to move. The magnetic levitation guidance system is installed in vehicles designed to control

superconducting magnets, so on the side of the rail, the magnetic field generated by the coils is relatively comparable to the acting force of the train, and allows the train to maintain the correct direction of movement.

(3) Propulsion system.

Due to the rise to a certain height, the magnetic train does not interact with the wheels with the rails, so it is impossible to use conventional traction motors. In this regard, the traction force arising from the friction force between them does not move the train forward, so that the traction device with a linear motor is used as the traction force of the train.

There are two types of linear motors used in magnetic trains. Linear motors evolved from rotating electrical machines. Its basic structure and operation principle are similar to the ordinary electric rotary electric machine. It's like cutting a rotating electric machine in a radial direction. Thus, the transmission mode changes from rotational motion to linear motion [1].

2. Permanent EMS type magnet (electromagnetic suspension)

(1) suspension system.

The permanent EMS type magnet is a maglev type electromagnetic cable. An electromagnetically oriented magnet is mounted along the entire length of the train. A magnetic train is mounted on an electromagnetic maglev (suspended electromagnet) Electromagnetic field generated by the magnet lifts the train above the surface, the gap between the vehicle and the rail surface is inversely proportional to the force of attraction. In order to ensure the reliability of the suspension and the smooth operation of the train, and to make the linear motor have a higher power, the current in the electromagnet must be controlled so that the magnetic field can maintain a stable force and levitation force, so that a gap of 10-15 mm is maintained between the train and the guide surface. This shape is an electromagnetic suspension.

(2) The guidance system and propulsion system are similar to the superconducting magnetic repulsion type EDS.

**Magnetic railroad power supply system**

1. Remote power supply. The magnetic levitation system is a long-station synchronous linear motor mode, the LSM ground synchronous motor is used, and the three-phase alternating current in the ground power winding is controlled by a powerful converter located on the ground. The traction conversion station required by the linear motor converts the electrical power of the public grid into variable frequency AC voltage according to the speed required by the traction control system. And the AC is synchronized with the vehicle speed to supply power to the linear motor. The power conversion system consists of a rectifier, three sets of

inverters, and a DC breaker that is braked by a resistor. Since the motor windings are distributed throughout the line but divided into separate sections, it is possible to energize only the section in which the vehicle is moving in order to improve the power factor of the linear motor.

## 2. Train power supply

(1) Power supply is individual, i.e. one power converter corresponds to one train. Therefore, the power converter supplies power to the train only when the train is moving in the precinct station.

(2) Automatically controls the operation of the train on the line. The magnetic train controls the movement of trains in the substation, and not like a regular train moves with the help of a driver. The substations are equipped with an electronic computer system for automatic operation.

(3) High precision position detection. In order to work simultaneously with the LSM synchronous linear motor, it is necessary to provide accurate and position detection of the ground traction winding and the built-in superconducting magnet to realize synchronous control.

(4) Electricity is supplied only in the running gear of the train. In the drive system of a synchronous linear motor, the movement of the train is connected only with the longitudinal windings of the stator along the road, so the power supply is controlled only on the ground winding of the section in which the train moves [2].

## **Characteristic of superiority of magnetic iron**

### Features of the magnetic railway

The magnetic railroad and the traditional railroad have quite big differences and characteristics. Trains running on traditional railroads have locomotives as traction force and, by applying pressure on the track structure, experience friction between the wheels and rails. A train running on a magnetic rail uses the attractive or repulsive force generated by the electromagnetic system to lift the vehicle, so that the entire train is suspended on the rail and controlled by the electromagnetic force. The linear motor directly converts electrical energy into traction.

A linear motor is an electric motor in which one of the elements of the magnetic system is open and has a deployed winding that creates a traveling magnetic field, and the other is made in the form of a guide that provides linear movement of the moving part of the motor [3].

Now there are many designs of linear motors, but all of them can be divided into two categories - low acceleration motors and high acceleration motors.

Low acceleration engines are used in public transport (maglev, monorail, subway). High acceleration motors are quite small in length and are typically used to accelerate an object to high speed and then release it. They are often used for research into hypervelocity collisions such as weapons or spacecraft launchers.

Linear motors are also widely used in machine tool feed drives and in robotics. located either on the train, or on the way, or both there and there. A serious design problem is the large weight of sufficiently powerful magnets, since a strong magnetic field is required to maintain a massive composition in the air.

According to the Earnshaw theorem (S. Earnshaw, sometimes written by Earnshaw), static fields created by electromagnets and permanent magnets alone are unstable, unlike the fields of diamagnets. Diamagnets are substances that are magnetized towards the direction of the external magnetic field acting on them. In the absence of an external magnetic field, diamagnets have no magnetic moment and superconducting magnets. There are stabilization systems: sensors constantly measure the distance from the train to the track and, accordingly, the voltage on the electromagnets changes.

### **Benefits of magnetic railway**

1. High speed, short travel time.
2. Safety and reliability. The magnetic levitation system, using guide rails, provides a smooth ride, eliminates the possibility of derailment and rollover of the vehicle, and improves the safety and reliability of train operation.
3. Low energy consumption, environmentally friendly, no pollution. No noise, vibration, exhaust and environmental pollution.
4. Fewer problems, low maintenance. The main components are single and solid, resulting in fewer faults and lower maintenance costs than high-speed and traditional railways.

### **Disadvantages of magnetic railway**

1. High cost of creating and maintaining a track.
2. Weight of magnets, electricity consumption.
3. The electromagnetic field generated by the maglev may be harmful to train crews and/or nearby residents. Even traction transformers used on AC electrified railways are harmful to drivers, but in this case the field strength is an order of magnitude greater. It is also possible that maglev lines will not be available to people using pacemakers.
4. It will be required at high speed (hundreds of km/h) to control the gap between the road and the train (several centimeters). This requires ultra-fast control systems.
5. Complex track infrastructure is required.

## **References**

1. *Dzenzersky V. A. et al. High-speed magnetic transport with electrodynamic levitation. — Kyiv: Naukova Dumka, 2001. - 479 p.*

2. *Electric railways: a textbook for students of the specialty 18.07.00 "Electric transport (railways) / under. ed. prof. Yu.E. Prosvirova. - Samara: SamIIT, 1997. - 192 p.*

3. *High-speed rail transport and systems with magnetic suspension of carriages - applicants for one transport niche / I. P. Kiselev // Transport of the Russian Federation: a journal about science, economics, practice. - 2010. - No4. - P. 12-14.*

DOI 10.34660/INF.2022.74.84.148

高铁牵引供电系统  
**HIGH-SPEED RAIL TRACTION POWER SUPPLY SYSTEM**

**Li Yiyuan**

*Master's degree Student*

**Volodin Anatoly Alexandrovich**

*Candidate of Technical Sciences, Associate Professor*

*Emperor Alexander I St. Petersburg State Transport University*

注解。 本文根据高速铁路牵引供电需求, 确定各种供电系统中的供电方式, 通过对比分析确定最适合的供电方式, 并概述优缺点。

关键词: 接触网, 供电系统, 直接供电方式, 自耦变压器供电方式(AT供电方式), 吸流变压器供电方式(BT供电方式)。

**Abstract.** *This article determines the power supply modes in various power supply systems based on the traction power supply requirements of high-speed railways, determines the most suitable power supply mode through comparative analysis, and outlines the advantages and disadvantages.*

**Keywords:** *catenary, power supply system, direct power supply mode, autotransformer power supply mode (AT power supply mode), current-absorbing transformer power supply mode (BT power supply mode).*

The traction power supply system of a high-speed railway must meet the following requirements:

1. To satisfy the relationship between the pantograph and the catenary for high-speed operation.
2. To meet the requirements of a reliable and stable power supply.
3. To meet the requirements of maintenance and resistance to environmental damage.
4. Automatic IMPS rephasing
5. Power supply capabilities adapt to the requirements of high speed and high density.
6. To have comprehensive and integrated remote monitoring capabilities.

The power supply system is divided into two modes: multi-phase power mode and in-phase power mode.

First, we will analyze the technology of anti-phase power.

1. Direct power

This is the easiest way to supply power. On the line, the power supply of the locomotive is formed directly by the catenary, by the way and by the ground, and no special measures for protection against communication interference are added. Most electrified railroads use this power method early. This power supply method is the simplest, the investment is the most economical, the traction network impedance is small, the power loss is low, and the power supply distance is shorter usually 30-40 km. The single load current of the electrified railway returns to the traction substation from the catenary along the rail. The rail and the ground are not isolated, and part of the reversible flow flows down the rail to the ground. Therefore it has an inductive effect on the communication line, which is a disadvantage of the direct power method. It is usually used in a section where there is no overhead communication line along the railway, and the communication line is made with an underground shielded cable and, if necessary, also moves to a longer distance.

The method of direct power supply with a return line is to install the return line parallel to the rail on a catenary pole, which is called the negative feeder. The mutual inductance between the catenary and the return line is used to return the return line flows back to the traction substation, reducing the electrical space, so it can partially compensate for the interference of the catenary to neighboring communication lines, but its anti-interference effect is not as good as that of (BT) method of power supply. This power supply method can be used in the area where the requirement for communication line noise immunity is not high, which can further reduce the impedance of the traction network, and the performance of the power supply is better, but the cost is slightly higher.

2. Suction transformer power mode (BT power supply mode)

Power supply mode (BT) is a power supply mode in which a suction return transformer is installed in the catenary. The transformation ratio of the current drain transformer is 1:1, its primary winding is connected in series to the catenary, and the secondary winding is connected in series to the return line, specially designed to reverse the flow of traction current to the traction substation, so it is called the power mode for suction transformer --- reverse line. In the middle of the two suction transformers, the rail and the return line are connected by the suction line, forming a circuit in which the load current of the electric locomotive flows from the rail to the return wire. The distance between two suction transformers is called the BT section. Usually the length of the BT section is 2-4 km. When the traction current flows through the winding, the secondary winding is forced to flow into the return line through the suction line. Since the electrical space between the catenary and the return line is very close. The currents flowing are

approximately equal and opposite, so most of the electromagnetic induction on adjacent communication lines is compensated, thereby reducing interference to communication lines. In this power mode, the current-absorbing transformer is connected in series with the catenary, so that the impedance of the catenary is about 50% larger than that of the direct power mode. The power consumption is also high, and the power supply distance is also short (single line is usually about 25km, double line is usually about 25 km (it is about 20 km), and the investment is also more than with direct electricity supply.

### 3. Autotransformer power supply (AT power supply mode)

The AT power supply method was developed in the 1970s, it can not only effectively reduce catenary interference on the communication line, but also adapt to the operation of high-speed and powerful electric locomotives, so it is used in many countries. In this power supply mode, the autotransformer is connected between the catenary and the positive feeder every 10 km, and its neutral point is connected to the rail. The autotransformer doubles the supply voltage of the catenary, while the voltage supplied to the electric locomotive is still 25 kV. After the electric locomotive is powered from the catenary, the traction current, as a rule, flows from the rail, and under the action of the autotransformer, the current flowing from the rail returns to the substation through the autotransformer winding and the positive feeder. When the locomotive current flows through one winding of the autotransformer, the other winding of the autotransformer induces a current to power the electric locomotive. The traction network resistance of the autotransformer power mode is very small, about 1/4 of the constant power mode, so the voltage loss is small, the power loss is low, the power supply capacity is large, and the power supply distance is two long, up to 40-50 km. As the distance between traction substations increases, the number of traction substations decreases, as well as the engineering costs of the power system for the power supply of railways. Due to the complexity of traction substations and traction networks, investment in electrified railways has increased. This power supply method is commonly used on heavy-duty, high-speed and other electrified railways with heavy loads.

### 4. Power supply over coaxial cable (CC power supply mode)

CC Power Supply - This is a new type of power supply. Its coaxial power cable (CC) is laid along the railway line, the inner core wire is connected to the catenary as a power supply line, and the outer conductor is connected to the rail as a return line every 5-10 km. The advantage of the CC power supply is that the supply and return lines are in the same cable, with a small spacing, and are arranged coaxially, which increases the mutual inductance. The impedance of a coaxial power cable is much smaller than that of a catenary and rail, so traction current and return flow pass almost entirely through the coaxial power cable. The current of the cable core conductor and the outer layer are equal and opposite, and the magnetic fields gen-

erated by them cancel each other out. There is almost no interference to adjacent communication lines. Low impedance and long supply distance. However, coaxial power cables are expensive and currently only used in some particularly difficult applications.

Comparative analysis of the power supply mode, suitable for high-speed rail

1. Suction transformer power mode (BT power supply mode)

Due to the high speed and high current of high-speed electric traction, the power supply quality of the power supply system should be high, and the number of electrical phases and electrical segments should be minimal. Although the BT power supply method has the best characteristics in terms of noise immunity of communication lines, it is not suitable for high-speed traction, since it has a current-absorbing transformer in series with the contact wire and is accompanied by a spark gap, because the contact wire of the power supply arm is divided into many sections Electric traction. Compared with BT power supply mode, many features of AT power supply mode and direct power mode (including negative feeder power mode) can meet the requirements of high-speed electric traction.

2. Autotransformer power supply (AT power supply mode)

The AT power supply mode has a large distance between substations. Firstly, the number of electrical phases can be significantly reduced, and the impedance of the traction network is small, which can significantly reduce voltage losses in the traction network, improve the quality of power supply and ensure high-speed train traffic; Secondly, a power source is selected that can closely cooperate with the power grid to supply electricity to the electrified railway in order to reduce the cost of the project. In addition, the power supply method of AT has little effect on the communication line, which is equivalent to the power supply method of BT. For the above reasons, the AT power supply mode is widely promoted in high-speed railways around the world, and Japan is promoting the AT power supply mode as the standard system for electrified railways.

3. Direct power supply

The direct power supply method has a large traction network impedance, a small distance between substations and, accordingly, a large number of electrical phases, and the protection of the communication line is not as good as that of the BT and AT power supply methods. However, the direct-mode traction network has a simple structure and can be applied in areas with low electromagnetic interference requirements. Some specifications of the direct power mode are between the BT and AT power supply modes, and it is also an additional mode for high-speed electrified railways.

### References

1. *V.E. Rozenfeld, I.P. Isayev, N.N. Sidorov Theory of electric traction M.: Transport, 2005. 436 p.*
2. *Marquardt K.G. Power supply of electrified railways. - M.: Transport, 1982. - 528 p.*
3. *Pochaevets V. T. ACS devices for power supply of railways. - M.: Route, 2003. - 318 p.*

HXD2型电力机车单相牵引变流器的电能可以更好地返回牵引网  
**THE ELECTRICAL ENERGY OF HXD2 ELECTRIC LOCOMOTIVE  
SINGLE-PHASE TRACTION CONVERTER CAN BE BETTER  
RETURNED TO THE TRACTION NETWORK**

**Gao Qi**

*Master's degree Student*

**Vikulov Ilya Pavlovich**

*Candidate of Technical Sciences, Associate Professor*

*Emperor Alexander I St. Petersburg State Transport University*

抽象的。本文以HXD2大功率机车牵引交流变流器为研究对象。通过理论分析和仿真表明,在单相牵引整流器(4QS)中,来自交流侧的电流可以很好地跟随市电电压,并能稳定地保持直流侧电容器上的电压。验证了所提控制策略的正确性。当机车从牵引状态转变为制动状态时,单相整流器可以很好的转移到逆变器工作状态,从而使电能更好地返回牵引网,牵引效果更好。

关键词: HXD2型电力机车; 牵引驱动系统; 四象限整流器(4QS); 功率因数。

**Abstract.** *In this article, the HXD2 high power locomotive traction AC converter is used as the object of study. Through theoretical analysis and simulation, it is shown that in a single-phase traction rectifier (4QS), the current from the AC side can follow the mains voltage well and maintain the voltage on the DC link capacitor stably. The correctness of the proposed control strategy has been verified. When the locomotive changes from the traction state to the braking state, the single-phase rectifier can be well transferred to the inverter working state, so that the electric energy can be better returned to the traction network with better traction effect.*

**Keywords:** *HXD2 electric locomotive; Traction drive system; Four quadrant rectifier (4QS); Power factor.*

There are different modes of transport in China. In land transport, the main mode of transport is rail transport.

The energy sector in my country is characterized by rich coal reserves, and it is one of the few countries that uses coal as the main source of energy. The share of coal in the production and consumption of primary energy in the country has re-

mained above 70% for a long time. It has been scientifically proven that increasing the weight of a train to 20,000 tons can significantly increase throughput. No. 1 in the world in this regard, a powerful AC freight electric locomotive HXD2 has appeared.

"Express, big load" is my country's freight development policy. Therefore, it is necessary to comprehensively improve the technical level of railway vehicles and equipment in my country.

A more comprehensive and in-depth study of high power AC drive systems and their control is required. The HXD2 electric locomotive system is developed in cooperation with Dalian Electric Locomotive Co., Ltd and French Alstom (Alstom). The system is mainly composed of a side contact network circuit, a main transformer circuit, a traction converter unit and a traction motor. The schematic diagram and structural composition of the traction electric drive system are shown in Figure 1.

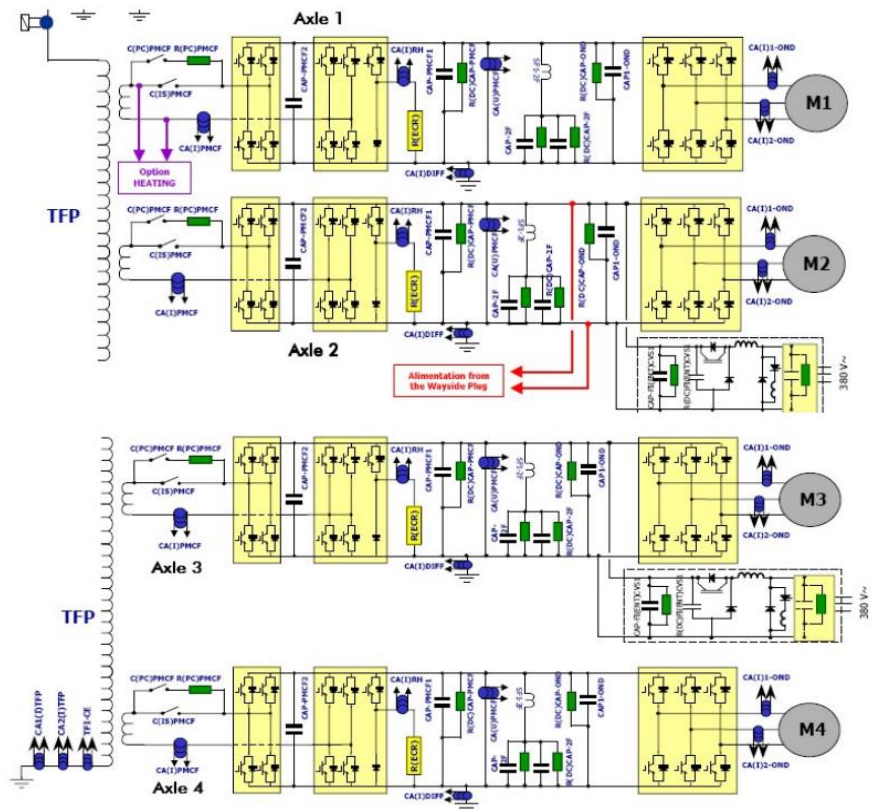


Figure 1. Structural diagram of the electric traction drive system

**Overhead side line circuit:** The voltage of overhead line in my country is 25kV/50Hz single-phase AC. And the mains side circuit mainly implements the overhead line input into the car through the collector to provide power to the locomotive.

main traction transformer: HXD2 electric locomotive main transformer adopts ABB technology and is a combined transformer structure, consisting of main transformer, auxiliary reactor, second harmonic filter reactor and other auxiliary equipment.

**Traction Converter:** HXD2 electric locomotive consists of two connected single machines. A single locomotive includes two bogies, each bogie includes two drive shafts. The single machine has 4 axles, and the whole car has an 8-axle structure. Each bogie contains two traction converters, the locomotive has four bogies in total, and a total of 8 sets of independent traction converter units, which can realize one-to-one control of traction motors.

**Asynchronous traction motor:** The traction motor (YJ90A) of the HXD2 electric locomotive is an AC induction motor produced in cooperation with Alstom in France.

The rectifier part of the HXD2 electric locomotive adopts the structure of a single-phase PWM rectifier (VSR) as shown in Figure 2, also known as a four-quadrant converter (4QC). The structure converts the single-phase AC input voltage on the secondary side of the main transformer to DC voltage to power the intermediate DC circuit. The term "four-quadrant converter" (4QC) means that the phase angle between voltage  $V_{ae}$  and current  $I_L$  is fully adjustable in both traction and braking conditions. By controlling the phase angle between voltage and current, four-quadrant AC operation can be achieved. Among them, L is the filter inductance on the AC side, C is the storage capacitor on the DC side, and R is the simulated load on the DC side.

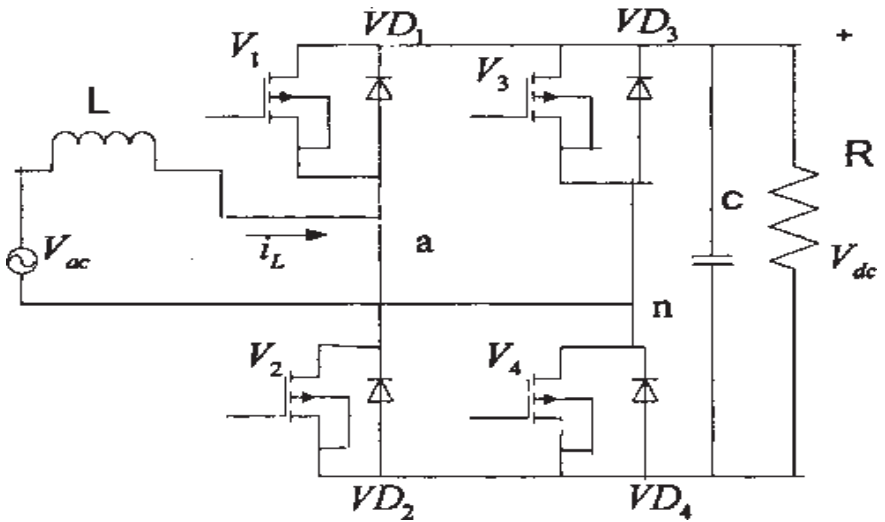


**Figure 2.** The structure of a single-phase rectifier with a PWM voltage source (VSR)

The rectifier input voltage range for the HXD2 electric locomotive is about AC900V (that is, the main transformer secondary voltage), the DC output side is about 1800V. It is worth noting that HXD1 and HXD3 also use this structure.

The so-called four-quadrant operation means: In the conventional coordinate system, let the grid voltage be on the abscissa and the grid current on the ordinate. Under traction conditions and regenerative braking conditions, it is guaranteed that the grid voltage and current can operate in the four quadrants of the coordinate system according to positive and negative correspondence.

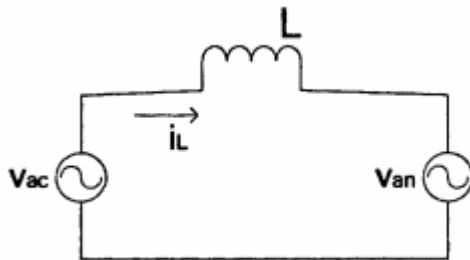


**Figure 3.** Equivalent circuit diagram

**basic principle:** The amplitude of the output voltage  $V_{an}$  on the AC side of the single-phase fully controlled four-quadrant bridge rectifier changes, and the change range switches between  $V_{dc}$ , 0 and  $-V_{dc}$ . If the corresponding control pulses are applied to the four switches of the circuit, then  $V_{an}$  responds accordingly to the change in the control pulse. If the control circuit is set to sinusoidal change, then from the  $V_{an}$  side, it will be equivalent to an AC source with variable phase and amplitude.

**Power factor:** The rectifier part of Chinese HXD electric locomotive uses single-phase PWM rectification without exception, this structure can realize four-quadrant operation, is composed of two-phase modules (half-bridge). B on the secondary side of the main transformer.

This structure is suitable for large power converters. In the main circuit of the HXD2 locomotive, it can mainly provide stable DC power for the intermediate circuit. At the same time, it can cause less distortion from the grid side. Compared with the earlier phase-controlled rectification method, the power factor of the four-quadrant rectifier is close to 1, so there is less interference and pollution of the power grid, and this structure is often used in modern high-power rectifier circuit.

Therefore, the power factor is of great importance for the circuit. In particular, for high power converter systems, the influence is especially noticeable. The locomotive itself is a powerful load, and its electric power comes from the catenary network above the roof, and the power supply of the catenary network from the power grid. The locomotive itself has a huge impact on the power system as a source of quality pollution electricity.

Previous DC electric locomotives mostly used bridge rectifier circuits. Due to the frequent opening and closing of the switch tube and the limitation of the control strategy, the current supplied by the train back to the contact network during operation is seriously distorted, and the power factor is extremely low, which not only affects the normal operation of the surrounding communication equipment, but also affects the power grid which in itself causes pollution. Although with the improvement of technology, some multi-segment bridge technology has been applied to the rectifier circuit of locomotives, but the effect is still not very good. So look forward to the emergence of a new type of schema application form and related control strategies.

To fully understand a circuit, you first need to understand the concept of power factor. By definition, in a circuit, the cosine value of the phase difference generated between voltage and current during operation is called power factor, which is denoted by the symbol  $\text{COS}\Phi$ . Power factor refers to the ratio of active power to apparent power of a circuit.

$$\text{COS}\Phi = \frac{P}{S} \quad (1)$$

P-active power                  S-apparent power

The power factor value (COS $\Phi$ ) ranges from 0 to 1, and the power factor is usually determined by the nature of the load. Loads such as incandescent lamps or electric resistance furnaces are purely resistive loads with a power factor of 1; Induction motor or synchronous motor refers to inductive load and capacitive load, and their power factor is less than 1.

In the power grid, because the voltage is clamped by the power grid, there is little misrepresentation. But because the current waveforms are different, they are greatly affected by the load carried by the grid.

Thus, its definition can be expressed as follows:

$$\lambda = \frac{P}{S} = U \cos \Phi_1 \quad (2)$$

In the formula, U is the ratio of the rms value of the main wave current to the rms value of the total current, called the coefficient of the main wave, which reflects the distortion coefficient (degree of misrepresentation) of the current;

P is active power,                  S is apparent power,  
this is still the fundamental wave power factor angle.

At this time, the power factor must contain two factors:

1-factor of angular phase displacement 2-shape distortion factor.

The lower the power factor of the circuit, the more energy the circuit uses to convert the alternating magnetic field, resulting in more reactive power. In the long run, more reactive power will have many adverse effects on the power system. In addition, harmonic interference caused by a circuit with a low power factor will cause great harm to the power grid and electrical equipment.

To reduce this effect and damage, power factor correction technology has been developed. This technology ensures that the input voltage and current have the same frequency and phase, which effectively improves the performance of the circuit.

For traction converters, it consists of a single-phase rectifier and a three-phase inverter connected by a DC link capacitor. The pantograph is connected to 25kV AC power through the traction network, and 950V AC power is output through the traction transformer, after which it is converted into 1800V DC power through a single-phase rectifier, and then 1800V DC power is supplied through the traction transformer. and then 1800V DC power is supplied through the traction transformer. It is obtained through an intermediate DC circuit and fed to a three-phase traction inverter to obtain a three-phase voltage of 950 V for the motor drive.

Modeling in Matlab a Single-Phase Rectifier with PWM (VSR)

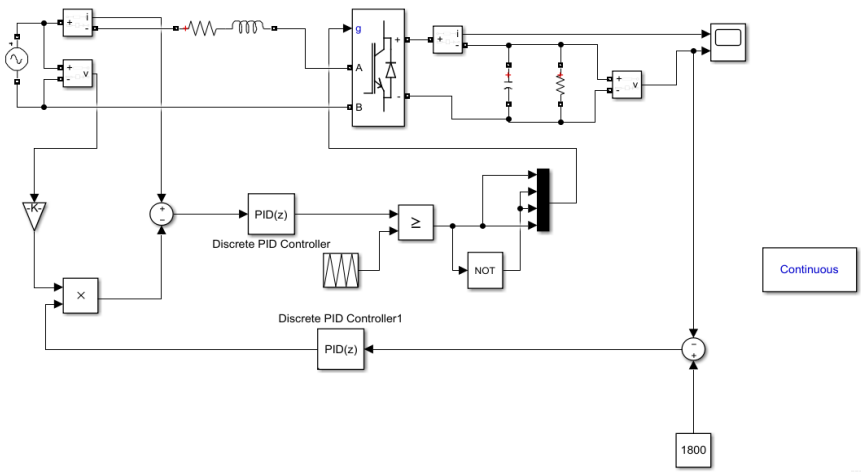


**Figure 4.** Simulation model of a section of a single-phase traction rectifier

From the results, it can be seen that the DC bus capacitor voltage is stable at 1800V, the AC side current of the single-phase traction rectifier can follow the grid voltage well, and the grid-side voltage-current power factor is 1.

### References

1. Zhang Chongwei, Zhang Xing. *PWM rectifier and its control [M]*. Beijing: Engineering Industry Publishing House, 2003
2. Zhang Yucheng. *Investigation of Single-Phase PWM Modulated Rectifier (VSR) [D]*, Huazhong University of Science and Technology, Wuhan City, Hubei Province, 2007
3. Zhang Shuguang - Chief Editor of *HXD2 Electric Locomotive / China Railway Press, 2009 (HXD Type High Power AC Locomotive Technology Series)*
4. Wu Lin. *Simulation study of the traction converter[D]*. Southwestern Jiaotong University. 2010
5. Wu Xiaoyan, *HXD2 Electric Locomotive Traction Converter Study [D]*, Southwest Jiaotong University, 2013.

DOI 10.34660/INF.2022.79.60.150

混合动力机车和再生制动系统提高了机车的能源效率  
**HYBRID LOCOMOTIVES AND REGENERATIVE BRAKING SYSTEMS  
INCREASE THE ENERGY EFFICIENCY OF LOCOMOTIVES**

**Xu Jiale**

*Master's degree Student*

**Wu Yansong**

*Master's degree Student*

**Volodin Anatoly Alexandrovich**

*Candidate of Technical Sciences, Senior Research Officer, Professor  
Emperor Alexander I St. Petersburg State Transport University*

抽象的。 文章分析了混合动力机车的发展,几种混合动力机车的储能方式,同时介绍了利用再生能源提高混合动力机车能效的三种技术。

关键词: 储能系统, 能源效率, 再生制动, 混合动力机车。

**Abstract.** *The article analyzes the development of hybrid locomotives, several hybrid locomotive energy storage methods, at the same time, introduces three technologies for using regenerative energy to improve the energy efficiency of hybrid locomotives.*

**Keywords:** *energy storage systems, energy efficiency, regenerative braking, hybrid locomotives.*

In China, building an ecological civilization is an important strategic plan of the country. As the country's awareness of green energy and environmental protection grows to meet the noise and emission requirements of urban shunting operations, hybrid (electric) shunting locomotives have become the direction of the future demand for the shunting market.

A hybrid locomotive refers to a locomotive whose drive system consists of two or more sets of single drive systems that can operate simultaneously. The so-called hybrid locomotive usually refers to a gasoline-electric hybrid locomotive, that is, a conventional diesel engine and a power battery are used as a power source.

Classification and characteristics of hybrid locomotives. The hybrid system can be divided into three categories depending on the transmission.

(1) Series hybrid system: In this system, all the mechanical energy of the diesel

engine is converted into electrical energy to drive the electric motor. This system allows the diesel engine to run at its most efficient rpm range, thereby maximizing fuel economy and reducing emissions.

(2) Parallel hybrid drive: The system includes two sets of drive systems: diesel engine and electric motor. The diesel engine is connected in parallel with the electric motor and both can drive the wheels. The electric motor can also work as a generator to charge the battery, eliminating the need for an additional generator. When the train is moving, the system uses the diesel engine as the main power source, when the train starts or accelerates, the engine works as an auxiliary driving force. When the diesel engine is in a state of low efficiency at low load, the function of the electric motor changes to that of a generator to charge the battery. When a train brakes or slows down on a descent, the Brake Energy Regeneration system is used to regenerate braking energy.

(3) Hybrid drive system: It is a combination of series and parallel drive. The control strategy of the hybrid drive system is as follows: when the train is moving at low speed, the drive system mainly operates in sequential mode.

When the train is moving steadily at high speed, parallel operation is the main method. The advantage of such a structure is that the management is convenient, and the disadvantage is that the structure is more complex.

City rail transport.

With the rapid popularization and rapid development of urban rail transport, its inherent characteristics, such as high operating density and short operating distance between stations, become more and more obvious, resulting in serious loss of braking energy during frequent starts and stops. locomotives. Theoretically, 30~40% of the traction energy required by the locomotive can be compensated by the regenerated braking energy, and the energy saving potential is huge. By efficiently recovering the braking energy, the temperature rise in the underpass can be reduced, the operating costs of urban rail transport can be reduced, and the energy load can be reduced. Therefore, the governments and research institutions of various countries have carried out a series of key technical research and development in the field of safe, reliable, high efficiency, low loss and large-scale urban rail regenerative braking system. Resistance dissipation type and chemical battery energy storage type are gradually changing to inverter recovery type, supercapacitor type and flywheel energy storage type.

The flywheel energy storage system mainly includes a flywheel rotor, a high-speed storage energy motor/generator, a support system, a power electronic converter, and a vacuum chamber.

In a battery, direct conversion of chemical energy into electrical energy occurs as a result of spontaneous oxidation, reduction and other chemical reactions inside the battery, which are carried out respectively on two electrodes. The active mate-

rial of the negative electrode consists of a reducing agent with a negative potential and stable in the electrolyte, such as active metals such as zinc, cadmium and lead, and hydrogen or hydrocarbons.

The positive active material consists of oxidants with a positive potential and stable in the electrolyte, such as metal oxides such as manganese dioxide, lead dioxide, nickel oxide, oxygen or air, halogens and their salts, oxo acids and their salts, etc. Electrolytes are the materials with good ionic conductivity, such as aqueous solutions of acids, bases and salts, organic or inorganic non-aqueous solutions, molten salts or solid electrolytes.

When the external circuit is disconnected, although there is a potential difference (open circuit voltage) between the two poles, there is no current and the chemical energy stored in the battery is not converted into electrical energy.

Common battery types: Regulated lead acid battery,

Lead Acid Gel Battery, Nickel Cadmium Battery, Nickel Metal Hydride Battery.

Supercapacitors appeared in the 1960s. Compared to batteries, they have higher performance and are more environmentally friendly. This is a very practical way to store energy. In recent years, supercapacitors have shown a booming trend in my country's emerging energy field. Many Western countries have included research projects related to supercapacitors as key national R&D projects.

The structure and capacitance principle of supercapacitors are different from traditional energy storage devices. Its operating principle is based on the capacitance effect of the electrical double layer. The electric double layer capacitor consists of four parts, including current collector, electrolyte, polarized electrode and separator. Capacitor characteristics are affected by the polarized electrode and electrolyte.

Development direction and prospects of regenerative braking technology

The new type of electric train/electric locomotive prioritizes the use of regenerative braking during the braking process and generates a lot of regenerative braking energy. Under the influence of line conditions, traffic organization, etc. The number of electric trains leaving and arriving at the railway junction is large, and the frequent deceleration and braking of the electric train makes the regenerative braking energy of the junction very rich. Usually, after the regenerative braking energy is consumed by the single-lever traction electric train and traction power supply equipment, about 50% of the regenerative braking energy is still returned to the external power grid through the traction transformer.

There are the following problems with returning a large amount of regenerative braking energy to the power grid: ① The energy efficiency is poor and the economy is poor. The recovered regenerative braking energy is billed in the form of a back-calculation or back-positive calculation (accounted as consumed elec-

tricity), which has led to huge economic losses for the railway sector; ☐ Exacerbate the power quality problem, the three-phase asymmetry of the regenerative braking return energy will have a certain impact on the power quality of the power grid (grid voltage fluctuation, harmonics, negative sequence, etc.).

The existing regenerative braking energy utilization technologies mainly include the following three types: Direct use; Feedback and use; Energy storage use.

Direct use by optimizing the organization and operation of the train, the regenerative braking energy generated by the train is consumed in a high-power resistor to avoid the regenerative braking energy being fed back into the power grid and causing power quality problems. The energy-intensive regenerative braking energy utilization scheme is easy to operate and easy to install. This is a scheme that used to be commonly used in locomotives. Since the development of power electronics technology and power electronic devices at that time, it was impossible to develop a more efficient system for using the energy of the regenerative braking of the locomotive. Installing resistors to consume the braking power generated by the locomotive was the most popular solution at the time. This technology will result in low flexibility in propulsion mechanisms, combined with a short single leg length of the traction power supply (typically 20 km) on AC electrified railways, so the regenerative braking energy utilization rate is low.

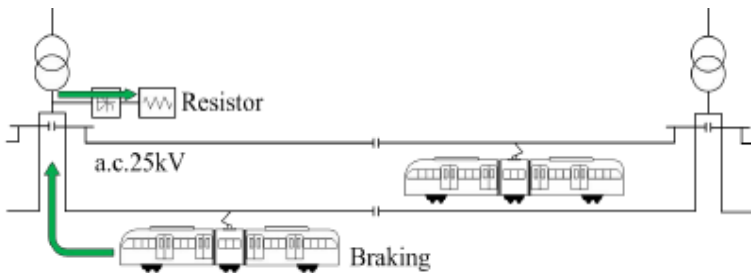


**Figure 1.** Energy dissipation of regenerative braking on a braking resistor

In recent years, the technology of energy storage and use has been actively developing in the DC power supply system of urban electric transport. The technology accumulates or releases regenerative braking energy through energy storage equipment, recuperates and uses regenerative braking energy while suppressing voltage fluctuations in the traction network, and has shown excellent performance in practical applications.

However, due to differences in power supply standards, the structure and control strategy of the energy storage system applied to the urban electric transport power supply system is not suitable for electrified railways using the AC power

supply system. To this end, an energy storage scheme based on a railway power air conditioner (RPC) has been proposed. However, compared to urban rail transport systems, the braking power of a single braking process in electrified railways is larger, the duration is longer, and the total regenerative braking energy is larger. There is more demand for the rated power and rated capacity of the energy storage system, which in turn results in higher investment costs.

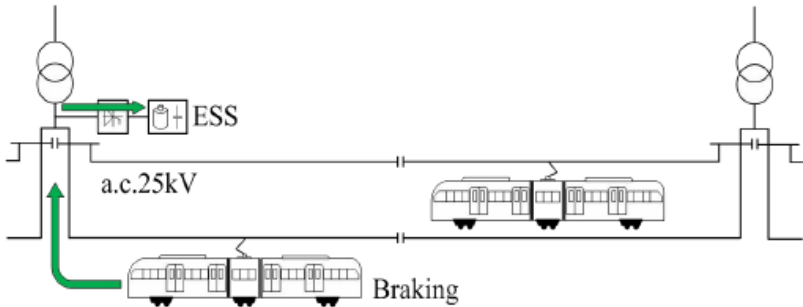


*Figure 2. Energy storage system*

The feedback technology feeds the regenerative braking energy back into the distribution network, which is called feedback inverter type. The inverter feedback circuit is designed to return the regenerative braking energy of the locomotive to the large public power grid. The principle is shown in Figure 2. According to the current concept in the field of electricity consumption, the complexity of this feedback method lies in the measurement of electricity consumption, which must be solved in consultation with the power supply distance. And since the AC railway traction load has single-phase characteristics, the single-phase regenerative braking power generated by the locomotive will cause an imbalance in the three-phase power grid when it is fed back into the power grid, thereby affecting the normal operation of other parallel three-phase loads. And there is no evidence that the returned regenerative braking power has been effectively used. In addition, when the single-phase regenerative braking power generated by the locomotive is directly fed back to the substation, it may cause the substation protection relay to malfunction and affect the normal operation of the traction power supply system. At the same time, feedback of regenerative braking energy to the power system can also cause problems such as overvoltage in the power system and the introduction of harmonics to reduce power quality in the power system. Therefore, this method of using the direct supply of regenerative braking energy back to the public power grid has certain limitations.

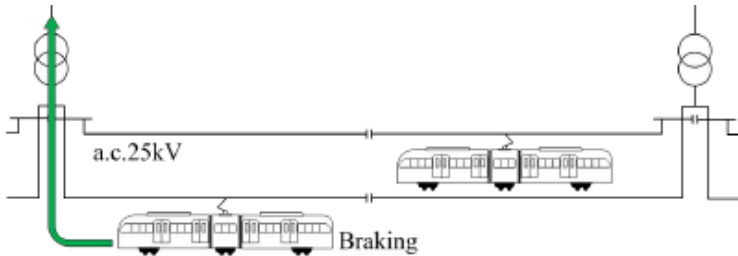


Figure 3. Supply to the general network

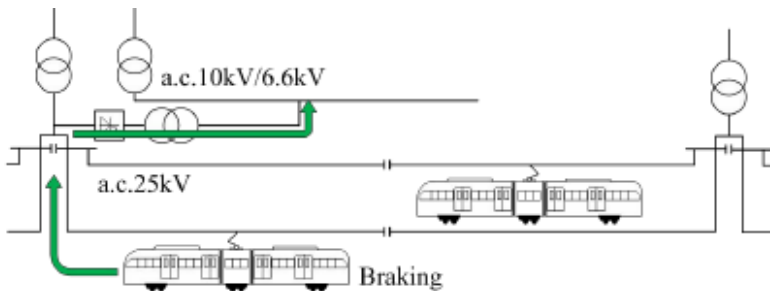


Figure 4. Supply to the distribution network

## References

1. Hao Zhiyong, Yue Dongpeng, Li Jianguo Current status and development prospects of hybrid electric vehicle research [J] // Railway rolling stock, 2003, 23(Appendix 1): 206-208.
2. Yang Jian, Li Fayang, Song Ruigang, et al. Status and Progress of Research on Brake Energy Recovery Technology for Urban Rail Vehicles [J], Journal of Railways, 2011, (2): 26–32.
3. Shang Weilin, Research of the Brake Energy Recovery Optimization Method of Fuel Cell Hybrid Electric Tram[D], Southwest Jiaotong University, 2019.
4. Huang Wenlong, Hu Haitao, Chen Junyu, Ge Yinbo, Shi Zhanghai, Energy Management and Management Strategy of the Regenerative Braking Energy Utilization System in Nodal Type Traction Substations, 2021, Issue 3 of the Journal of Electrical Technology.
5. Zhang Qiurui, Bi Daqiang, Ge Baoming. Investigation of a closed-loop inverter device for subway regenerative braking energy[J].Power Electronics Technology. 2012, 46(09): 61-63.

DOI 10.34660/INF.2022.58.51.151

混合动力机车 HXN6 和 CKD6E6000  
**HYBRID LOCOMOTIVES HXN6 AND CKD6E6000**

**Wu Yansong**

*Master's degree Student*

**Xu Jiale**

*Master's degree Student*

**Volodin Anatoly Alexandrovich**

*Candidate of Technical Sciences, Senior Research Officer, professor*

*Emperor Alexander I St. Petersburg State Transport University*

抽象的。 本文主要介绍两种不同类型的混合动力机车, 分析其运行状况, 分析国外机车的发展情况。

关键词: 混合动力机车, HXN6, CKD6E6000。

**Abstract.** *This article mainly introduces two different types of hybrid locomotives, analyzes their operating conditions, and analyzes the development of foreign locomotives.*

**Keywords:** *hybrid locomotives, HXN6, CKD6E6000.*

Diesel-electric hybrid locomotive (including diesel electric train) refers to a locomotive that can be powered by a diesel engine and a battery. Compared to a traditional diesel-powered locomotive, it has lower emissions, lower noise and lower energy consumption costs and other benefits. Currently, domestic and foreign companies are conducting research in the field of hybrid rolling stock.

Some well-known power plant suppliers have also committed themselves to the development of hybrid integration solutions and have achieved some results. The following are mainly two hybrid locomotives HXN6, CKD6E.

The HXN6 hybrid shunter locomotive is an AC hybrid diesel-electric shunter developed by CRRC under the leadership of China Railway Corporation in 2015. This type of locomotive is equipped with a NY6240ZJA EFI diesel engine and a lithium iron phosphate battery. It uses an AC drive system with main and auxiliary DC links. The maximum working power of the diesel engine is 1250 kW, and the maximum discharge power of the battery is 1500 kWh. The maximum hourly power of the DC intermediate link of the locomotive is 2200kW, the wheel

diameter is 1250mm, the drive type is C0-C0, the axle load is 25t, the minimum curve radius of 100m can travel at a speed of 5km/h. According to different loads and working conditions, the locomotive running mode is divided into traction battery running mode, diesel running mode, and mixed running mode (driven by diesel engine and battery). According to the different uses of the locomotive, the locomotive also has a shunting mode (power battery priority) and a small mode (diesel engine priority). When the locomotive is shunting at the marshalling yard, the shunting operation mode is adopted, the locomotive is first driven by the power battery, and the diesel engine is not running. When the power of the locomotive is insufficient or the power battery needs to be recharged, the diesel starts to work, and the speed is stable within the optimal range of fuel consumption. At this time, when the locomotive needs more power, the diesel engine and the power battery can jointly drive the locomotive (mixed state). When the power demand of the locomotive is low, the excess power of the diesel engine can be used to charge the battery. When the locomotive performs small work, the low work mode with diesel engine priority is adopted. During this time, the diesel engine continues to run. In case of insufficient diesel power, a power battery is supplemented. When the locomotive is moving downhill, the braking energy can be recuperated through dynamic braking,

<b>Main technical parameters of the locomotive</b>	
ambient temperature	-40 °C + 40 °C
traction drive	AC
Rail gauge	1435mm
Type of drive	C0-C0
rated power	1090 kW
shaft mass	27 t
maximum speed	80 km/h
traction force	480kN

Based on the design of CKD6E5000 and HXN6 hybrid locomotives, CRRC Ziyang Locomotive Co., Ltd. comprehensively considered the platform, modular design and standardization requirements, and combined with the customer's requirements for high-power traction Rizhao Iron and Steel Holding Group Co, Ltd., developed the CKD6E6000 heavy hybrid shunting locomotive.

CKD6E6000	
ambient temperature	-20 °C+40 °C
traction drive	AC
Rail gauge	B0-B0
Type of drive	2200 kW
Locomotive mass	150 t
maximum speed	80 km/h
traction force	560kN

The locomotive body consists of a frame and various modules. The frame consists of traction beams, side bearing beams and side beams.

The locomotive has 2 sets of two-axle bogies, and the rest of the front and rear bogies are exactly the same, except that the rear end bogies are equipped with a hand brake device. The whole bogie is mainly composed of frame, wheelset drive device, main and auxiliary suspension devices, traction device, engine suspension device, main brake device, sandbox device, accessories, etc.

During shunting work, ground-based charging equipment is primarily used. Secondly, the diesel engine is used to charge the power battery in a high-efficiency and economical area, and the power battery has a low discharge rate to complete traction. The diesel engine operates in the high efficiency region, avoiding the losses caused by the traditional shunting diesel locomotive operating in the low efficiency region and idling for a long time. When the locomotive runs in the high power section, start the diesel engine, let the diesel engine run in the high efficiency economic zone, and the lack of power is made up by the power battery. When the low position of the handle is necessary to start the diesel engine for traction, let the diesel engine run in the economic zone with high efficiency. On the one hand, it provides power of locomotive traction, on the other hand, excess energy is used to charge the power battery.

For small hauls over short distances, the diesel engine is used primarily to provide power. The diesel engine operates in the high efficiency region. When the power is excessive, the power battery is charged and the battery is kept as high as possible to meet the demand for traction.

When the driver applies the brakes of the locomotive to stop, the locomotive automatically applies dynamic braking to recover energy. When the battery is almost fully charged or the dynamic braking is not working, the air brake is automatically applied to ensure the safety of braking the locomotive. Brake Energy

Regeneration can be used to regenerate energy by engaging the driver controller with more braking power or by applying the brakes in "air-electric hybrid braking" mode. In the case of "air-electric hybrid braking", the locomotive predominantly implements electric braking, and in case of insufficient braking power, it is supplemented with air braking to reduce the need for external energy.

#### **Development of foreign hybrid locomotives**

In 2001, Canadian Railway Power Technology Corporation upgraded the American GG20B diesel shunter, released the Green Goat hybrid locomotive, and developed the GenSet series of hybrid locomotives.

In 2009, the French company ALSTOM converted the V100 series of diesel locomotives with hydraulic transmission, which used a 238 kW diesel generator set and a 102 kWh nickel-cadmium battery as a power source.

In 2010, the Japan Railway Freight Company developed the HD300 diesel-electric AC hybrid shunter locomotive, which uses a diesel engine to generate electricity and a lithium-ion battery, has a brake energy recovery function, and uses a permanent magnet direct drive traction motor.

In 2013, the French company ALSTOM developed a 3-axle hybrid AC shunter type H3 using diesel power and a nickel-cadmium battery for energy storage.

In 2018, at the 12th Berlin International Railway Technology Exhibition, France, ALSTOM introduced the H4 multi-power shunting locomotive, which has a "diesel engine + lithium battery", "grid + diesel engine" hybrid mode. There are 3 working modes, including dual power supply mode and mains + lithium battery dual power supply mode. The dual power supply mode significantly reduces the noise and carbon dioxide emissions of this type of locomotive, which can reduce carbon dioxide emissions by 6,000 tons per year.

At present, at least 5 foreign countries have developed a total of 8 series of hybrid shunting diesel locomotives, of which 6 have been mass-produced and put on the market.

Looking at the products and developments of hybrid electric locomotives at home and abroad, it can be seen that: 1. With the world's increasingly serious energy and environmental problems, more and more railway equipment suppliers are committed to the research and application of hybrid electric technology. As of 2018, there are at least 9 out of 6 countries in the world.

Railway equipment suppliers are engaged in the research and development of hybrid shunting locomotives, and from 2010 to 2018, each supplier launched a total of 10 types of hybrid shunting locomotives, 5 of which were launched only in 2018. It can be seen that the hybrid shunting diesel locomotive is the direction of development of the shunting diesel locomotive of the future.

## References

1. Meng Yu, He Guofu, Liu Shongguo, et al. *Research on shunting adaptability, economy, and environmental protection of the HXN6 hybrid shunting locomotive [J]. Railway rolling stock, 2018, 38(1): 37-42.*
2. Juan Lucy. *New developments of hybrid electric locomotives in the country and abroad [J]. Railway locomotives and electric trains, 2018(6): 1-5.*
3. Zhu Yandong, Ren Cong, Meng Yufa, Peng Changfu *CKD6E6000 Locomotive Electric Drive 2020 High Axle Load Hybrid Shunting Locomotive Design (1)*

交流机车电气设备  
AC LOCOMOTIVE ELECTRICAL EQUIPMENT

**Jing Chao**

*Emperor Alexander I St. Petersburg State Transport University*

抽象的。使用交流牵引电动机的交流机车根据牵引电动机的性质,还可分为单相整流电力机车、分离电力机车、同步电力机车等。中国交流电力机车,现代直流电力机车,接触电压单相电源,频率25KV,功率3200~4800KW,用于干线电力牵引。韶山4号交流机车,开发于1980年代,功率6400kW,最大牵引力628kN,最高时速100km/h,机车综合效率82%以上,功率因数为大于0.85。

关键词: 阀门、VL80S电力机车变压器、车顶设备

**Abstract.** *AC locomotives using AC traction motors can also be divided into single-phase rectifier electric locomotives, separator electric locomotives, synchronous electric locomotives, and so on according to the nature of their traction motors. Chinese AC electric locomotives, modern DC electric locomotives, contact voltage single-phase power, frequency 25KV, power 3200~4800KW, used for mainline electric traction. Shaoshan type AC locomotive 4, developed in the 1980s, has a power of 6400 kW, a maximum traction force of 628 kN, a maximum speed of 100 km/h, an overall locomotive efficiency of more than 82%, and a power factor of more than 0.85.*

**Keywords:** *Valve, VL80S Electric Locomotive Transformer, Roof Equipment*

An AC locomotive consists of two parts: the electrical system and the mechanical structure. The electrical system includes a collector, a main switch, a high power traction transformer, 4 to 6 traction motors, two sets of drive control equipment, a set of converters consisting of thyristors or tripping thyristors, auxiliary motors of various capacities and a large number of electrical and electronic devices. In addition, there are communication facilities, instruments, and some electric locomotives are also equipped with computer control devices. The traction motor is mounted on the axle and bogie, and the traction force is transmitted through the gears. The collector is mounted on the roof, while the rest of the electrical equipment is inside the car. The mechanical structure is mainly composed of car body, frame and steering frame. The body of the car is attached to the bogie through the frame, and the bogie distributes the weight of the locomotive evenly

on each wheel pair through an elastic support device and an axle box. The load capacity of each axle of Chinese electric locomotives is 23t

### **An overview of the electrical equipment of an AC locomotive**

The power of a four-axle diesel locomotive with a three-phase AC drive is limited not by the bogie, but by the mass and volume of electrical equipment installed on the body of the locomotive. The use of a small-sized traction motor without a commutator makes it possible to reduce the weight of the bogie, which is also beneficial from the point of view of running technology. On the body of the locomotive, in addition to a relatively heavy 16 Hz transformer, a braking resistor and an auxiliary transmission device, a converter and a smoothing element are also installed.

The transformer supplies power to four converters through four secondary windings. The converter consists of a four-quadrant regulator and a pulse inverter, the intermediate link of which is a constant voltage. The 4-quadrant controller generates 4x phase shift pulses for optimum network conditions. Each two converters have a common set of control and adjustment devices and are connected to the same group of three-phase buses to drive the traction motor on the bogie.

In the field of high clutch utilization, the advantages of using busbars in traction technology have been proven by the experience of operating diesel locomotives, industrial and mine locomotives driven by three-phase alternating current. In addition, the use of a busbar system on the bogie can reduce the cost of control and adjustment devices (represented in economy), and there is hope that the use of two sets of transfer devices can be used to improve the performance of the locomotive. using a trolley type power supply. The power frequency is 16% Hz, the locomotive axle type is B-B, the power of its wheelset is 6.6 MWh, the intermediate link voltage is 2.8 kV, and the thyristor components used can be obtained economically, be well matched to the power of the engine and the power of the transformer installed on the locomotive.

In order to fully exploit the potential of the installed power, the best solution is to connect a preset motor choke between the inverter and the motor. This can reduce high order harmonics, allowing the inverter and motor to have a large continuous current in the low speed range. To get higher thrust in the high speed range, a three-phase contactor shunted to a given choke will short it out. The transformer must be designed to continue to pull the load required for transport while maintaining the weight limit of that heaviest component. A certain amount of thermal power must be taken into account in the conditions of passenger transport. It can be expected that the temperature of the transformer will not reach the limit value even with a locomotive pull of up to 700 tons.

### Features of alternating electric current

The properties of alternating current are significantly different from the properties of direct current, we know this from the course of physics. One of its very positive properties is the possibility of transformation, that is, the magnitude of the current can be changed, increased or decreased, so to speak, transformed. This is achieved by using such electrical devices as current transformers, which are both step-down and step-up. It is with the use of transformers that the voltage is adjusted on the traction motors of AC electric locomotives.

But after all, DC traction motors (TM) are installed on these electric locomotives, how do all these devices work in one circuit? Basically, it's easy. Alternating current before entering the TM after passing through the transformer is rectified in installations called rectifying devices (RD). Semiconductor rectifiers are installed in them - diodes, called in the professional language "avalanche valves" (AV), and from the physics course, we certainly know that the diode has the property of "rectifying" alternating current into direct current (remember p-n junctions, hole conductivity and all such).

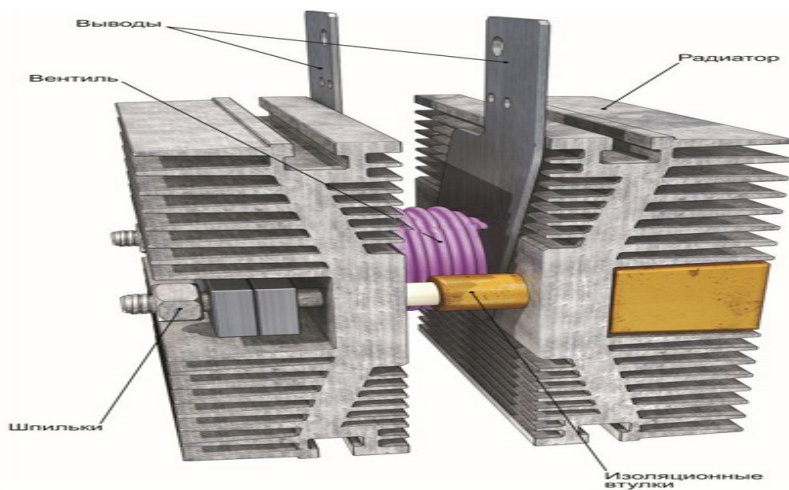


*Figure 1. Valve (rectifier diode)*

Direct current is constant because it flows invariably from plus to minus, without changing direction and anything else, it can be depicted as just a straight line. But the alternating current behaves differently, it constantly changes its direction and amplitude, if we draw it on a graph, we will get a wave pattern. So the top and bottom of this very wave we have drawn are called half-cycles, and a diode

(valve) is a semiconductor device that passes current in only one direction (one half-cycle), so the rectified current becomes more or less similar to direct current.

#### **AC locomotive device**

The roof equipment includes, in addition to the collector, the main switch (MS), fan air shutters, insulators, busbars and intersection shunts, main air tanks connected by pipelines.

The power circuit of the electric locomotive is connected to the current collector by the main switch (MS) - a pneumatic contactor, which also turns off the power circuit in case of overloads and abnormal operating modes. In terms of dimensions, it is smaller than the high-speed switch (HS) of DC electric locomotives, therefore, unlike the HS, it is installed on the roof, and not in the body.

#### **These are installed in the body:**

- the traction transformer itself (usually in the middle), rectifier installations (usually above each bogie),
- rectifier excitation unit (REU),
- fan motors,
- motor-compressors,
- phase splitters,
- reversers,
- brake switches,
- installations for switching air (UPV),
- ballast resistors (for electric braking),
- power electro-pneumatic and pneumatic contacts, contacts of control circuits and other devices necessary for the operation of an electric locomotive.

All these devices are placed in a high-voltage chamber (HVC), divided into blocks of power devices (BPD). Low-voltage electrical contacts and control circuit relays are located on panels that are not covered by protective shutters.

There are more fans installed than in permanent ones, from 3 to 4. In freight electric locomotives, one motor-compressor is installed in a section, and two in single-section passenger ones. The traction transformer is a rather large structure, it is placed in a large housing, inside which transformer oil is filled, cooled in the cooling circuit by distilling the oil through the external cooling sections with a special oil pump, on the roof of the transformer its main input and outputs are located on insulators.

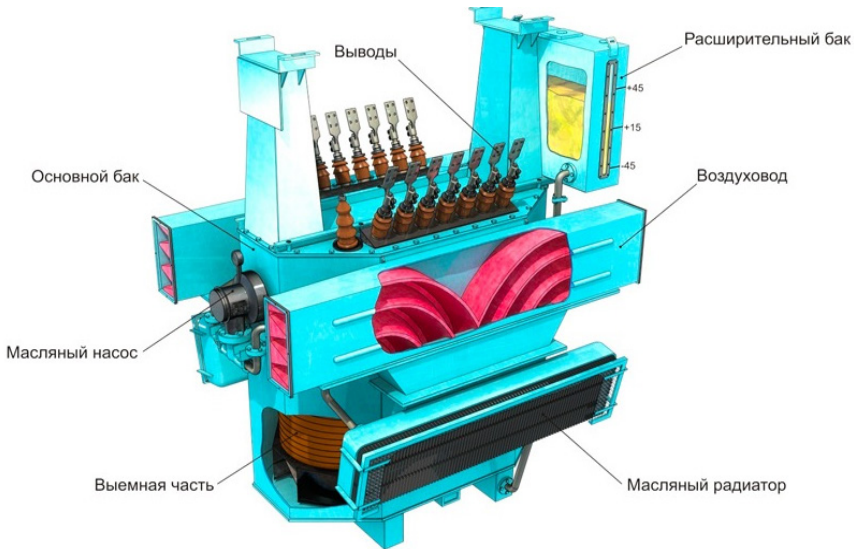


*Figure 2. Electric locomotive VL80S transformer*

Fans cool all TMs, rectifiers, ballast resistors during electric braking. Electric motors of fans, motor-compressors and oil pump are asynchronous, alternating current, this whole group is called - auxiliary machines.

How much? Of course, this is why the electric locomotive is heavier and more complicated. And how does it all work? Let's start to figure it out.

#### Using

##### 1. Collector

###### (1) Basic structure of collector

TSG3-630/25 single arm collector is composed of chassis, pincer chain mechanism, nose head, transmission mechanism, control mechanism, etc.

###### (2) Role of collector

The pantograph is a current-collecting device of electric locomotives and electric vehicles for receiving current from the contact wires of the contact network. It is installed on the roof of electric locomotives and electric vehicles through insulators. When the collector is raised, its retractable plate is in direct contact with the contact wires, and the current is taken from the contact wires and transmitted inside the locomotive through the busbar on the roof for power.

###### (3) Maintenance and service

Before use, check whether all fasteners are in good condition, whether the soft braided wire is intact and whether it is necessary to replace the broken wires in

time, whether the insulator is clean and not cracked, whether the arc of the sled is flat, whether the connection is smooth and worn to the limit. Sliding plate and grease should be replaced in time.

## 2. Gear switch

### (1) Structure of TKX4 type transfer switch

The TKX4 type switch is mainly composed of a frame, a drum, a pin rod, a transmission cylinder, a chain foot, and so on.

### (2) The role of transfer switch TKX4

Before starting the locomotive, the driver must first determine whether the position of the locomotive direction switch matches. This switching is carried out by the driver manipulating the reverse handle. When the switch completes the conversion work, the cam mounted on the rotating shaft and the blocking contact installed on the bottom plate are also converted, opening and closing the corresponding blocking contact in the control circuit, so that the automatic switch will not be converted into a non-blocking contact working state.

## 3. High voltage connector

### (1) The role of high voltage connectors

The high voltage connector is mainly composed of a mechanical transmission mechanism and an electrical connection mechanism.

When two cars are to be connected together and work in reconnection, the two connectors are slowly approached by the pulling force of the two car couplers when they are connected. Insert it into the plug from the other side, and connect the high voltage circuit on the primary side of the two vehicles. At the same time, the extension spring on the fork holds the half ring. Since the relative displacement of the two connectors is absorbed and controlled by the extension spring and the return spring, the contact pressure between the fork and the half ring can be maintained. constant, thus can provide better electrical performance.

When two cars are separated, they can be automatically separated by the traction force, when the two cars are separated, and the high voltage circuit of the primary side of the two cars is cut off, and the tension spring is restored.

The current path of the high-voltage connector in the on state: from the high-voltage circuit of one car to the current conductor, through the connecting wire, to the current conductor, and then through the soft wiring of the flared head, half ring, plug, to other plug, half ring, conductive bus, etc. of the station connector, and then to the roof rail of another car.

## 4. Main circuit breaker

### (1) Basic structure of the main circuit breaker

The air circuit breaker TDZ1A-10/25 is limited by a lower plate made of cast aluminum sheet, installed on the roof of the locomotive, and is divided into upper and lower parts. The high voltage part is exposed on the roof, mainly including arc

chute, non-linear resistance china bottle, supporting china bottle, isolation switch and rotating china bottle. The low pressure part, installed at the bottom of the bottom plate, mainly includes the storage cylinder, the main valve, the delay valve, the transfer cylinder, the starting valve, the auxiliary switch and other components.

(2) The role of the main switch

The main switch is connected between the collector and the primary winding of the main transformer and is installed in the middle of the roof of the locomotive. And it is the main power switch of the electric locomotive and the general protection device of the electric locomotive. locomotive. When the main switch is turned on, the locomotive receives power from the contact network through the pantograph and is put into operation in case of a short circuit, overload, grounding, etc. the signal passes through the corresponding control circuit to make the main circuit breaker automatic shutdown to cut off the main power supply of the locomotive, to prevent the fault range from expanding.

(3) The role of the main switch

The main switch is connected between the collector and the primary winding of the main transformer and is installed in the middle of the roof of the locomotive. And it is the main power switch of the electric locomotive and the general protection device of the electric locomotive. When the main switch is turned on, the locomotive receives power from the contact network through the current collector and is put into operation if a short circuit occurs in the main and auxiliary circuits of the locomotive.

In the event of a short circuit, overload, grounding and other faults, the fault signal will automatically open the main switch through the corresponding control circuit, cut off the main power of the locomotive, and prevent the fault from expanding.

### **Conclusion and perspectives**

A three-phase AC drive system for locomotives powered by 182 Hz AC, developed in stages since 1971 in close cooperation with the Munich Federal Railway, can provide a locomotive with versatile traction performance. In order for the B-B axis formula

The locomotive can be installed with the required large power, and great efforts must be made to design each part and its reasonable location on the locomotive, cable laying, air and oil cooling.

Thanks to the close cooperation of companies such as KraussMaffei, Krupp and Thyssenenschel, as well as the clear goals of the Munich Railway Administration, the locomotive was successfully completed on time.

This new drive technology, like all prototype devices used to enter a new technological era, first requires restarts and various tests. Therefore, the system must

be in optimal condition so that sea trials of the five locomotives can be carried out successfully and more smoothly. Sea trials and trials should be carried out as soon as possible in order to create conditions for the production of the diesel locomotive type 120.

### References

1. *Publication used in preparation for the lesson*
2. *Translated from West German <EB> 1977, N10, 272-283 Translator: Luo Yuanmou, proofreader: Fan Junhua.*
3. *Zhang Dayong. Development of electric drive technology for Chinese locomotives [J]. Electric locomotive drive, 2007(3): 1-4*
4. *Li Chunyan. Development of power electronic devices and electric traction drives [J]. Scientific Chinese, 1998(5): 54-56.*

无刷牵引电机在牵引机车车辆上的应用前景  
**PROSPECTS FOR THE USE OF BRUSHLESS TRACTION MOTORS  
ON TRACTION ROLLING STOCK**

**Huang Jingxuan**

*Master's degree Student*

**M.Yu. Izvarin**

*Candidate of Technical Sciences, Associate Professor*

*Emperor Alexander I St. Petersburg State Transport University*

抽象的。无刷电机是一种新的电机技术，被迅速引入高科技电器和电动汽车（如特斯拉 Model S），以替代有刷直流电机。它们在爱好飞机中也非常常见，包括多引擎飞机。因为无刷直流电机没有换向器或电刷（显然），所以它们的工作不受有刷直流电机的许多限制。

关键词：无刷电机，异步牵引电机，电机技术，电机设计

**Abstract.** *Brushless motor is new motor technology rapidly being introduced into high-tech appliances and electric vehicles (such as the Tesla Model S) as a replacement for brushed DC motors. They are also extremely common in hobby aircraft, including multi-engine ones. Because brushless DC motors don't have a commutator or brushes (obviously), they work without many of the limitations of brushed DC motors.*

**Keywords:** *Brushless motors, Asynchronous traction motors, motor technology, motor design*

### **1. Increasing power and traction.**

In accordance with the trends that have developed in recent years, the traction force of an electric locomotive when starting off should be 300-320 kN for a four-axle section, and the end of the hyperbolic section of the traction characteristic is in the region of speed 120-160 km/h for freight and 200-220 km/h for passenger locomotives and multi-unit electric trains. The continuous power of such an electric locomotive must be at least 6000 kW with the possibility of its short-term increase to 6400 kW. This does not mean that such power is typical for all types of electric locomotives, but it is obvious that it will be higher than 1100-1500 kW per axle.

If until recently, the main traction motor of domestic manufacturers was a

commutator, and foreign - asynchronous, then over the past 2 years, almost all the world's major manufacturers of EPS have also PMSM - traction motors based on permanent magnets. Such a significant advancement of this technology is associated with the creation of new alloys with an induction approaching 1.5 T. Will traction motors with permanent magnet excitation replace collector and asynchronous motors? The question is not entirely clear. The advantages are obvious - brushless motors have more power for the same volume and weight.

## **2. How a brushless DC motor works**

Brushless DC motors are commonly used in multi-engine aircraft because of their high speed and efficiency.

Like brushed DC motors, brushless motors work by reversing the polarity of the windings inside the motor. The magnetic fields created when the windings are energized exert a pushing effect on the permanent magnets located around the outer casing.

On a brushless DC motor, it is not the motor shaft that rotates, but the outer casing. Because the central shaft to which the windings are attached is stationary, power can be applied directly to the windings, eliminating the need for brushes and a commutator.

Without brushes, brushless motors wear out much less quickly than brushed DC motors. They operate with much less audible and electrical noise and are capable of operating at much higher speeds.

Brushless DC motors have only recently come into use in consumer products and hobby projects because they are difficult to control.

While brushed DC motors simply use the rotation of the motor itself to change the polarity of the windings, brushless DC motors are actively controlled and require complex winding control circuitry that must also scale with increasing speed.

Only because microcontrollers have become cheaper and more affordable has it become possible for low-cost systems to be able to maintain the correct rate of rotation needed to run an engine.

## **3. Technical characteristics of trains with asynchronous motors**

The desire to use the simplest electric machine - an asynchronous squirrel-cage motor - is associated with the entire history of the development of electric traction. However, the question of the widespread introduction of asynchronous traction motors was raised only after the advent of power semiconductor controlled devices - thyristors. The rapid development of semiconductor technology is the key to success in the widespread use of electric rolling stock (ERS) with asynchronous traction motors, which began in the 70s.

On the first domestic electric locomotive VL80 with asynchronous traction motors (ATD), thyristors TL200 for a current of 200 A and an operating voltage of 800 V were used. Thyristors for currents up to 2500 A and an operating voltage of up to 4500 V were created and used. 180 thyristors TL200. As the production

of thyristors for one traction motor develops, 6-12 thyristors will be used in the inverter link. If the mass of the thyristor converter per 1kV·A power was at first 5–8  $\kappa\gamma/(\kappa\text{B}\cdot\text{A})$ , then for the more advanced electric locomotive E-120 this figure is 1.05  $\kappa\gamma/(\kappa\text{B}\cdot\text{A})$ . Even more striking are the successes in the development of the elemental base of control systems—microelectronics. Integrated circuits and microprocessors dramatically simplify the design of control systems and increase their reliability. The pace of development in this area is such that every 5-10 years a new generation of instruments appears.

Converters of many types require forced switching of thyristors, which is associated with the need to complicate the converter circuit and use capacitors, the mass of which is still significant. Thyristors of a new type are being developed and are already being used, which are locked along the control electrode. Their widespread use will make it possible to drastically reduce the mass of converters per unit of power, simplify them, and increase reliability.

Thus, there are sufficient prerequisites for the widespread introduction of an asynchronous traction drive both in railway and urban transport.

When using an asynchronous traction drive in electric traction, the following advantages can be realized:

1. significant simplification of the traction motor in comparison with the collector one and increase in its reliability (there is no need for daily inspection of the collector-brush assembly);

2. increasing the reliability of body electrical equipment due to the use of non-contact power conversion devices;

3. improvement of the traction properties of electric locomotives due to the use of a rigid traction characteristic during boxing. There are experimental results showing the possibility of increasing the friction coefficient by 20–40% [1];

4. increase in the power and torque of the traction motor with the same overall dimensions (there are no collector, windings of additional poles and compensation);

5. the possibility of full automation of the train driving mode;

6. improving the performance of ERS due to the implementation of the benefits of paragraphs. 3-5;

7. reduction of copper consumption for the manufacture of traction motors. According to the results of designing the latest samples of pulsating current collector traction motors and asynchronous traction motors, the consumption of copper for the manufacture of the latter is reduced by 2–2.5 times.

These advantages leave no doubt about the advisability of widespread introduction of asynchronous traction motors in electric traction. The available experience in the design and operation of ERS with these engines fully confirms that.

The load modes of traction motors are determined not by the type of motor, but by the operating conditions for a particular type of ERS. For example, a freight

electric locomotive (Figure 2.1, a) is characterized by the greatest realizable traction force  $F_{max}$  during acceleration (speed range) and, accordingly, an increase in power  $P$  in this section, proportional to the increase in speed  $v$ , conservation of power in the speed range, where, naturally, traction force  $F$  decreases. Finally, at speeds, the power decreases in accordance with the shape of the traction characteristic in this section.

Freight electric locomotives are characterized by a ratio of maximum speed to nominal, approximately equal to 2. The power developed by the traction motor at maximum speed for freight electric locomotives is less than the nominal one and usually amounts to (0.5-0.6)  $P_{nom}$ . The forms of load curves (see Figure 2.1, a) are due to the need to develop the highest power at the end of the acceleration of the electric locomotive and maintain it when moving on the leading rise.

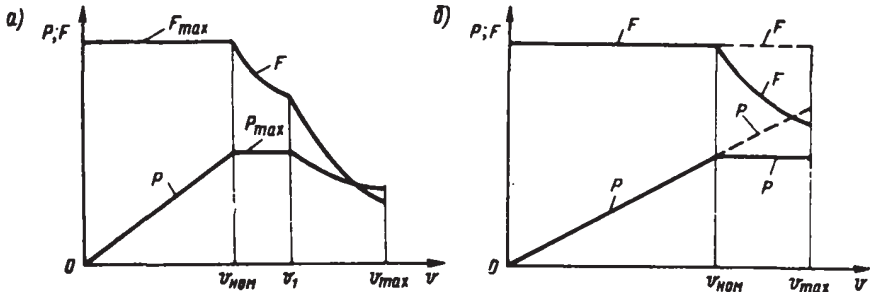


**Figure 2.1.** Characteristic dependences of power and traction force on the speed of movement for freight electric locomotives (a) and passenger electric locomotives and electric trains (b)

When the train moves on the site in the speed range, the required traction force is sharply reduced.

The ratio of the maximum speed to the nominal speed is usually 1.4–1.6 (Figure 2.1, b) for passenger electric locomotives and electric trains with a maximum speed of 130–160 km/h. Due to the significant influence of the aerodynamic resistance of the train on the overall resistance to movement for passenger electric locomotives and electric trains, it is desirable to maintain the design power in the speed range.

If the maximum speeds of electric locomotives or electric trains are increased to values of 200–250 km/h, then the power and traction curves will look like those shown in Figure 2.1, 6 dashed lines. At high speed, aerodynamic drag will dominate over all components of rolling resistance, including ascent resistance. For this reason, it will be necessary to develop maximum power at maximum speed. Naturally, the traction force must remain the greatest both during acceleration and

at maximum speed.

Electric rolling stock with an asynchronous traction motor powered by a thyristor converter must implement efficient electric braking with braking energy return to the network. For the considered ERS, the power of the electric brake, as a rule, does not exceed the power of the traction mode. Therefore, the power and braking force curves are usually close to the corresponding traction mode curves.

Subway electric trains are subject to specific power requirements. In traction mode, the starting power  $R_p$  is usually limited by the throughput of power supply devices (maximum current per car). This causes the ratio of velocities at the level  $v_{max}/v_{HOM} = 2.54-3.5$ . In the electric braking mode, there are no severe restrictions on power supply devices, since the recuperated energy is largely consumed by neighboring trains operating in traction mode.

In other words, the power of the traction motor in the braking mode should be at least 2 times the starting power of the traction mode. In this case, the speed of the start of intensive braking is usually 2 times higher than the speed of reaching the starting power in the traction mode, since the limiting traction and braking forces should be approximately the same. Sometimes at speed  $v_{max}$ , it may be necessary to reduce power in traction and braking modes due to the condition of static stability of asynchronous traction motors.

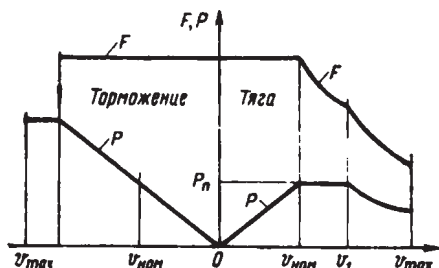


*Figure 2.1. Characteristic curves of power and traction for electric subway trains*

The curves shown in Figure 2.1, 2.2 give an idea of the loads of different types of ERS asynchronous traction motors. Quantitative ratios are approximate. They are specified in the terms of reference for the design of a specific ERS sample.

According to the given power curves, it is possible to obtain current load curves if we set the pattern for changing the voltage of the traction motor in the entire range of speed changes from 0. Here and below, the phase voltages and currents of the traction motors, as well as the connection of the stator windings into a star, will be taken into account.

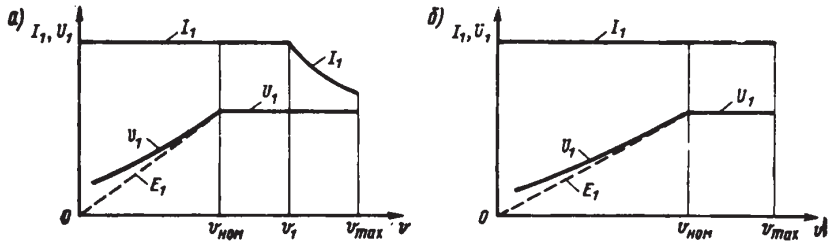


**Figure 2.3.** Curves of phase voltages and currents for a freight electric locomotive (a) and a main high-speed electric train (b) ( $E_1$ —phase EMF of the stator winding)

For most types of ERS, it is advisable to combine the rated voltage  $U_{nom}$  with the rated speed, assuming that it will remain unchanged in the speed range, i.e.,  $take = const$  here. Sometimes it may be appropriate to slightly increase the voltage and in the speed range.

To ensure the greatest and constant traction force in the acceleration zone, the largest phase current is required,

also unchanged in value. These considerations, given the nature of the change in power, completely determine the current loads of traction motors for the considered ERS. They are shown in Figure 2.3, a and b as an example for a freight electric locomotive and a main high-speed electric train.

Naturally, the curves shown in Figure 2.3, a and b, only approximately reflect the true current loads, which are specified for a particular type of ERS.

The electromechanical characteristics of traction motors determine the traction characteristics of the ERS, which largely reflect its traction properties and load conditions in operating modes. For any type of traction motors, traction characteristics must meet two requirements:

1. the number of characteristics should be such that, if possible, the entire traction area is covered, taking into account the restrictions;
2. The control system must provide the possibility of continuous operation at any point in the traction area.

With regard to asynchronous traction motors, two additional requirements should be introduced:

1. the specified traction characteristics must be provided under operating conditions without significant complication of the control system;
2. The control system must shape the traction characteristics in such a way as to ensure their rigidity during boxing, regardless of the shape of the characteristic in the traction mode.

Since the asynchronous traction drive has the ability to smoothly adjust the voltage and frequency, the 1st requirement is easily met. There are no difficulties for fulfilling the 2nd requirement. The expediency of taking into account the 3rd requirement will be shown below.

The slope of the characteristics is not of great importance, which is important, for example, for DC traction motors. It is only necessary that the 4th requirement be met, i.e., the traction characteristic can be soft, like in sequential excitation engines, but it must become “hard” when the clutch is broken. This requirement can also be provided by means of regulation by delaying the increase in the frequency of the supply voltage when the load is dropped at the traction motor in the event of a clutch failure. In this case, there will be no reduction in the traction force of the electric locomotive.

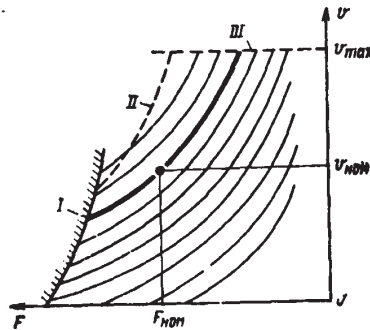


Figure 2.4. Traction characteristics of an electric locomotive

Figure 2.4 shows the traction performance of an electric locomotive with limitations common to electric traction drive. Traction characteristics are "soft" and roughly correspond to the characteristics of constant power. Curve I is the linkage constraint; curve II - by power; curve III - by design speed. The thickened curve in Figure 2.4 corresponds to the tractive characteristic, on which the point with the nominal parameters is located.

The material of paragraphs 1.1-1.3 basically exhausts the general operating conditions and requirements for the output parameters of asynchronous traction motors. Further evaluations must be made when considering an asynchronous traction motor in combination with a converter feeding it, which will be presented below.

### Conclusion

Advantages and disadvantages of brushless DC motors.

Low wear—The only physical interface between the rotating outside of the motor housing and the stationary windings inside are ball bearings, which means

brushless DC motors wear out very slowly.

**High Speed**—Brushless motors have much less friction than brushed DC motors, so they can run at higher speeds.

**High Efficiency**—Compared to other types of motors, brushless motors have very high running efficiency, which means lower power consumption for the same output compared to DC brushed motors.

**Very High Control Complexity**—Brushless DC motors require specialized controllers and complex control algorithms to operate properly.

**High price**—The cost of the motors themselves is not too high, but when the cost of the controller is added, the overall cost of using a brushless DC motor in a project becomes relatively high.

**Need for Specialized Gears**—In applications such as Dyson vacuum cleaners, brushless DC motors must be equipped with a gear to convert high speeds to the correct speed.

## References

1. *Boyko E. P. General purpose asynchronous motors E. P. Boiko, Yu. V. Gaintsev, Yu. M. Kovalev, and others; edited by V. M. Petrov and A. E. Kravchik. Moscow: Energiya, 1980.*
2. *Bulgakov A. A. Frequency control of asynchronous electric motors: A. A. Bulgakov. 2nd edition: Nauka, 1966.*

铁路车辆车钩缓冲装置磨损分析  
ANALYSIS OF THE WEAR OF THE BUFFER DEVICE OF THE  
RAILWAY VEHICLE COUPLER

**Zhang Chunyang**

*Master's degree Student*

**Xu Yiming**

*Master's degree Student*

**Chudokov Alexander Ivanovich**

*Candidate of Technical Sciences, Associate Professor*

*Emperor Alexander I St. Petersburg State Transport University*

抽象的。卡车牵引缓冲装置的主要磨损件是牵引台、牵引销孔和从动板。采用光学显微镜、扫描电镜和X射线能谱仪对运行磨损后的离合器缓冲装置进行切割取样,分析离合器缓冲装置主要磨损部位的表面磨损情况和断面及其磨损失效情况。机制揭晓。结果表明:磨损和分层是离合器牵引台配合面的主要磨损机制。冲击磨损是离合器销孔的主要部分,其破坏机制主要是磨粒磨损和分层;冲击磨损和磨粒磨损是主要的磨损机理,磨损机理主要是磨粒磨损、分层和氧化。

关键词: 离合器缓冲装置; 故障分析; 穿。

**Abstract.** *The main wear parts of the truck hitch buffer device are the hitch traction table, the hitch pin hole and the follower plate. By cutting and sampling the clutch buffer device after operational wear using an optical microscope, a scanning electron microscope and an X-ray energy spectrometer, the surface wear conditions and sections of the main wear parts of the clutch buffer device are analyzed and its wear failure mechanism is revealed. The results show that: abrasion and delamination are the main wear mechanisms on the mating surface of the clutch traction table. Impact wear is the main part of the clutch pin hole, and the damage mechanism is mainly abrasive wear and delamination; impact wear and abrasive wear are the main wear mechanisms, and the wear mechanisms are mainly abrasive wear, delamination and oxidation.*

**Keywords:** *Clutch buffer device; failure analysis; wear.*

The coupler buffer is a vehicle component used to connect vehicles and vehicles, locomotives and vehicles to each other, transfer and absorb the traction and

shock force generated by the train during operation, and plays an important role in ensuring the safe transportation of vehicles. With the ever-increasing speed and load of rail traffic in my country, coupler failures often occur due to inadequate maintenance and use of the daily coupler's buffer device.

#### 1 Principle of operation and operating parameters of the coupler buffer device

The hitch buffer device, as a key component for traction and impact reduction, is used in almost all vehicle couplings. The reasonable connection method not only ensures the reliable operation of vehicles, but also reduces the impact between vehicles, and its various characteristics are also directly related to each other. The hitch buffer device is usually installed at both ends of the bottom of the vehicle as a whole. Regardless of whether the hitch buffer is subjected to traction or impact force, the longitudinal force must be transmitted through the buffer. When the hitch buffer is tensioned, the force transmission process is as follows: clutch → hitch frame → rear pusher plate → buffer device → front pusher plate → front pusher plate seat → draw bar. When the clutch acts on the buffer device, the force transfer process is as follows: clutch → front driven plate → buffer device → rear driven plate → rear driven plate seat → traction beam. When analyzing the longitudinal dynamics of a train, adjacent test coupler buffers are often connected in series to maximize the coupler buffer energy in tension (compression), the buffers are deformed. The main operating parameters of the hitch buffer device are stroke, maximum force, capacity and absorption rate.

#### 2 Overview of clutch wear

##### 2.1 The main factors affecting the breakage and separation of the hitch

1) The strength of the coupling is reduced when it is found that the crack of the coupling is repaired and heat treated, it is difficult to meet the technological requirements due to welding repair and heat treatment. Strict control of temperature, holding time and cooling rate is an important guarantee that the coupling meets strength requirements. An incorrect control process often makes it difficult to remove old cracks and causes welding defects, and may even lead to additional stress concentration and reduced coupling strength. 2) There are cracks or defects in the loaded part of the coupling. According to statistics, due to stress concentration, the stress on hitch hook eye, hook neck, hook arm and other parts is much larger than other parts. In addition, in 2014, Xining East Depot's repair cart hitch tongue failure rate was 10.42%, and most of the reasons for failure were cracks in the hook at the corners of the medial side of the tongue. Therefore, damage occurs most often in these parts. 3) Misuse of the locomotive or abuse of emergency braking. Maneuvering speeding, illegal decompression, or emergency braking during use often results in violent collisions between locomotives and vehicles, and between vehicles. This collision force is very detrimental and often causes failures such as deformation and damage to accessories.

## 2.2 The main parts of the coupling are damaged

1) Clutch breakage causes separation, mainly including hook tongue breakage, hook ear breakage, hook neck breakage, hook tail breakage, plate breakage, plate seat breakage, etc. 2) The shock absorber is damaged or out of order, or broke off the plate, causing the buffer device of the clutch to break under the influence of a large impact force, which led to the separation of the clutch. 3) The clutch frame is broken, causing the clutch to separate. 4) The hitch bolt or hitch pin is broken, causing the hitch pin to fall off and the hitch to separate. 5) The hitch beam or hitch assembly bolts are torn off, causing the hitch beam to fall and the hitch to separate. 6) The rivet on the seat of the plate is broken, which led to the separation of the coupling.

## 3 Wear analysis and discussion

Most of the wear parts are under the hook body and eye holes, followed by the side wall of the hook lock cavity, the anti-jump platform in the hook lock cavity, and the butt and tail side of the hook. The wear of the connector will weaken the strength of the connector, which will greatly affect the efficiency of using the connector. Once the jump protection platform is worn out, it will even cause the clutch to lose its jump protection function.

### 3.1 Hook hole

The clutch pin hole connects the clutch to the clutch frame through the clutch pin to allow the vehicle to perform the coupling, traction and buffering functions. When the truck is running, there will be working conditions such as starting, stopping, accelerating, decelerating, crossing a curve, driving up and down a slope. Because the hook pin hole and the hook pin are installed with clearance, there will be shock and friction between them. Wear and other effects will cause wear on the curved surface of the hook pin hole. If the rolling marks on the wear surface are multi-directional and relatively disordered, this indicates that the wear surface has experienced multi-directional friction and rolling force, which can be mainly due to the fact that it is caused by relative slip and impacts in different directions in the mating surfaces between the hook pin hole and the hook pin during starting, braking or shifting of the railway freight car, and plastic deformation obviously occurs. The shape of this rolling track is determined by the state of movement of the clutch during actual operation.

### 3.2 hook tongue piece

Two faults - cracks and wear - are the most important faults that occur on a joint. The vast majority of cracks occur at the top and bottom corners of the inside of the steering knuckle, and cracks can often occur at the drawbar, knuckle pin hole, and at the base of the shock arm. The most common part where wear occurs is the inside of the hook, followed by the tail side of the hook and the hole for the hook pin.

### 3.2.1 Failure cause analysis

The failure of the hook tongue is mainly caused by a relatively large impact force or a defect in the manufacturing process.

### 3.2.2 Prevention and treatment measures

1) When performing segmental repairs, flaw detection must be carried out at the corners of the traction surface of the hook tongue and at the upper and lower corners. 2) Welded repair - when the total length of cracks in the upper and lower corners of the inner side of the steering knuckle is not more than 30 mm. After welding, it must be subjected to heat treatment. If exceeded, replace. If the length of the crack in the middle part of the drawbar of the bogie hitch does not exceed 60 mm, it should be repaired by welding. 3) Welding should be carried out when the total length of arcuate cracks at the base of the hook traction lug does not exceed 30 mm. If part of the protective flange of the hole for the trunnion pin is damaged, it is repaired by welding. If the crack does not protrude into the finger hole by more than 10 mm, it is also repaired by welding. 4) When the remaining thickness of the inner side of the tongue of the hook is less than 68mm, it must be welded on. 5) If the wear of the surface of the tongue lock exceeds 3 mm, surfacing is carried out until it is even. After hardfacing of socket No. 13 on the hook lock cover, the minimum fit should be at least 45mm, and then measure the distance from the hardfacing to the top, hook pin hole or bushing. If the wear diameter exceeds 3mm, the bushing must be inserted or replaced. The measured position is based on the end of the pin flange going inward 30mm into the hole.

## Conclusion

In the hitch buffer device, the driven plate and frame of the hitch play the role of transmitting the longitudinal force (traction force or impact force), in addition, when the vehicle passes the turn and the meandering movement occurs, both the normal force and the side force act on the end of the plate, and the wear is more serious. When a sample of a rotating follower plate is placed under the RM, obvious macroscopic traces of grooves can be found on its friction surface, indicating that the local position of the surface of the sample has been heavily ploughed. The occurrence of these phenomena is closely related to the fact that the rotating driven plate carries large normal and lateral impact forces simultaneously. When analyzing the profile of the rotating driven plate, there is an obvious peeling and removal phenomenon, which may be due to the fact that the surface of the driven plate is under a lot of stress in the process of mating with the hook frame, which contributes to ductility. Deformation of the surface, when exposed to damage to the delamination mechanism, the exfoliated material rolls into wear residues between the contact surfaces and accumulates on the surface of the driven plate. At the same time, there are deep grooves of varying degrees on the worn surface, which

is consistent with the traces of grooves observed macroscopically, indicating that strong plowing was experienced from local positions on the surface of the plate, and some grooves were filled with wear residues. The surface of the material was subjected to significant abrasive wear. Consequently, the surface of the rotating driven plate is subjected to more severe impact and abrasive wear.

### References

1. Wang Xingcai. *Analysis of the causes of failure of the rear hitch, hook and rear frame of the truck [JJ]. West Railway Technology, 2000(4).*
2. Li Huali, Deng Rui, Wang Wei *Discussion of the relationship between the buffer device of the railway vehicle coupler and the strength of the car body [J] Railway locomotives and electric trains, 2014.*
3. Liu Zhiyuan, *Truck Construction and Maintenance [M], Beijing: China Railway Press, 2005.*

DOI 10.34660/INF.2022.89.41.155

SS7e型电力机车电气设备电磁兼容研究  
**RESEARCH OF ELECTROMAGNETIC COMPATIBILITY OF  
ELECTRIC EQUIPMENT OF SS7E ELECTRIC LOCOMOTIVE**

**Du Peidong**

*Master's degree Student*

**Volodin Anatoly Alexandrovich**

*Candidate of Technical Sciences, Associate Professor*

*Emperor Alexander I St. Petersburg State Transport University*

抽象的。随着电子工业的发展,电磁兼容问题变得越来越重要。作为电子设备,它可以受到外界的电磁干扰,也可以作为干扰源干扰外部设备。因此,系统的电磁兼容性直接关系到系统的性能和可靠性。

本文分析了SS7e电力机车控制系统的EMI防护措施。

关键词: 电力机车SS7e; 控制系统; 电磁干扰; 电磁兼容。

**Abstract.** *With the development of the electronics industry, the problem of electromagnetic compatibility has become more relevant. As an electronic device, it can be subject to electromagnetic interference from the outside world, and can also be used as a source of interference to interfere with external equipment. Thus, the electromagnetic compatibility of a system is directly related to the performance and reliability of the system.*

*This article analyzes the EMI protection measures of the SS7e electric locomotive control system.*

**Keywords:** *Electric locomotive SS7e; Control system; Electromagnetic interference; Electromagnetic compatibility.*

### **1. Source of interference for electric locomotives**

Generally speaking, electromagnetic interference sources are divided into two categories: natural interference sources and artificial interference sources. Natural interference sources mainly come from the celestial noise of the atmosphere and space noise of the Earth's outer space. Artificial interference sources are electromagnetic energy interference generated by electromechanical or other artificial devices. Some of them are devices specially used for the transmission of electromagnetic energy, such as radio equipment such as radio waves, communications

equipment, radars, etc., which are called deliberately transmitting interference sources. The other part is the emission of electromagnetic energy, which is associated with performing its own functions, such as vehicles, electrical machines, power lines, etc., which is called an unintentional source of interference.

As for the main sources of interference in electric locomotives, they can be divided into two categories: sources of interference within the system and sources of interference outside the system.

### **1.1 Source of interference in the system**

Most of the interference in the system is generated by airborne equipment, so they can be summarized as follows depending on the type of equipment.

#### **1.1.1 Interference in the operation of the main transformer and converter equipment**

The electric locomotive is equipped with a transformer with a capacity of more than 5000 kVA, which forms a strong magnetic field around it, which affects the surrounding equipment.

For a power electronic device, which is the main converter, its conversion process is based on switching or modulating current or voltage. A power electronic switch or switching system that converts the input of one frequency to the output of another frequency is at the center of the power conversion process. As we all know, high-order harmonic components can appear at both input and output terminals. This situation is unavoidable in electronic power conversion devices. Such harmonic components can also propagate through connected circuits or fields, causing interference.

#### **1.1.2 Interference in the operation of inductive electrical equipment with a control switch**

Electric locomotives have a lot of inductive equipment such as traction motors, fan motors, air compressor motors, etc., as well as small devices such as circuit contactor coils. These are all inductive loads with iron core coils. When the contacts of a switch or contactor are turned on and off, very steep transient voltage disturbances are generated in the circuit. The total rise time is from S to nS, the peak voltage can reach several hundred volts, the duration is up to 1ms, and the frequency is 1MHz ~ 10MHz.

#### **1.1.3 Inductive conduction interference**

A high-current converter on a locomotive and a pulsed current generated by an electric motor or braking resistor, as well as a capacitive stray current connected by the converter to the earth system, will generate a magnetic field in the rail and in the locomotive chassis. In principle, this magnetic field will interfere with all inductive systems communications and signaling.

## 1.2 Extra-system interference

Interference other than electric locomotive interference is mainly due to lightning interference, solar and space noise interference, and interference from other equipment on the ground. They will also affect the entire electric locomotive system.

## 2. Measures to suppress electromagnetic interference

According to the basic principles of electromagnetic interference, the electromagnetic compatibility of a system can be improved by limiting the interference source, isolating the communication path, and protecting sensitive equipment. The main methods include optimizing grounding, shielding interference sources or sensitive equipment, adding filtering equipment, and adding special equipment (such as isolating transformers, photoelectric conversion means, lightning arresters, varistors, etc.).

### 2.1 Flat shell shielding design

The shielding effectiveness and the attenuation generated depend on the interference frequency, the distance between the interference source and the shielding housing, the thickness of the shielding housing and the shielding material. For electromagnetic interference, the shielding effect is as follows: one part of the incident wave is reflected on the front surface of the shielding housing, one part is absorbed, and the other part is transmitted in figure 2.1.

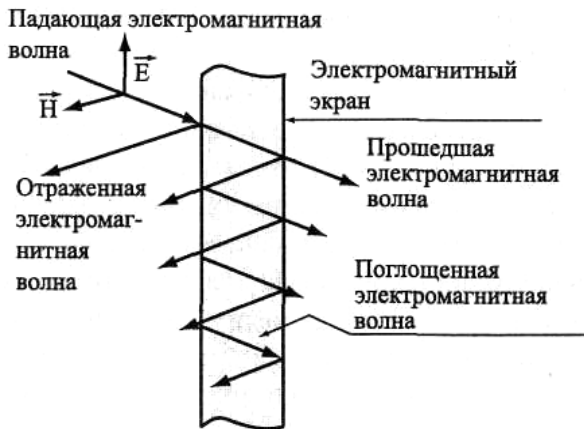


Figure 2.1. Flat shell shielding design

### 2.2 System grounding

EMC test results show that the reliability of system control and communication is largely dependent on the correct grounding of the system. Therefore, it is necessary to seriously consider the locomotive grounding scheme, which is also

a key point in the design of the electromagnetic compatibility of electric locomotives. Grounding is mainly intended to ensure a stable reference potential for all parts of the system. On electric locomotives, grounding can be mainly divided into the following types:

(1) Grounding. “Ground” in locomotives refers to the body, outer shell or special grounding bar of electronic equipment connected to the body of the locomotive, and the shielding layer of the shielding wire is usually connected to the cabinet body and ground, so it is also called shielding ground;

(2) 0V reference grounding, i.e. low voltage 0V reference conductor (+5V, ±15V, ±24V);

(3) 110V control power supply negative line;

### **2.3 Wiring**

There are many types of cables used in electric locomotives, including high power main circuit cables, auxiliary circuit cables, control cables, signal lines, communication lines, data buses and other cables with different power levels and purposes. Moreover, due to space constraints and electric locomotive design, cables with different power levels, different uses and large differences in current-carrying frequencies are located very close. Therefore, the electrical wiring has a greater impact on the electromagnetic compatibility of electric locomotives, and the electric wiring of electric locomotives is mainly carried out in accordance with the following requirements;

(1) Try to separate the locomotive cables according to different power levels and uses. For example, main circuit line, auxiliary circuit line, 110V circuit line, ±5V circuit line, ±15V circuit line, ±24V circuit line, the data bus and the signal line are distributed in different slots. At present, some locomotives have achieved separation of the wiring of the main, auxiliary and control circuits, but there is no further separation of other types of lines.

(2) Take measures to shield the related wiring, such as when different types of cables are crossed that cannot be separated, shielding materials such as pulika tubes are used for shielding and insulation, and shielded cables are used for signal cables, communication cables and data buses.

(3) keep away from interference sources such as auxiliary converters and output power cables of the main converter for circuit wiring that is subject to interference.

### **2.4 Other measures**

There are many other measures in the electromagnetic compatibility scheme of electric locomotives, such as an electronic control device to obtain DC/DC isolation power supply technology, and an electronic control device to add filtering technology. In order to avoid overvoltage that occurs when the mechanical switch is turned on and off, all relays, contactor coils, solenoid valves, etc. connected to

varistor absorbers to improve conduction immunity and reduce conduction interference emission.

Another key element in the electromagnetic compatibility of electric locomotives is the electromagnetic compatibility test. Every electrical equipment and control device used in the locomotive must be tested for electromagnetic compatibility in accordance with standard requirements.

### References

1. Bai Tongyun, Lu Xiaode. *EMC design [M]*. Beijing: Beijing University of Posts and Telecommunications Press, 2001
2. Zhao Mingsheng. *Electrical Engineer's Handbook [M]*. Beijing: Machinery Industry Press Office, 2001
3. Zhao Shudong, Shaoshan 8 type electric locomotive, Beijing: China Railway Press, 1998.
4. Yang Yonglin. Shaoshan type 7E electric locomotive. Beijing: China Railway Press, 2006.
5. Chen Chunyan. Design of anti-interference electric locomotive control electronic circuit. *Electric locomotive transmission*, 1994[4]: 6-11

提高电力牵引系统的能源效率

## IMPROVING THE ENERGY EFFICIENCY OF ELECTRIC TRACTION SYSTEMS

**Xi Faxiang**

*Master's degree Student*

**Rolle Igor Alexandrovich**

*Candidate of Technical Sciences, Associate Professor*

*Emperor Alexander I St. Petersburg State Transport University*

抽象的。本文主要对相关的铁路电力牵引系统进行详细讨论。随着社会经济的快速发展,铁路及相关交通运输行业在用电方面有了很大的提高。世界大力支持资源节约和环保系统,在引入智能电网的背景下,也对供电系统的质量和性能提出了更高的要求。本文借助电子技术和电能的利用,对以上两个内容进行了巧妙的探讨。

关键词: 滤波补偿装置, 牵引变电站。存在较高的电流和电压谐波。

**Abstract.** *This article mainly discusses the relevant railway electric traction systems in detail. With the rapid development of the social economy, the railway and related transportation industries have greatly improved in the use of electricity. The world strongly supports the system of resource saving and environmental protection, and in the context of the introduction of smart grids, it also puts forward increased requirements for the quality and performance of the power supply system. This article intelligently discusses the above two contents with the help of electronic technology and the use of electrical energy.*

**Keywords:** *Filter compensating devices, traction substations. Presence of higher current and voltage harmonics.*

The quality of electricity largely depends on a large number of factors that can change its parameters beyond the specified limits. For example, the voltage may become too high due to an emergency at a power plant. Low values may occur in the evening when people turn on many different household devices. According to regulatory documents, some fluctuation in the parameters of electrical energy is allowed. In low-quality power networks, it is necessary to use special devices that bring the parameters of electricity to standard indicators, called voltage stabilizers. Rospotrebnadzor (Russian Federal State Agency for Health and Consumer Rights)

is the supervisory authority over the quality of food networks, to which you can file claims if problems arise.

Factors affecting the quality of electricity: Voltage fluctuations associated with the periodic connection of powerful loads. Change in air humidity. Low tides, as well as high tides in offshore power plants. At wind farms - changing the strength and direction of the wind. Icing of supply wires. The quality of electrical wires, their aging. The need to comply with the main characteristics

The quantitative indicator and permissible deviations of the network characteristics are established by regulatory documents. These parameters were approved by law due to the likelihood of fires due to the ignition of electrical devices, as well as the disruption of sensitive devices operating at military facilities, in scientific laboratories and in medical organizations. Power quality indicators are updated periodically as new electronic consumers with higher power requirements appear. Electricity is considered as a supplied product, which must meet the specified indicators. With large deviations of these parameters, a system of administrative responsibility can be applied to energy suppliers. In the case of people who suffered through their fault, the matter can reach criminal liability. Possible consequences of deviations Mains power quality characteristics affect the duration of operation of electrical devices, especially in industry. As a result, the efficiency of the lines is reduced, and the consumption of electricity increases. In electric motors, when the network characteristics deteriorate, the torque decreases, the lighting devices begin to flicker, which affects the cultivation of vegetables in the greenhouse, and the duration of the lamps decreases. It also has a significant effect on various biochemical processes. As is known from physics, a decrease in voltage at a constant load on the motor leads to a significant increase in current strength, which contributes to failures in the operation of protection systems. As a result, the wire insulation can melt, which will lead to negative consequences: failure of electronic systems, destruction of electric motor windings, etc. In such a situation, metering devices will record excessive energy consumption, which increases financial costs. Quality rating indicators: Voltage tolerance (connected devices are able to operate normally). There are two types of deviation mode:

- normal - deviation +5%;
- limiting - deviation + 10%. Voltage should be restored in no more than 2 minutes. The voltage range is the difference between the values of the amplitude and effective voltage for one oscillation cycle. This indicator should not be more than + 10%.

The dose of flicker is divided into long-term (about two hours) and short-term (10 minutes). This parameter indicates the degree of susceptibility of the human eye to the flickering of lighting, which has arisen due to fluctuations in the power supply. To measure the dose of flicker, there is a special device - a flickermeter,

which determines the amplitude-frequency characteristic. The data obtained are compared with the sensitivity of the human eye. The standards set the permissible limits for this parameter:

- short-term fluctuations - no more than 1.38;
- long fluctuations - no more than 1.0. For incandescent lamps, this parameter should be no more than 1.0 and 0.74, respectively.

Voltage dip is a sharp decrease in its value. After some time, this parameter is restored to the initial value again. The duration of the failure can be up to 30 seconds. The impulse voltage acts for a duration of several microseconds or more, depending on the cause of the impulse. Its permissible values are not standardized by regulatory documents. A powerful voltage pulse can occur from a lightning strike, as well as due to the simultaneous connection of a large number of loads. Regulatory documents set the voltage recovery time, which does not affect the operation of consumers:

- impulses due to a lightning strike - no more than 15 microseconds;
- impulses from uneven load connection - no more than 15 milliseconds. Coefficients that determine the quality of electricity:

- distortion of sinusoidality;
- temporary overvoltage;
  - asymmetry of zero and reverse sequence;
  - harmonic vibrations.

The deviation of the frequency of the current leads to malfunctions of the electrical equipment. The maximum deviation occurs if the power consumption increases gradually and the power reserve of the network is not enough. Permissible normal frequency deviation of 0.2 hertz up and down. The maximum deviation value is +0.4 Hz. In emergency cases, a deviation of +0.5 -1 Hz is allowed.

At present, in the conditions of saturation of the electrical networks of buildings and structures with such non-linear electrical receivers as computer equipment, solving the problem of higher harmonics in these networks is not only relevant, but topical. In the monograph, some theoretical provisions and ideas that were presented in the early publications of the authors were further developed. This, first of all, refers to the development of new methods of analysis and improvement of models of low voltage networks with non-linear loads by additionally taking into account the parameters of the main elements of the electrical networks of buildings.

This standard specifies the requirements for electromagnetic compatibility (hereinafter - EMC) in terms of immunity and electromagnetic emission of electrical equipment operating from a power supply or battery with a voltage of less than 1000 V AC or 1500 V DC or from an electrical circuit in which measurements are made.

Higher harmonics are currents or voltages whose frequency exceeds the fundamental oscillation of 50/60 Hz and is a multiple of this frequency of the fundamental oscillation. The higher harmonics of the current do not contribute to the active power, but only have a thermal load on the network. Because higher harmonic currents flow in addition to "active" sinusoidal oscillations, they introduce electrical losses within the installation, which can lead to thermal overload.

Regenerative braking is a type of electric braking in which the electricity generated by traction motors operating in generator mode is returned to the electrical network.

Regenerative braking is widely used in electric locomotives, electric trains, modern trams and trolleybuses, where, when braking, electric motors begin to work as electric generators, and the generated electricity is transmitted through a contact network either to other electric locomotives or to the general power system through traction substations.

The same principles are used in electric vehicles, hybrid vehicles, where the electricity generated during braking is used to recharge the batteries. Some e-bike motor controllers implement regenerative braking.

Experiments were also carried out on the organization of regenerative braking of other principles on cars. Flywheels, pneumatic accumulators, hydraulic accumulators and other devices were used to store energy.

## References

1. Beseckersky V. A., Popov E. P. *Theory of automatic control systems*. - St. Petersburg: "Professiya" Publishing House, 2003. – 752 p.
2. Sharikov V.A. Dmitriev A.V., Razin E.A., Sharikova O.L. *Method for calculating the main indicators of the operating modes of the traction battery of an electric bus*

为直流电动火车的机械部分开发诊断支持  
**DEVELOPMENT OF DIAGNOSTIC SUPPORT FOR THE  
MECHANICAL PART OF A DC ELECTRIC TRAIN**

**Li Kexin**

*Master's degree Student*

**Zelenchenko Alexey Petrovich**

*Candidate of Technical Sciences, Associate Professor*

*Emperor Alexander I St. Petersburg State Transport University*

抽象的。 该文章证明了改善通勤直流电动火车«ЭР2Т»机械部分的诊断支持的相关性。 确定电动列车动力部分力学元件状态的选定方法和手段。

关键词: 机械部件, «ЭТ2М»电动火车, 技术诊断。

**Abstract.** *The article proves the relevance of improving the diagnostic support of the mechanical part of the commuter DC electric train «ЭР2Т». Selected methods and means to determine the state of the elements of the mechanics of the power part of the electric train.*

**Keywords:** *mechanical part, «ЭТ2М» electric train, technical diagnostics.*

The strategic direction in the development of the repair system for suburban electric trains is the transition from a planned preventive repair system to a repair system based on the actual condition.

The problem is solved by using a complex diagnostic system.

The article presents the developed diagnostic support for the mechanical part of a commuter DC electric train. In particular, the following questions are reflected:

- Decomposition of suburban electric train as an object of technical diagnostics has been developed;
- The composition of the complex diagnostic system was determined;
- Selected equipment for floor diagnostic system;
- Selected equipment for the on-board diagnostic system;
- An internal depot diagnostic system has been developed.

As a result of the study of the diagnostic model of the diagnostic object, diagnostic signs, direct and indirect parameters and methods for their evaluation are established, and a diagnostic algorithm is developed. The totality of these data is called diagnostic support.

Purpose and functions of the diagnostic complex:

The diagnostic complex is a device that allows solving the following tasks of determining the state of the EPS:

- Technical condition control;
- Finding a place and determining the cause of failure (malfunction);
- Forecasting the technical condition.

Technical condition control is a verification of the compliance of the values of the object parameters with the requirements of technical documentation and the determination on this basis of one of the specified types of technical condition at a given time, for example, serviceable, operable, faulty, inoperable, etc.

The purpose of forecasting the technical condition may be to determine, with a given probability, the time interval (resource) during which the state of the object is assessed as serviceable.

When determining the technical condition of an object, the following approaches are used:

- Working technical diagnostics - diagnostics, in which working influences are applied to the object;
- Test technical diagnostics - diagnostics, in which test actions are applied to the object;
- Express diagnostics - diagnostics on a limited number of parameters for a predetermined time.

The paper proves the relevance of the development of diagnostic support for the mechanical part of the electric train.

A block diagram of an electric train as an object of diagnostics has been developed, shown in Figure 1.



**Figure 1.** Structural diagram of an electric train as an object of diagnosis

The mechanical part includes parts and assemblies of the wheel-reduction unit and the undercarriage of the electric train.

The reliability of the mechanical part is analyzed.

A comprehensive system for diagnosing electric rolling stock, shown in Figure 2, includes a number of subsystems.

- On-board (embedded) systems installed on an electric locomotive;
- Intradepot stationary and portable systems;
- Floor units

The on-board systems mainly control the state of the electrical equipment of the electric locomotive during its movement.

Internal depot devices diagnose the locomotive in full.

Floor-standing devices, for example, DISK-B, make it possible to carry out operational monitoring of the condition of axleboxes when an electric locomotive moves under a train on the line.

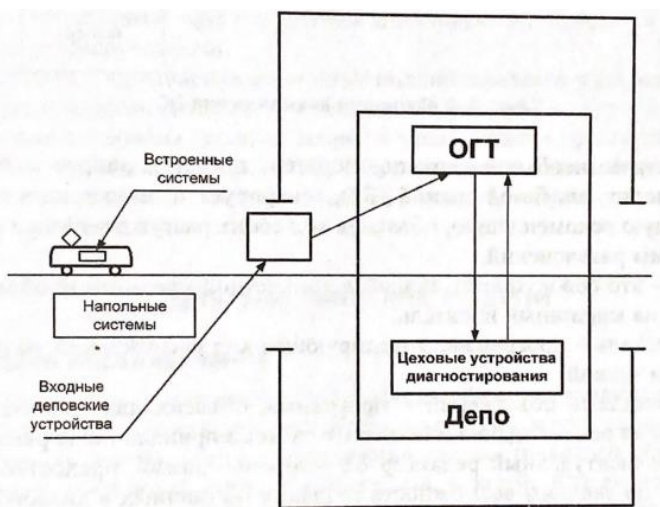


*Figure 2. Integrated system for diagnosing an electric locomotive*

The diagnostic equipment of the floor system for diagnosing the mechanical part of the electric train was selected in the work. In particular, the proposed complex KCM-02.

The KCM-02 complex is a system for automatic monitoring of the technical condition (diagnostics) of rolling stock, consisting of subsystems for detecting malfunctions of axle boxes, wheel sets, brake and coupler equipment, drawing parts, violations of the side or top clearance, etc.

The KCM-02 complex consists of station and floor distillation equipment connected via communication channels to the CPC APM and via the SPD OTN network to the CPC railway APM.

The subsystems for monitoring the condition of axleboxes and brake wheels KCM-02 are equipped with small-sized floor cameras (KNM-05) with fastening to the rail sole in fig. 3.

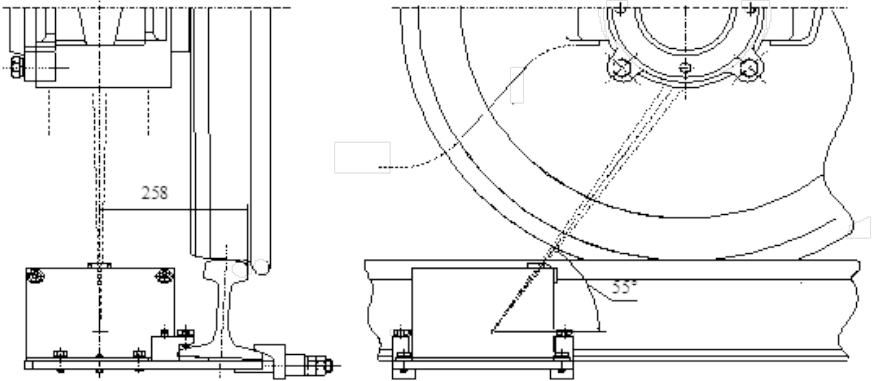


*Figure 3. Scheme of orientation of the KNM-05 IR receiver on the axle box*

In the work, equipment for the on-board diagnostic system was selected.

Figure 4 shows the classification of methods for diagnosing traction drive bearings.

Currently, the state of bearing units on the railway network is determined by:

- visual control;
- by heating temperature;
- according to vibroacoustic manifestations.

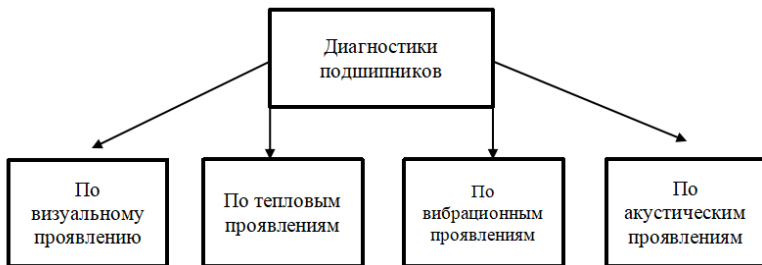


*Figure 4. Classification of bearing diagnostic methods*

During visual inspection, such phenomena as a change in the color of the bearing, lubricant leakage, traces of metal chips, etc. act as signs of a bearing defect.

Bearing heating temperature is checked:

- touch by hand;
- special non-contact pyrometers;
- according to the intensity of infrared radiation of the heated node.

In addition, the heating temperature can be determined using sensors specially built into the assembly.

The analysis of vibroacoustic manifestations makes it possible to carry out in-place diagnostics of bearing assemblies in the conditions of repair enterprises by the following methods:

acoustic;

diagnostics by the general level of vibration;

diagnosing nodes according to the spectra of vibration signals;

diagnostics by spectra of envelope vibration signals;

shock pulse method;

acoustic emission method.

The article also presents an internal depot system for determining the state of the elements of the mechanical part of an electric train.

Selection of magnetic particle flaw detectors (MD)

Let us analyze the main types of flaw detectors and ND used in magnetic particle testing of parts, their technical characteristics and purpose.

Magnetic particle flaw detector MD-12p.

MD-12P flaw detector (TU 32TsSh 2603-83) is available in three modifications: MD-12PSH (cervical); MD-12PE (eccentric); MD-12PS (saddle-shaped).

Flaw detectors MD-121 of all modifications consist of a control unit and an NL of the corresponding type, shown below in Figure 5.

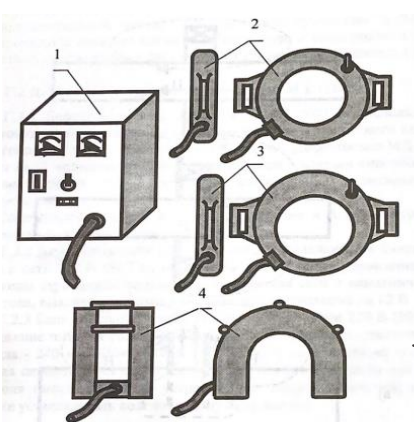


**Figure 5.** The main blocks of the flaw detector MD-12P of all modifications.

1 - power supply; 2 - solenoid of flaw detector MD-12PSH;

3 - eccentric solenoid of flaw detector MD-12PE;

4 - saddle-shaped device of the MD-12PS flaw detector

The control unit is designed to power the HL and the portable lamp with a voltage of 36 and 12 V, respectively. On the front panel of the control unit there is a connector and a socket for connecting the LV and the portable lamp, respectively, switches for the mains and portable lamp, as well as pointer indicators of the mains voltage and magnetizing current.

ND flaw detectors MD-12P of all modifications have a coil placed in a plastic case, through which an alternating current is passed. There is a toggle switch on the NU case to turn it on.

The MD-12PSH flaw detector is designed to inspect the axle journals of wheel sets and other parts with a diameter or maximum cross-sectional size of not more than 160 mm. The flaw detector NL is made in the form of a round solenoid with a working hole with a diameter of 200 mm. The magnetic field decreases symmetrically with distance from the ends of the solenoid body. The extended parts of constant section placed inside the solenoid are magnetized symmetrically with respect to the ends of the solenoid body, as shown in Figure 6.

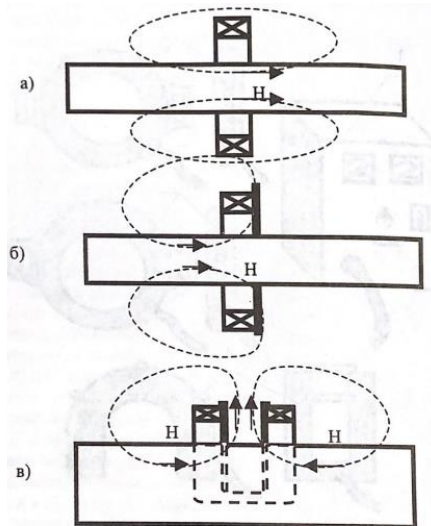


**Figure 6.** Lines of force of the magnetic field created on the surface of the part by the magnetizing devices of flaw detectors MD-12PSH(a); MD-12PE(b); MD-12PS(v). Eddy current flaw detectors (VD) are also selected

The principle of operation of eddy current flaw detectors is based on the excitation of eddy currents in the controlled part using an eddy current transducer (ET). Inductive coils are usually used as a sensitive element of the VP, through

which an alternating or pulsed current is passed, which creates an electromagnetic field around the coil. When the EP is installed on a metal (electrically conductive) surface, the magnetic field of the coil induces eddy currents in the surface layer of the metal in the form of concentric circles, the maximum diameter of which is approximately equal to the diameter of the coil. Eddy currents penetrate to a depth of fractions of a millimeter to several millimeters, depending on the frequency of the exciting current. The higher the frequency of the exciting current, the smaller the depth of penetration of eddy currents.

The flaw detectors consist of an electronic unit and two interchangeable VPs with a diameter of 5 and 10 mm (types 1 and 2, respectively, for the VD-12NFM flaw detector).

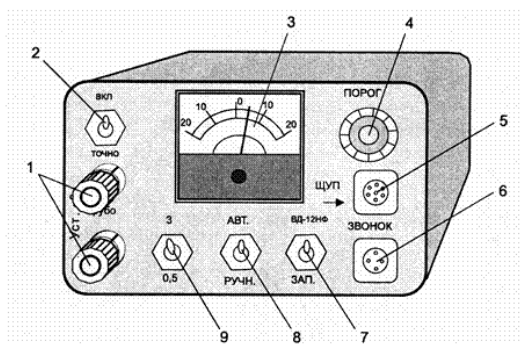


**Figure 7.** External view of the electronic unit of the VD-12NFM flaw detector

1 - knobs "Set. 0/Coarse" and "Set. 0/Exactly"; 2 - toggle switch "On." to turn on the flaw detector; 3 - pointer indicator; 4 - knob "Threshold" for smooth adjustment of sensitivity; 5 - "Probe" connector for connecting the transducer; 6 - "Call" connector for connecting headphones; 7 - toggle switch "Zap." to set the mode of remembering the operation of the sound and light indicators; 8 - toggle switch "Manual / Auto." to switch the mode of detuning from interference; 9 - toggle switch "3 / 0.5" for switching the sensitivity level.

VD-12NFM flaw detector allows scanning parts in dynamic and static modes of operation. Scanning in the dynamic mode is used to inspect parts with a flat and curved surface with a radius of curvature of more than 20 mm, while the light and sound indicators are triggered when the VP crack is crossed.

Findings:

- The relevance of the development of diagnostic support for a commuter DC electric train has been proved;

- Decomposition of suburban electric train was developed as an object of technical diagnostics;
- The composition of the complex diagnostic system was determined;
- Selected equipment for floor diagnostic system;
- Selected equipment for the on-board diagnostic system;
- An internal depot diagnostic system has been developed.

用于电力机车和电力列车牵引制动控制系统设计的初始数据  
**INITIAL DATA FOR THE DESIGN OF TRACTION-BRAKING  
CONTROL SYSTEMS FOR ELECTRIC LOCOMOTIVES AND  
ELECTRIC TRAINS**

**Chu Mingjing**

*Master's degree Student*

**Rolle Igor Alexandrovich**

*Candidate of Technical Sciences, Associate Professor*

*Emperor Alexander I St. Petersburg State Transport University*

注解。 文章详细讨论了电动机车车辆牵引制动方式控制系统的研究 随着社会经济的快速发展, 铁路及相关交通运输行业在用电方面有了很大的提高。 世界大力支持资源节约和环保系统, 在引入智能电网的背景下, 也对供电系统的质量和性能提出了更高的要求。

关键词: 电力机车牵引制动, 电力列车, 功率因数转换器。

**Annotation.** *The article discusses in detail the study of control systems for the traction-braking mode of electric rolling stock With the rapid development of the social economy, the railway and related transport industries have greatly improved in the use of electricity. The world strongly supports the system of resource saving and environmental protection, and in the context of the introduction of smart grids, it also puts forward increased requirements for the quality and performance of the power supply system.*

**Keywords:** *traction-braking of electric locomotives, electric trains, power factor converters.*

Under the traction force of an electric locomotive is meant the sum of the traction forces developed by all wheel pairs of an electric locomotive.

Thus, the main ways to increase the traction force of an electric locomotive should be considered to be an increase in the number of wheel sets (the number of sections for an electric locomotive) or the torque of traction motors; however, the increase in torque has its limitations, which will be discussed below. It should be noted that with the same current of traction motors, electric locomotives with wheels worn in diameter have a slightly greater traction force (but also a lower speed). Thus, the thickness of new tires of freight electric locomotives is allowed

up to 100 mm, and extremely worn tires - 40 mm (including rolled products 7 mm), i.e. the largest difference in diameters of new and worn wheels is 120 mm, which is almost 10% of the total wheel diameter. An electric locomotive with new tires develops a traction force 10% less than with extremely worn ones.

#### Train resistance

The friction forces arising during the movement of the train in the nodes of the rolling stock, the forces of interaction between the rolling stock and the track, the outer surfaces of the rolling stock and the surrounding air, as well as the force of gravity that manifests itself on the slopes of the track, are attributed to the forces of resistance to the movement of the train. The resultant of all these forces is usually directed against the direction of motion and coincides with it only on steep descents. The values of all resistance forces do not depend on the driver, however, he must know that these forces, due to various reasons, change, and in accordance with this, when driving the train, adjust the operating mode of the electric locomotive.

The total resistance to the movement of the train (locomotive and wagons)  $W$  is divided into the main  $W_0$  and additional  $W_d$

$$W = W_0 + W_d$$

Basic resistance to movement. It is the sum of all forces that impede movement on straight horizontal sections of the track, and arises as a result of mutual friction of parts of the rolling stock, resistance from interaction; track and rolling stock, as well as air resistance in the absence of wind.

Resistance from mutual friction of rolling stock parts. This resistance, first of all, depends on the friction force in the axle bearings of the wheel pairs, it is determined by the type and condition of the bearings, the quality and quantity of lubricant, the outside air temperature (affects the viscosity of the lubricant), the speed of the train and the pressure of the bearing on the axle neck. In roller journal bearings, instead of sliding friction, rolling friction acts, which provides a significant reduction in friction forces; it should be taken into account that the pressing force on the axle box of the wheel pair axle of an electric locomotive exceeds 10 tf, and for fully loaded cars it reaches 9 tf.

The internal resistance to the movement of an electric locomotive is also due to friction in the gear train, anchor and motor-axial bearings, between brushes and collectors of traction motors, etc. Internal resistance decreases with proper care and good condition of these units.

Resistance from the interaction of the track and rolling stock. It results from rolling friction and sliding friction between wheels and rails. With a high hardness of the material of the wheels and rails, they are less pressed into each other and the rolling friction decreases; Applications of seamless track and heavier type rails also reduce this friction. Sliding friction between the wheel and the rail oc-

curs when the wheel diameters of one wheel pair are unequal, the ridges of the bandages come into contact with the side faces of the rail heads and cross-slip during the wobbling of the bogies. The higher the speed, the more these phenomena hinder the movement.

It is also necessary to take into account the shocks from the running of the wheels on the ends of the rails at the joints, crosses of turnouts. This resistance can be reduced by improving the maintenance of the railroad bed and rails, and by increasing the length of the rails. Irregularities of the rails or wheel tires (potholes, ovality) also increase the resistance to movement, since during the vertical movement of the chassis, part of the energy of the locomotive is absorbed by the parts of the spring suspension, both of the electric locomotive itself and of the cars; in addition, there are energy losses in the rubberized parts of the leashes of the axle boxes.

Air resistance. It is caused by air pressure on the frontal surface of the rolling stock, rarefaction of air behind the rear end wall of each car, and friction of the rolling stock surface against the air. The value of this resistance is most influenced by the speed of trains, the shape of the cars and the locomotive.

Measures to reduce the main resistance to movement:

- full loading of wagons; correct formation of trains (concentration of cars of the same type in groups - gondola cars, platforms, etc.);
- closing doors and hatches, which improves the air flow around the cars;
- elimination of friction of brake pads on the wheels;
- improvement of the state of the superstructure of the track;
- reduction of parking time, facilitating the starting of trains, especially in winter.

Calculation of the main movement resistance: The total main movement resistance of the train  $W_o$  is the sum of the main movement resistances of the locomotive  $W'o$  and the train  $W''o$ , i.e.

$$W_o = W'o + W''o.$$

Additional resistance to train movement. This resistance occurs when driving in curves, on slopes, at low outside temperatures and strong head and side winds.

To reduce additional resistance to movement, the track profile is softened, the radii of curves are increased, lubricating the side surfaces of the outer rail heads in the curves or the ridges of the tires with a special lubricant, the doors of freight cars are closed, and high-speed passenger cars are made more streamlined.

Slope resistance. The steepness of the slope is defined as the ratio of the height difference (from the horizontal line of the beginning and end of the slope to the length of the section on which the slope is located, i.e.

$$I = MH/MO.$$

Resistance from curved sections of track. When moving along curves, under

the action of inertia, the ridges of the wheel pair tires are pressed against the side surface of the outer rail head, which leads to friction between them. With a large curvature of the track, a small lateral run-up of wheel sets in three-axle bogies, not only the end wheelsets are pressed against the outer rail, but also the middle ones (2nd and 5th) against the inner rail. In addition, there are additional forces in the body supports and shock-traction devices, both for locomotives and wagons. All this causes additional resistance to movement in the curve.

Wind resistance. Head or side wind causes additional resistance to movement, especially increasing at high speeds; a tailwind helps to increase the speed of movement. Side wind, pressing the wheel flanges to the rails, leads to a significant increase in resistance to movement, especially for cars following with open doors and hatches.

Resistance to movement from low outside temperatures. At low temperatures, the resistance to movement increases mainly due to an increase in the viscosity of the lubricant in the friction units. It is recommended to take it into account at temperatures below  $-25^{\circ}\text{C}$  as a percentage of the main resistance to movement; for example, for freight cars at a speed of 80 km/h and an air temperature of  $-30^{\circ}\text{C}$ , this increase in resistance is assumed to be 7%.

Coupling of wheels with rails, limitation of traction force according to adhesion conditions

The adhesion of the wheel to the rail is the stronger, the greater the force  $R_0$  (see Fig. 2), with which the wheel pair presses on the rail. The grip required for the implementation of the traction force can be obtained only on the condition that a certain fraction of this force  $P_0$  will be greater than the traction force  $F_{kd}$  developed by the given wheelset.

If the traction force exceeds the adhesion force, then the adhesion will be broken, the wheel will begin to slip along the rail, while the adhesion force will sharply decrease, the wheel, as it were, will lose its stop and begin to rotate faster and faster. This phenomenon is called boxing; with it, the torque developed by the engine and implemented by the wheel pair drops (due to a decrease in current and friction coefficient) and the traction force decreases, which primarily causes a decrease in the speed of the train; it is also possible that the switching of the locomotive engines is disturbed.

To determine the maximum permissible traction force of an electric locomotive, it is necessary to know the value of the friction coefficient.

The adhesion coefficient depends on many factors: the condition of the rail surface (oil stains, peat or coal dust, leaves reduce adhesion, sand increases it); general condition of the track; radius of curvature and elevation of the rails on curved sections of the track. With light rain, the friction coefficient decreases, but with heavy rain washing dirt off the rails, there is no decrease in the friction coefficient.

The adhesion coefficient is also affected by factors that depend on the state of the electric locomotive. Thus, the increased rolling of tires, the difference in diameters along the rolling circle of a set of wheel sets or wheels of one wheel set, large transverse run-ups of wheel sets, a difference in the stiffness of springs and springs, and an unsuccessful selection of traction motors according to their characteristics worsen adhesion, especially with increasing speed. Large inertia (mass, diameter) of the rotating parts associated with the engine prevents the development of boxing.

The adhesion coefficient for AC electric locomotives up to a speed of 50 km/h is higher than for DC electric locomotives; this is a consequence of the fact that on AC electric locomotives the traction motors are connected in parallel, and on DC electric locomotives they are connected in series or series-parallel. For VL80R electric locomotives, the friction coefficient at speeds corresponding to the starting mode is even slightly higher due to a smooth (not stepwise) increase in the starting current and torque of the traction motors.

When using three or four sectional electric locomotives VL80S and VL11, the indicated values of the traction force increase proportionally by 1.5 or 2 times, respectively, but they do not exceed the values corresponding to the strength of the SA-3 automatic couplers and the upgraded SA-ZM automatic coupler, designed for a force of 250 tf .

### References

1. *Automated control systems for electric rolling stock. Part 1//ed. L.A. Baranova and A.N. Savoskin. - M.: GOU UMTs for education on the railway transport, 2013. - 400 p.*
2. *Yakushev A.Ya. Automated control systems for electric rolling stock, Tutorial. - M.: GOU UMTs for education on the railway transport, 2016. - 301 p.*

电动巴士电池的选择  
**SELECTION OF A BATTERY FOR AN ELECTRIC BUS**

**Vorobyov Alexander Alfeevich**

*Doctor of Technical Sciences, Full Professor*

**Sychugov Anton Nikolaevich**

*Postgraduate*

**Wang Meilun**

*Master's degree Student*

**Wang Peng**

*Master's degree Student*

*Emperor Alexander I St. Petersburg State Transport University*

注解。 文章讨论了电动公交车，这是一种相对较新的节能环保交通工具。 它的电源由电池供电。 电动公交车根据获取电能（充电）的方式和续航里程进行分类。 文章提出了一种使用 MatLab 计算电池最优参数的算法。 开发的算法将允许为电动巴士自动选择电池。 所选电池提供：

- 指定的动力储备；
- 抗最大工作电流；
- 最小尺寸和重量；
- 预定的使用寿命。

关键词：电动客车、电池组、计算算法

**Annotation.** *The article discusses electric buses, which are a relatively new energy-saving and environmentally friendly mode of transport. Its power is supplied from the battery. Electric buses are classified according to the method of obtaining electrical energy (charging) and the range. The article proposes an algorithm for calculating the optimal parameters of a battery using MatLab. The developed algorithm will allow automatic selection of a battery for an electric bus. The selected battery provides:*

- *specified power reserve;*
- *resistance to maximum operating currents;*
- *minimum dimensions and weight;*
- *predetermined service life.*

**Keywords:** *electric bus, battery pack, calculation algorithm*

Currently, energy efficiency issues are one of the priority areas of scientific research worldwide. Transport, as one of the most important consumers of the country's energy resources, is constantly being improved. Do not forget that with the growth of consumption of energy resources, the load on the ecological system will also increase, which is especially important for large cities. Therefore, one of the priority tasks of scientific research is the search for such technical solutions that would simultaneously provide a reduction in energy consumption and ensure environmental requirements. As one of the possible solutions, it is proposed to organize the operation of electric buses in large urban agglomerations. This is an innovative transport - an electric bus. Eco-friendly, flexible, safe. It is not tied to a contact network - it is charged at the final stops and in parks. This type of transport allows you to solve two problems at once. The successful experience of operating an electric bus on urban routes in Moscow allows us to conclude that this experience should be applied in other large cities [1].

To date, the following classification of electric buses has been adopted according to the method of obtaining electrical energy (charging) and the power reserve (Figure 1):

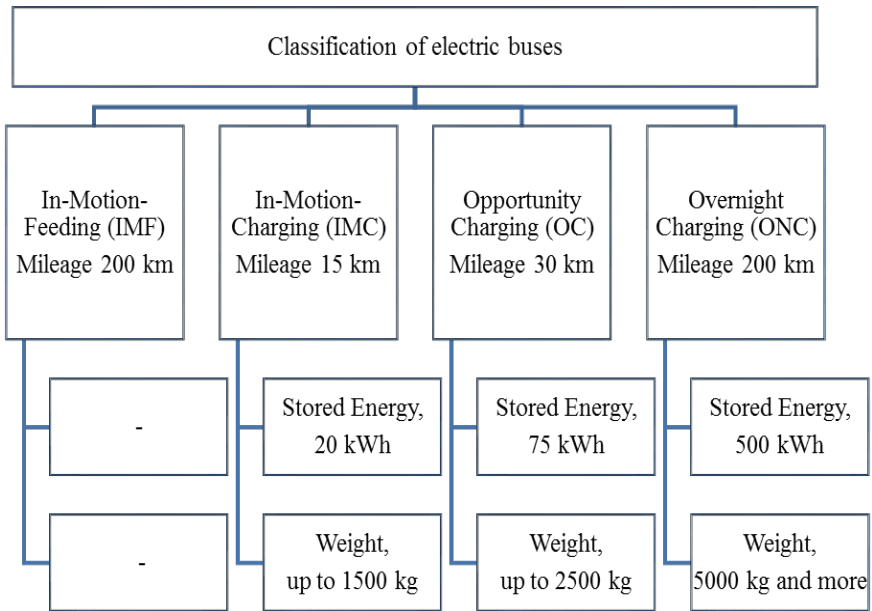


**Figure 1.** Technologies of electric grid buses - electric buses

Electric buses powered by In-Motion-Feeding (IMF) include modern electric buses that are powered by a contact network.

Electric buses with dynamic charging In-Motion-Charging (IMC) are a relatively new class, they have become widespread recently and are an electric bus with an installed traction battery (TAB) and a charger. Such an electric bus can operate on routes partially consisting of existing routes, and then follow part of the path without a contact network, receiving power from the TAB.

Opportunity Charging (OC) charging electric buses and Overnight Charging (ONC) depot/overnight charging electric buses (ONC) differ from each other in range and in the way the TAB is charged. [2]

To power the traction motors, batteries are installed on the electric bus. Table 1 shows the comparative characteristics of some batteries [3,4].

Model	Qty. batteries	Module configuration	Length, mm	Width, mm	Height, mm	Capacity, Ah	Energy, kWh	Max. discharge current Dur, A	Max. discharge current Short, A	Voltage Max, V	Voltage Min, V	Weight, kg
PE340-394B	96S- 2P	4S-2P	804	546	303	35	11,8	70	105	394	240	150
PE350-394A	96S- 2P	12S-2P	804	546	303	35	12,3	70	105	394	240	150
PE350-394B	96S- 2P	12S-2P	804	546	303	35	12,3	70	105	394	240	150
PE350-689	168S- 2P	12S-2P	1094	877	310	35	21,5	70	105	689	420	265
PE700-394	96S- 4P	12S-2P	1047	918	300	70	24	140	210	394	240	181
PP320-394B	96S- 2P	12S-2P	804	546	303	32	12	120	480	394	240	295
PE320-689	168S-2P	12S-2P	1094	877	332	32	19,6	120	245	689	420	310
PE168-110-RD-ВТ	6S- 4P	30S-8(16)P	810	848	356	168	18,9	37,5 (75)	75 (150)	124,5	90	250
ЛИАБ 78ТК Т02			2040	445	610	170	78	170	600	535	449	1250
СНЭ 88ТТИВ			1140	540	350	145	88	144	430	710	560	880
СНЭ 88ТТИГ			1140	540	350	14	88	144	430	710	560	900

When choosing a storage battery, one should be guided by the criteria of economic efficiency, minimum weight and size indicators, while unconditionally ensuring a given power reserve and the required service life. The article proposes an algorithm for calculating the optimal parameters of a battery using MatLab. To do this, a program code was developed that allows, according to the given initial data, to determine the main energy indicators of movement: consumed / recuperated energy, power consumed during acceleration, power recuperated during braking.

The energy required for acceleration can be determined as follows:

$$E_{\text{раз}} = \frac{P_{\text{раз}} \cdot T_{\text{раз}}}{\eta} = \frac{m_{\text{ПЦ}} \cdot (\alpha_{\text{ПЦраз}} \cdot T_{\text{раз}})^2}{\eta}, \quad (\text{Дж}) \quad (1)$$

where  $\alpha_{\text{ПЦраз}}$  – electric bus acceleration,  $\text{m/s}^2$ ;  $T_{\text{раз}}$  – acceleration time,  $\text{s}$ ;  $m_{\text{ПЦ}}$  – weight of the electric bus.

Kinetic energy accumulated by the energy storage during deceleration:

$$E_{\text{топм}} = P_{\text{топм}} \cdot T_{\text{топм}} \cdot \eta = m_{\text{ПЦ}} \cdot (\alpha_{\text{ПЦтопм}} \cdot T_{\text{топм}})^2 \cdot \eta, \quad (\text{Дж}) \quad (2)$$

where  $\alpha_{\text{ПЦтопм}}$  – electric bus deceleration,  $\text{m/s}^2$ ;  $T_{\text{топм}}$  – deceleration time.

The spent energy, taking into account the recovery for one cycle of movement on the site:

$$E_{\text{зат}} = E_{\text{раз}} - E_{\text{топм}}, \quad (\text{Дж}) \quad (3)$$

The energy required to provide the required autonomous movement can be determined as follows

$$E = E_{\text{зат}} \cdot \frac{S_{\text{зх}}}{350}, \quad (\text{Дж}) \quad (4)$$

where  $S_{\text{зх}}$  – specified power reserve,  $\text{M}$ .

The energy stored by the TAB is defined as:

$$E_{\text{ТАБ}} = 3600 \cdot C_{\text{ТАБ}} \cdot (U_{\text{ТАБМАХ}} - U_{\text{ТАБМИН}}), \quad (\text{Дж}) \quad (5)$$

Required number of TABs connected in parallel

$$n_{\text{вет}} = \frac{E}{E_{\text{ТАБ}}}, \quad (\text{шт}) \quad (6)$$

As noted above, the allowable charge / discharge current of the NE must be greater than or equal to the maximum current of the AEPS

$$\begin{cases} I_{\text{ТАБВЕТразРАЗРЯДmax}} \\ I_{\text{ТАБВЕТтопмЗАРЯДmax}} \end{cases} \quad (7)$$

The above calculation algorithm is implemented using a script in MatLab (Figure 2).

```

1      %Author
2      %Anton Sychugov, Alexanr Vorobiev, Wang Meilun, Wang Peng
3      %ver.1
4      %date 10/02/2022
5
6      %Исходные данные
7      m = 16; %Масса\ ЭТС т
8      Vmax = 38; % Скорость\ км/ч
9      S = 80; %Путь\ км
10     АКВ = 70; %Глубина разрядки АКБ\ (DOD в %
11     a = 0.9; %Ускорение, замедление\ м/с^2
12     КПД_TD = 0.81; %КПД тягового двигателя\ %
13     КПД_PP = 0.82; % КПД тягового преобразователя\ %
14     Uakb = 290; %Номинальное напряжение АКБ\ В
    
```

*Figure 2. Initial data for calculation*

As a result of the program execution, the most optimal accumulator for the entered initial data is selected (Figure 3).

```

Otbor =
5x6 table
      Model      EMKOST      GABARITS      MAX_emkost_Eab      MAX_Ves      VITOK
-----
'PE340-394B'    13.583    1.3301e+08    230.91    2550    17
'PE350-394A'    13.583    1.3301e+08    230.91    2550    17
'PE350-394B'    13.583    1.3301e+08    230.91    2550    17
'PE700-394'     27.166    2.8834e+08    244.49    1629    9
'PP320-394B'    12.419    1.3301e+08    235.95    5605    19

LOSE

Itog_AKB =
1x19 table
      Model      Gabarit      Emkost      Energi      MaxTokZarKor      MaxTokZarDlin
-----
'PE700-394'     2.8834e+08    70    24    210    140
    
```

*Figure 3. Calculation result*

### Conclusion

The developed algorithm will make it possible to automatically select a battery for an electric bus. The selected battery provides:

- specified power reserve;
- resistance to maximum operating currents;
- minimum dimensions and weight
- predetermined service life.

### References

1. <https://mosgortrans.ru/electrobus/>
2. *Possibilities of Sustainable Utilization of Braking the Energy of Electric Rolling Stock* / V. A. Sharyakov, A. V. Agunov, O. L. Sharyakova, A. V. Tret'yakov // *Russian Electrical Engineering*. – 2018. – Vol. 89. – No 10. – P. 607-611. – DOI 10.3103/S1068371218100085. – EDN YUYWZI.
3. <https://www.liotech.ru/products/batarei-i-nakopiteli/tyagovye-batarei-trolleybusov-s-avtonomnym-khodom/>
4. <http://enerz.ru/produkcija/akkumuljatornye-batarei/>

DOI 10.34660/INF.2022.59.67.160

永磁同步电机技术研究  
**STUDY OF PERMANENT MAGNET SYNCHRONOUS MOTOR  
TECHNOLOGY**

**Wang Helin**

*Master's degree Student*

**Vikulov I.P.**

*Candidate of Technical Sciences, Associate Professor*

*Emperor Alexander I St. Petersburg State Transport University*

注解。 大功率永磁同步电机最早用于电力机车的牵引驱动，与传统的感应电机相比具有许多优点，但设计非常复杂。 因此，从其磁系统结构的复杂性、风冷系统的设计、所用的永磁材料等方面对大功率直驱永磁电机的设计进行了分析。

关键词：永磁同步电机，电机发热，电机磁系统设计。

**Annotation.** *High power synchronous motors with permanent magnets were first used in the traction drive of electric locomotives, they have a number of advantages over traditional induction motors, but are very complex in design. Therefore, the design of a powerful direct drive permanent magnet motor is analyzed in terms of the complexity of the structure of its magnetic system, the design of the air cooling system, and the permanent magnet materials used.*

**Keywords:** *Permanent magnet synchronous motor, motor heating, motor magnetic system design.*

(1) The traction electric drive of the locomotive, containing a permanent magnet synchronous motor and a direct drive, has a total power of 7200 kW. The main feature of the direct drive is the absence of a gearbox. The output torque of the engine is directly transmitted to the wheels. The high efficiency of the traction drive is increased by about 2-3%, and the power consumption is also reduced by about 15% compared to the asynchronous traction drive, while eliminating the problems of maintenance and repair, high noise generated by the gearbox, etc., which in turn leads to lower operating and maintenance costs of the locomotive. The failures of the mechanical system of the locomotive are reduced - reducer cracks and oil leaks from the reducer. The permanent magnet synchronous motor, as a key component of the direct drive electric locomotive, plays an important role in improving its efficiency. The permanent magnet synchronous motor is being adopted in railways

because of its high power density, high power factor and high overload. Leading countries in railway equipment manufacturing, such as Europe and Japan, have successively developed permanent magnet synchronous traction systems, completed prototype trial production and line test evaluation, and gradually entered the design and commercialization stage. Compared to asynchronous traction motors, permanent magnet motors are used in rail transport. Stepper traction motors have the following advantages:

(2) (1) high efficiency; (2) high power density; (3) strong overload capacity; (4) low cost throughout the entire life cycle; (5) fully enclosed design; (6) gearless torque transmission to the wheelset. Although the permanent magnet synchronous traction motor has so many advantages, the design of the magnetic system and the evaluation of heat are complex tasks in motor design, and the solution of these problems determines the success or failure of the motor design.

A permanent magnet synchronous motor is mainly composed of a stator, a rotor and casing elements. As with conventional AC motors, the stator core is a lamellar structure to reduce iron losses due to eddy currents and hysteresis effects when the motor is running; windings are usually three-phase symmetrical structures, the selection of the parameters of the motor magnetic system is carried out by its own method. The motor rotor has various designs - a rotor with permanent magnets and with a starting squirrel-cage cage, as well as a rotor with permanent magnets built-in or mounted on the surface of the rotor. The rotor core can be solid or multilayer.

The magnetic fields of the rotor and stator are in a synchronized state during normal operation of a permanent magnet motor, so that there is no induced current in the rotor, there is no loss in rotor copper, hysteresis, and eddy current losses, and there is no need to consider the problem of rotor losses and heat generation. As a rule, the permanent magnet motor is powered by a special frequency converter and naturally has a soft start function. In addition, the permanent magnet motor is a synchronous motor which has the characteristic of controlling the power factor of a synchronous motor by means of an excitation force, so the power factor can be calculated to a predetermined value.

From a starting point of view, by starting a permanent magnet motor with a variable frequency power supply or an appropriate inverter, the process of starting a permanent magnet motor is not difficult and is similar to starting an induction motor using a variable frequency.

### 1. Engine structure

The direct drive permanent magnet synchronous motor has a sealed design and includes a rotor that realizes a hollow shaft design. The forced ventilation of the stator is designed to dissipate heat, and the closed rotor design improves the cooling effect of the motor. Considering the design of the rotor, the traditional

permanent magnet motor is usually made completely sealed, and the heat dissipation effect is limited. The engine is connected to the hollow shaft of the wheelset through a drive disk with end teeth. The 3D circuit diagram of the engine and the circuit diagram of the gas circuit of the engine are shown in Figure 1.

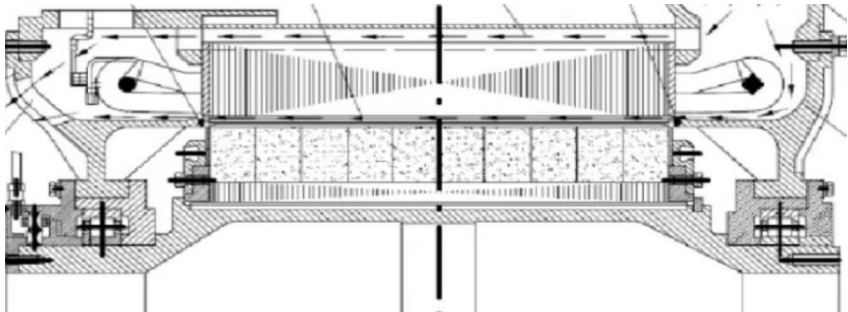
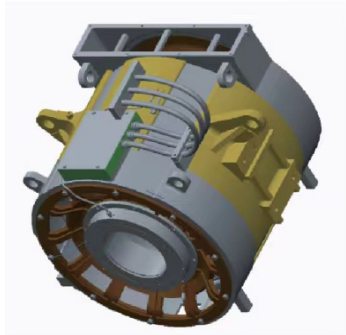
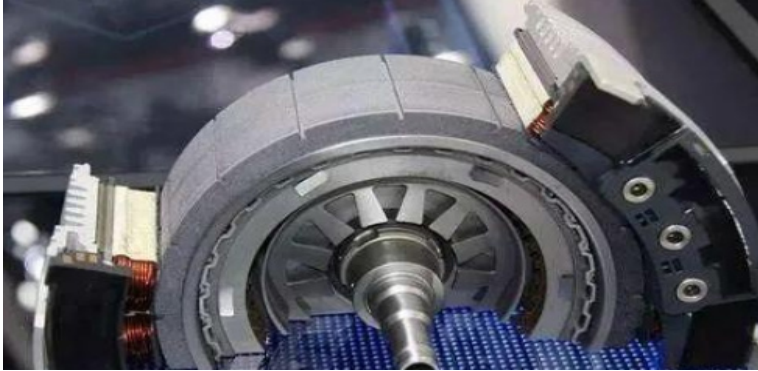


*Figure 1. Three-dimensional diagram and diagram of the air channels of a permanent magnet synchronous motor*

### 1.1 Stator part

The stator part of the engine frame is a fully multi-layer welded structure. The plates at both ends and the cast stator clamp ring are connected by pull plates, and the frame body is welded. The air gap is cooled, and the teeth of the stator core are made with ventilation channels, as shown in Figure 2.

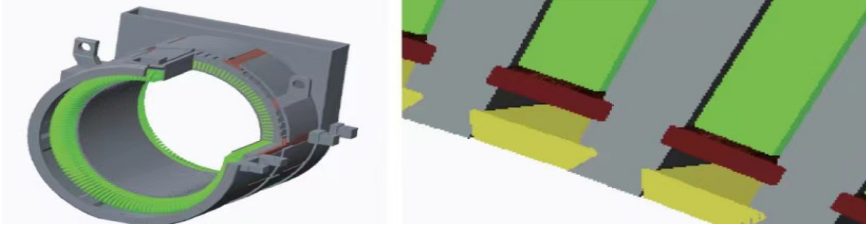


*Figure 2. Schematic diagram of the 3D stator and ventilation duct*

### 1.2 Rotor part

The rotor adopts a V-shaped magnetic circuit design, the iron core is formed by pressing the rings at both ends of the rotor and the forged parts of it, and then the permanent magnet is fixed in the groove with a special ring made of stainless steel. The magnetic steel grooves are filled with silicone rubber. A three-dimensional schematic diagram of the rotor is shown in Figure 3.

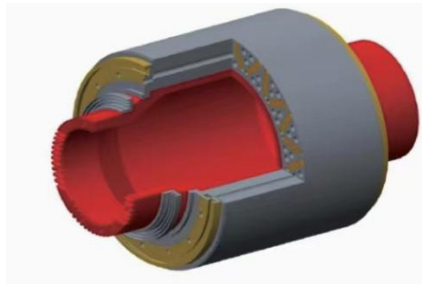


*Figure 3. 3D Rotor Diagram*

The development of permanent magnet synchronous motor is closely related to the development and progress of permanent magnet material technology. At present, the permanent magnet materials used in permanent magnet synchronous motors mainly include ferrite, AlNiCo and rare earth permanent magnet materials, among which ferrite has poor magnetization performance, so it is not suitable for use in electric locomotives.

**Table 1.**  
*Parameters of the magnetic steel of the rotor*

Characteristics of magnetic steel	Parameter
Material Grade	CN36EH
Magnetic remanence Br/KGs	12.2-12.9
Coercive force of magnetic induction Hcb/(KA * m <sup>-1</sup> )	≥ 892
Coercive force of magnetic polarization Hcj/(KA * m <sup>-1</sup> )	≥ 2388
Maximum product of magnetic energy (BH) <sub>max</sub> / KA * m <sup>-3</sup>	286-310
Working temperature (Tw)/°C	≤ 200
Curie temperature /°C	320

### 1.3 Dimensional drawing of engine components

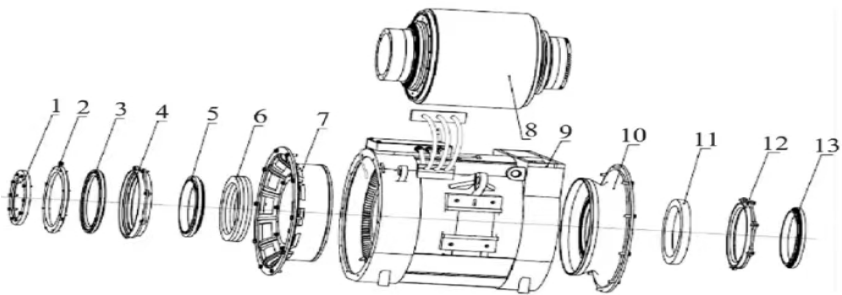


**Figure 4.** *Dimensional drawing of 3D engine components*

## 2. The design of the motor magnetic system

### (1) Dimensions and weight

According to the electromechanical principle, the usable motor size is related to the motor speed. Therefore, a gearbox is traditionally used, and the size and weight of the motor are small. At present, a DC commutator motor and an AC induction motor are used in the locomotive gear drive. But when there is no gearbox, the gear ratio is 1. To provide vehicle traction, the torque transmitted by the gearbox to the wheelset axle is equal to the engine torque multiplied by the gear ratio, while the speed of the wheelset is equal to the corresponding engine speed divided by the gear ratio. number. Since the effective working size of the motor is proportional to the motor torque, the torque ratio of the gear motor is doubled by its transmission by the gear.

In rail traction, since the operating size of the engine is limited by the wheel

diameter and the distance between the wheels, the size of the engine is required to be small, and at the same time, most of the engine mass acts on the bogie frame to reduce its effect on the wheelset. Also, the weight of the engine should be lighter to reduce its impact on the track structure.

The contradiction between the fundamentally large mass and size of the engine, with the smaller mass and small dimensions necessary for practical use of engines, creates huge problems in the design of the engine. According to the current technical scheme of permanent magnets, the volume ratio of the iron core is 1.48 times, with respect to the size of the motor is 1.6 times, and with respect to the mass ratio is 1.42 times. The high power density of permanent magnet motors provides low speed, high torque and direct drive. Table 2 shows the comparison of the technical parameters of a permanent magnet motor and an induction motor of the same power.

**Table 2.**  
*Comparison of motor parameters*

En- gine's type	Rated power, kW	Rated cur- rent, A	Constant power range, rpm	Rated torque, N*m	Power factor	Rated effi- ciency	Num- ber of pole pairs	Weight, kg
Perma- nent magnet motor	1225	477	353-706	33142	0.93	95.7	14	3430
Asyn- chro- nous motor	1225	395	1390-2896	10900	0.88	95.3	6	2450

(2) Back EMF

Permanent magnet motors have back EMF and require field weakening control at high speeds. Limited by the peak withstand voltage of the electronic components, the motor voltage must be balanced in performance and back EMF.

(3) Rotor magnetic circuit

The rotor magnetic circuit has a permanent magnet torque and a resistance torque. When the permanent magnet motor is running, it is advisable to place the permanent magnet on the surface of the rotor, which can make the motor get higher permanent magnet torque and reactive power. The resistance torque during acceleration is created by the inertia forces of the motor shaft. Reasonable layout requires finite element analysis. The results of the analysis of the magnetic flux density at motor load are shown in Figure 5.

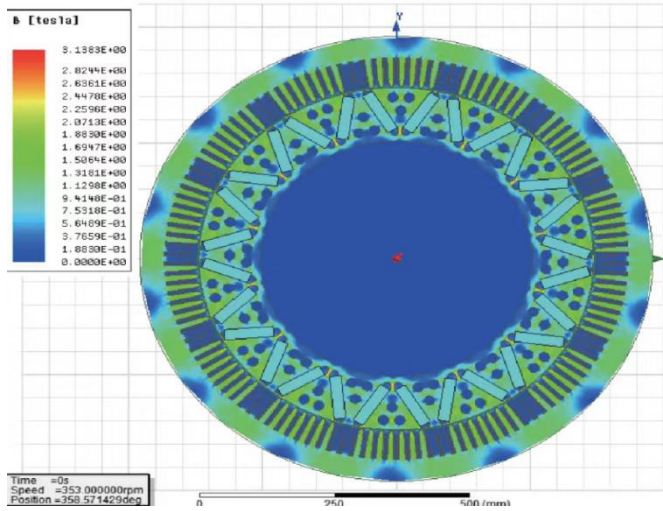


*Figure 5. Analysis of magnetic flux density*

A malfunction caused by demagnetization of the motor magnetic system is the main problem of a permanent magnet motor. When the current is too large or the temperature is too high, the current rises sharply and the temperature of the motor winding instantly rises, and the permanent magnet quickly loses magnetization. When driving a permanent magnet motor, an overcurrent protection device is installed to avoid the problem of burning the motor stator winding, but the loss of magnetism and equipment shutdown caused by this process is inevitable.

The permanent magnets and steel cores of the stator and rotor of a permanent magnet synchronous motor are prone to high eddy current losses and harmonics, which are reflected in the form of thermal energy, which increases the overall or local heating of the motor, and even causes the permanent magnets to lose their magnetism, which seriously affects for engine operation. Therefore, the permanent magnet synchronous motor has higher requirements for heat dissipation. For permanent magnet synchronous motors, heat dissipation inside the motor should be avoided as much as possible.

Consider several ways to cool engines.

The external cooling of a permanent magnet synchronous motor is mainly air-cooled, and the air circulation is usually forced by a fan. External cooling methods mainly include natural cooling, self-cooling and external cooling by fan.

1) Naturally cooled permanent magnet synchronous motor.

The motor does not have a special cooling device, but only relies on the radiation on the surface of the components and the natural convection of the cooling

medium to dissipate the heat generated inside the motor, so the heat dissipation power is limited, and this method is only suitable for small motors with low power and self-convection. Such motor cooling is used in cases where the environment does not allow the use of fans.

2) Forced cooling of permanent magnet synchronous motor. The motor rotor of a permanent magnet synchronous motor is equipped with a fan. When the motor rotates, the air flow generated by the fan is used to force the air to pass through and blow over the heat dissipation surface, thereby greatly improving the heat dissipation and dissipation capacity of the motor. According to the location of the fan, it can be divided into two types - internal self-cooling and external self-cooling. The internal self-cooling is suitable for open motors, the internal fan is mounted on a rotating shaft inside the end cap, the fan rotates with the rotor, forcing external cooling air into the machine, and blows the armature surface through the axial and radial vents. External self-cooling is suitable for closed motors. In addition to the built-in fan, the motor is equipped with an external fan. The air on the case is dissipated into the surrounding air, and the fan inside can continue to speed up the circulation of air inside the motor so that the temperature is evenly distributed and the heat is more easily transferred to the motor frame.

### 3. Improving the design of the permanent magnet motor

a. Increasing the thickness of the permanent magnet. From the point of view of design and manufacture of a permanent magnet synchronous motor, the relationship between armature reaction, electromagnetic torque and permanent magnet demagnetization should be taken into account. Under the combined action of the magnetic flux generated by the torque winding current and the magnetic flux generated by the radial power winding, the permanent magnets on the rotor surface are prone to demagnetization. Provided that the air gap of the motor remains unchanged, to ensure that the permanent magnet does not demagnetize, the most effective method is to increase the thickness of the permanent magnet accordingly.

b. Using a special layout of magnetic steel. The main features of the design are the special arrangement of magnetic steel elements on the surface of the rotor so that the parallel magnetic flux is relatively large, and the moment of resistance is relatively small. Such an arrangement of elements is beneficial for the full use of the torque generated by the magnetic flux, as well as increasing the stability of the motor.

c. There is a ventilation groove loop inside the rotor, which is an important factor in reducing the temperature rise of the rotor and affecting the reliability of the permanent magnet synchronous motor, as it reduces the possibility of permanent magnet demagnetization. If the rotor temperature is too high, the permanent magnet will cause an irreversible loss of magnetism. In the design, the internal

ventilation circuit of the rotor can be designed for direct cooling of the magnetic steel. Not only reduces the temperature of the magnetic steel, but also improves its efficiency.

d. Rare earth permanent magnet is used to reduce heat caused by excitation. Once magnetized, it can create a strong permanent magnetic field without additional energy. The rare earth permanent magnet motor, which is made to replace the excitation field source generated by electricity in the conventional motor, is not only efficient, but also simple in structure, reliable in operation, small in size and light in weight. Rare earth permanent magnet motors can not only achieve high performance (such as ultra-high efficiency, ultra-high speed, ultra-high running speed) unmatched by traditional electrically excited motors, but also can be converted into special motors that can meet specific conditions and requirements.

### Conclusion

The permanent magnet synchronous traction motor is a key component of the permanent magnet direct drive electric locomotive. After applying the considered solutions in the engine design, all parameters meet the design requirements and the engine operation process is stable, but this does not mean that the engine design is ideal. There are opportunities for its further optimization, which require further research.

### References

1. Dong Siming, *Working principle and structural characteristics of high-speed electric train [M]* Beijing: China Railway Press, 2007: 21-34.
2. Liu Yongqing, *Technical characteristics of modern electric locomotives [J]* *Economics of Science and Technology of Inner Mongolia*, 2017(19): 38-52
3. Feng Xiaoyun *on AC traction drive and permanent magnet synchronous technology [M]* Higher Education Press, 2009: 274-296.
4. Ding Ronjun. *Modern railway traction. Research and development of transmission and control technologies. Electric locomotive drive*, 2010, pp. 77-103.
5. Feng Jianghua, Gui Weihua, Fu Mingli et al. *Comparison of permanent magnet synchronous motors for railway traction systems [J]* *Journal of Railways*, 2007(5): 111-116.

南乌拉尔硫化物岩溶  
**SULFIDE KARST OF THE SOUTHERN URALS**

**Smirnov Alexandr Il'ich**

*Candidate of Geologo-Mineralogical Sciences,  
Mineral Reconnaissance Extraordinaire, Senior Research Officer  
Institution of Russian Academy of Sciences Institute of geology of the  
Ufimian scientific centre*

抽象的。证实了硫化物岩溶是该地区独立的岩性类型。给出了其发展的条件和因素，确定了其表现形式和分布区域。指出了硫化物岩溶地表岩溶管理研究作为黄铁矿铜矿床勘探特征的实际应用以及在绘制该地区岩溶图时需要考虑的必要性。

关键词：巴什基尔外乌拉尔山脉、矿石岩溶、沉降和充液漏斗、黄铁矿铜矿床。

**Abstract.** *Substantiation of sulfide karst as an independent lithological type of the region is given. The conditions and factors of its development are given, the forms of manifestation and areas of their distribution are established. The practical application of the study of surface karst management of sulfide karst as an exploratory feature of copper pyrite deposits and the need to take it into account when mapping the karst of the region are indicated.*

**Keywords:** *Bashkir Trans-Urals, ore karst, subsidence and suffusion funnels, copper pyrite deposits.*

### **Introduction**

The Southern Urals is located on the border of Europe and Asia, which runs along the eastern foot of the Uraltau ridge (fig. 1.) and is geologically and geomorphologically divided into the mountainous Urals and the flat Trans-Urals.

Along with the widespread carbonate karst in the Southern Urals, ore (sulfide) karst is locally found on its territory, which has not currently received due recognition by domestic karst scientists, although geologists pointed out the presence of ore karst in the region more than half a century ago.

**The purpose of the study** is to substantiate sulfide karst as its independent type in terms of the composition of karst rocks.

**The source materials for the research** were the collected and systematized archival and stock data, as well as the author's field research in the course of studying exogenous geological processes.



*Figure 1. Steles "Europe" and "Asia" on the highway Beloretsk-Uchaly*

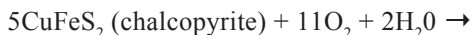
### Research results

**Issue status.** The term ore karst was first introduced into the scientific literature by Yu.P. Ivensen, by which he understood the karst process in ore bodies [4]. However, he did not give its unambiguous definition, which later led to different interpretations of this term [3]. Thus, some researchers considered ore karst as karst cavities of any origin, enclosing ores [5], others as voids and cavities arising in carbonate rocks under the action of sulfuric acid (oxidation product of sulfide ores) [7], yet others, after Yu.P. Ivensen, as karst developing directly in sulfide ore bodies [1, 2, 11, 12].

V.A. Garyainov, developing the ideas of Yu.P. Ivenson, V.A. Aprodov and N.I. Sokolov about the ore karst, defined ore karst not as a phenomenon of localization of ore matter in previously formed karst cavities (ore-bearing karst according to S.Yu. Lyakhnitsky [6]) and not as karst in limestones containing bodies of sulfide ores [7], but as karst in the ore-bearing bodies themselves. [2]. At the same time, he rightly used the term "sulfide karst", which clearly denotes (by analogy with sulfate, carbonate, etc.) a group of karst rocks.

**The substantiation of sulfide karst as an independent type** is based on the fact that sulfide ores are soluble formations. At the same time, they are able to pass into solution, which can be transported by groundwater outside the ore bodies, or migrate into its deeper horizons [2]. That is, the conditions for the development of sulfide karst are similar to the development of karst in any other karst rocks [9, 13].

The most common reactions of oxidation and leaching of sulfide ores in copper pyrite deposits are:



and (or)



When sulfides are leached from primary ores, up to 80-90% of their volume can be removed, while their porosity sharply increases and voids form [2]. It follows from this that the mechanism of development of the karst process in sulfide ores does not differ in any way from its development in other traditional karst rocks.

The intensity of the development of sulfide karst, as well as its other lithological types (carbonate, sulfate), is greatly influenced by both general geological-geomorphological and climatic-hydrogeological factors [9], as well as local factors of a mineralogical, structural, textural and other nature. Thus, the amount of pyrite in ores is very important for the development of sulfide karst, since this mineral, changing under surface conditions, speeds up the process of oxidation of other minerals [10]. The texture of ores also plays an important role: in dense massive ores and weakly permeable ores, oxidation and leaching occur more slowly than in fractured, druze, banded, and other varieties [1].

A great influence on the depth and intensity of the development of sulfide karst is also the nature of the rocks that "enclose" the ore bodies. The most optimal conditions for its development arise when sulfide ores are found among traditionally karst carbonate rocks. When sulfides are oxidized by natural waters, their dissolving power on host rocks simultaneously increases [2].

Among other factors favorable for the development of sulfide karst, one should also note the emergence in the "water-rock" system of environments suitable for the habitation of thionic bacteria. The latter, as J.I.E. Kramarenko (1974) points out, stimulate the oxidation of sulfide ores and promote the migration of chalcophile elements. In the presence of some of their species from copper-pyrite ores, it passes into a solution of iron by 200, and copper by 8 times more than in "sterile" samples [2].

**The distribution of sulfide karst** is confined to zones of sulfide mineralization and deposits of copper pyrite ores. It is developed locally in the Bashkir Trans-Urals (fig. 2).

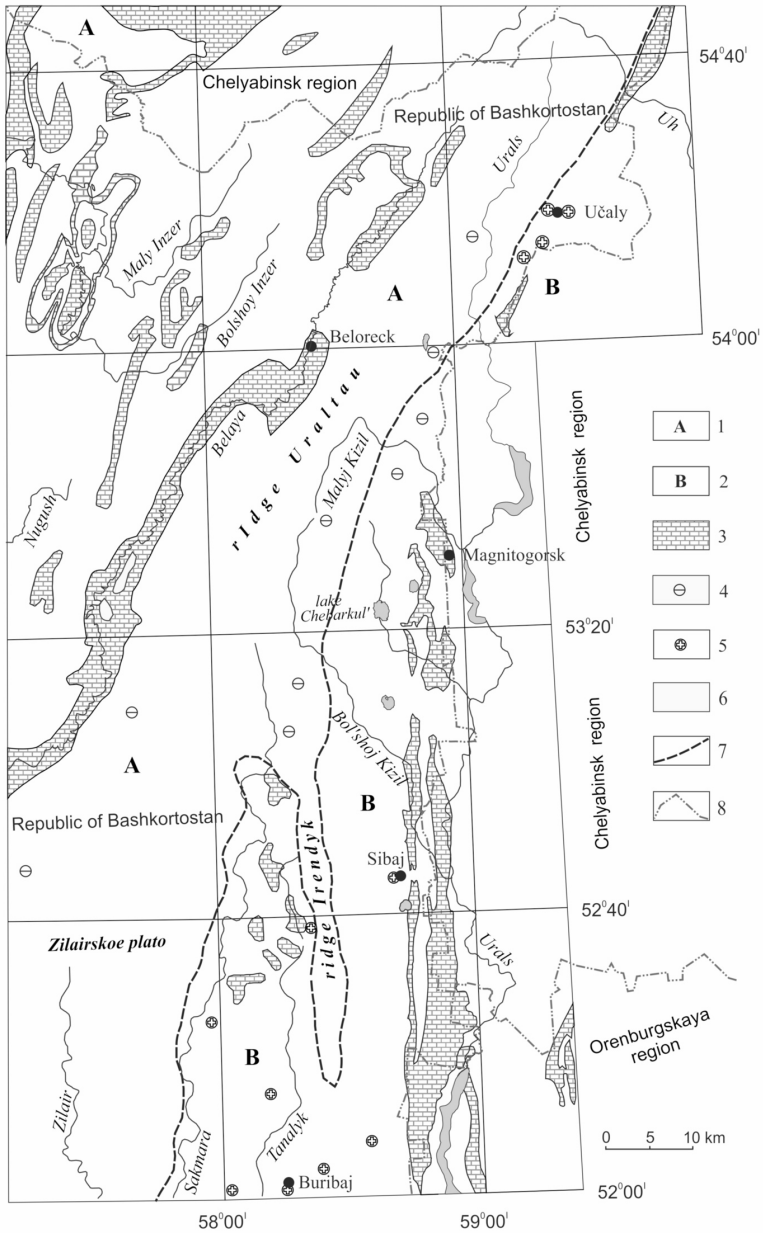


Figure 2. Carbonate and sulfide karst of the Southern Urals [by 8]

Ural karst country: 1 — mountain karst in dislocated and strongly dislocated formations of the Southern Urals, 2 — flat karst in folded-block deposits of the Bashkir Trans-Urals. 3 — carbonate karst. Local manifestations of karst: 4 — carbonate, 5 — sulfide. 6 — areas with no karst development. Borders: 7 — types of karst according to the nature of the relief and conditions of occurrence of rocks, 8 — subjects of the Russian Federation.

On the surface, sulfide karst is represented by rounded and elliptical saucer-shaped depressions, very rarely cup-shaped funnels. Their diameter ranges from several to tens of meters, and their depth varies from 0.5 to 1–2 m. The flat bottom of these funnels is often waterlogged [8].

Surface manifestations of sulfide karst are widely developed in the ore field of the Yubileinoe deposit, especially in the area of the third deposit, which emerges on the surface of the Paleozoic basement under the Jurassic deposits. They are also distributed in the southern part of the Zapadno-Podilsky section of sulfide mineralization, in the Makansko-Peter and Paul tectonic zone in the basin of the river. Makan and on the Buzavlyk-Tanalyk interfluve [8]. As M.Sh. Bikov and Yu.V. Aleksandrov (1978) point out, they also existed at the Buribai copper pyrite deposit.

At present, due to the development of copper pyrite deposits and the economic development of territories, the relief forms caused by the development of sulfide karst are mostly destroyed by technogenesis (fig. 3).



*Figure 3. Quarry of the Yubileiny copper pyrite deposit*

By genesis, the surface manifestations of sulfide karst are subsidence and suffosion, formed above ore bodies that were subject to leaching, which is recognized by all researchers.

According to Garyainov V.A. [2], surface manifestations of sulfide karst can serve as one of the search signs of new copper deposits.

### Conclusions

Sulfide karst in the Southern Urals, according to the conditions and factors of development, meets all the signs of a karst process to distinguish it as an independent lithological type. The presence of sulfide karst must be taken into account when mapping the karst of the region and areas of distribution of sulfide mineralization.

*The study was carried out within the framework of the State budget theme № FMRS-2022-0010.*

### References

1. Aprodov V.A. *Ore karst // General issues of karst studies. M., 1962. P. 116-129.*
2. Garyainov V.A. *Exogenous structures and their search value. Saratov: Publishing House of Saratov University, 1980. 208 P.*
3. Ezhov Yu.A., Lysenin G.P., Andreichuk V.N., Dublyansky Yu.V. *Karst in the earth's crust: distribution and main types. Novosibirsk, 1992. 76 P.*
4. Ivensen Yu.P. *Polymetals of Central Asia and South Kazakhstan. M.- L.: ONTI, NKTP, 1937. 56 P.*
5. Kreyter V.M. *Search and exploration of mineral deposits. M.: Gosgeolizdat, 1941. 789 P.*
6. Lyakhnitsky Yu.S. *Questions of terminology and classification of karst phenomena // Problems of studying, ecology and protection of caves. Kyiv, 1987. P. 13-23.*
7. Nikolaev N.I. *The main problems of studying karst // General questions of karst studies. M., 1962. P. 26-33.*
8. Smirnov A.I. *Types of karst and modern activity of its development in the Southern Urals and Cis-Urals In the collection: Karst studies XXI century: theoretical and practical significance. Proceedings of the international symposium. 2004. P. 90-94.*
9. Smirnov A. *Conditions and factors for karst development in the Southern Urals and Cis-Urals. In the collection: Process management and scientific developments. October, 13, 2021. Birmingham, united kindom. Part 1. Birmingham, united kindom, 2021. P. 133-143.*
10. Smirnov S.S. *Zone of oxidation of sulfide deposits. M., 1955. 150 P.*

11. Smirnov V.I. *Geological foundations of prospecting and exploration of ore deposits*. M., 1957. 220 P.

12. Sokolov N.I. *Typological classification of karst // Materials / Commission on the study of geology and geography of karst: Inform. coll. M., 1961. № 1. P. 140-153.*

13. Sokolov D.S. *Basic conditions for the development of karst*. M.: Gosgeoltekhizdat, 1962. 322 P.

DOI 10.34660/INF.2022.99.23.162

标准光学机械重力仪的自动化结果  
**RESULTS OF AUTOMATION OF A STANDARD OPTICAL-  
MECHANICAL GRAVIMETER**

**Dubovskoi Vladimir Borisovich**

*Candidate of Physical and Mathematical Sciences, Leading Researcher*

**Leontyev Vladimir Ivanovich**

*Candidate of Physical and Mathematical Sciences, Leading Researcher*

**Boev Ivan Alekseevich**

*Lead Engineer*

*Schmidt Institute of Physics of the Earth of the Russian Academy of  
Sciences*

注解。 这篇文章描述了标准光学机械重力仪ГAГ-3的创新,这使得在更高的技术水平上使用它成为可能。 给出了在各种物体上使用现代化 ГAГ-3M 重力仪的例子。

关键词: 重力仪, 重力变化, 微量。

**Annotation.** *The article describes the innovations made on the standard optical-mechanical gravimeter ГAГ-3, which made it possible to use it at a higher technical level. Examples of the use of the modernized ГAГ-3M gravimeter at various objects are given.*

**Keywords:** *gravimeter, gravity variation, microgal.*

In connection with the advent of onshore automated gravimeters of the Scintrex type, the use of optical-mechanical quartz gravimeters in geophysics has significantly decreased. However, the high cost of Scintrex gravimeters limits their availability. At the same time, the technical capabilities of "obsolete" gravimeters are far from being exhausted.

In order to test the use of standard optical-mechanical quartz gravimeters for recording gravity variations at the level of fractions of microgals, on the basis of one of the prototypes of the ГAГ-3 geodetic gravimeter, a gravimeter model with a magnetoelectric feedback system and a digital readout was made.

During the modernization of the sensitive system, a magnetoelectric feedback coil was installed on the lever of the range spring, and a magnetic system with a permanent magnet made of samarium-cobalt was installed on the body of the device.

As an optical displacement sensor, we used a laser displacement sensor, which was developed at the IPE RAS for the ИМУ-1П satellite accelerometer. The noise of the displacement sensor in the frequency range of 0.1-0.001 Hz does not exceed a few angstroms, which corresponds to the gravimeter noise of  $10^{-11}g$ . The standard reference of the sensitive system was used as a reference point for the photoelectric sensor with an injection laser.

Thus, the quartz elastic system of the ГАГ-3 gravimeter has not undergone significant changes and can be performed on standard optical-mechanical gravimeters, in which, as a rule, the zero-point shift decreases to 0.1-0.3 mGal/day over time.

The resolution of digital recording of the acceleration of gravity, implemented using an analog-to-digital converter built into the gravimeter case, was 0.1  $\mu$ Gal.

The gravimeter signal was filtered in accordance with the fundamental mode of storm microseisms. A series of measurements was carried out under stationary conditions, the root-mean-square deviation of a single reading from a linear drift for 40 min of measurements was  $\pm 1.5 \mu$ Gal, with an averaging time of 3.5 min -  $\pm 0.3 \mu$ Gal.

The possibilities of measuring small increments of the acceleration of gravity were tested by the null method (measurements at the same point with an interval between instrument settings of 2 min and a reading averaging time of 2 min). The root-mean-square deviation of a single reading from the gravimeter drift line was  $\pm 0.8 \mu$ Gal.

The minimum signal recorded by the gravimeter is determined by the Brownian noise of the sensitive system (1) [1].

$$\sigma(g) = \sqrt{\frac{w_0 \cdot \Delta f \cdot 4kT}{M \cdot Q}} \quad (1)$$

where  $\sigma(g)$  – gravimeter signal,  $w_0$  – natural frequency of the gravimeter sensitive system,  $\Delta f$  – filtering frequency,  $k$  – Boltzmann's constant,  $T$  – temperature,  $M$  – pendulum mass,  $Q$  – quality factor.

For most ground-based quartz gravimeters, Brownian noise is 0.1-0.4  $\mu$ Gal.

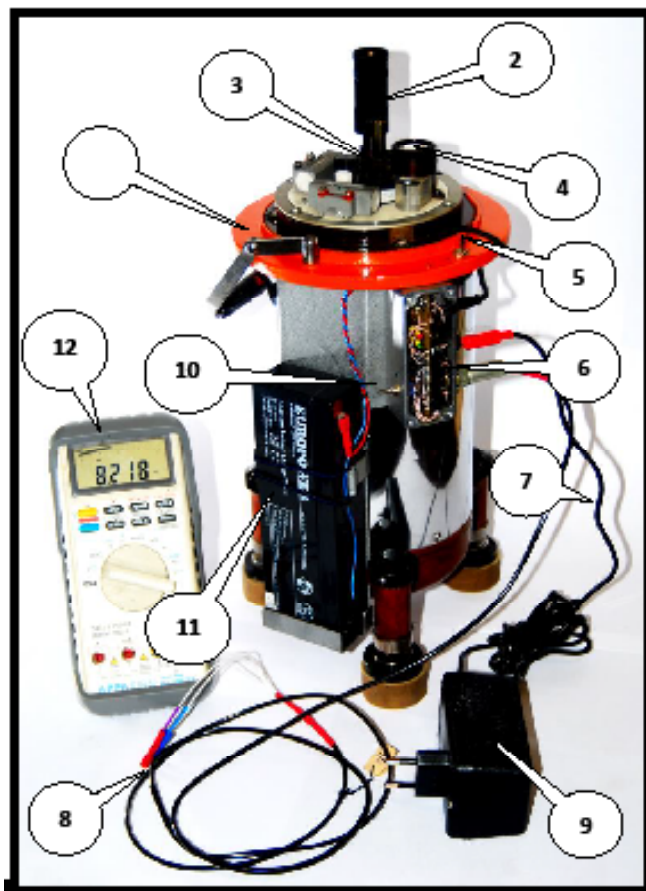
Table 1 shows the comparative errors of the optical-mechanical (A) and automated (B) ГАГ-3 gravimeters.

**Table 1.**  
*Comparison of measurement errors of the optical-mechanical (A) and automated (B) gravimeter ГАГ-3*

Source of error	Structural elements and test methods	Error $m_{\Delta g} \cdot 10^{-9} \text{ g}$
Resolution of the reading device	A. - Compensating measuring spring with micro screw	5-10
	- Tilt method $Dg = \pm 10^{-6} \cdot 5 \cdot 10^{-6} \text{ g}$	1,5 - 80
	B. - Compensation measuring spring, photoelectric displacement sensor, self-contained digital voltmeter	0,5 – 0,8
	- with an external precision voltmeter and the use of optimal signal processing on the PC	0,01
Reading device non-linearity	A. - Compensation spring with microscrew, measuring range $\Delta g = (1-5) \cdot 10^{-4} \text{ g}$	10-50
	B. - Digital readout, measurement range $Dg = \pm 10^{-6} \text{ g}$	0,1
Position averaging inaccuracy маятника	A. - Visual	5-20
	B. - Digital adaptive filter	0,3 – 0,8
Zero offset non-linearity	A, B - For 8 hours, taking into account the lunisolar tide for a thermostated device	0,5

It should be noted that when creating the ГАГ-3 gravimeter, an original effective thermostating system and the design of a range device were used, which practically excludes the effect of changes in atmospheric pressure when working in mountainous conditions, measures were taken to seismoacoustic protection of the device (Fig. 1) [2].

The modernized gravimeter ГАГ-3М was used on expeditions in Romania (Vrancea zone) and in Russia to determine the fine structure of the gravitational field at the site of the Leningrad Nuclear Power Plant (LNPP), register non-tidal variations of the Earth's gravitational field at the Leningrad test site, map density inhomogeneities at many critical structures Moscow.



- |                      |                           |
|----------------------|---------------------------|
| 1. Gravimeter body   | 7. Power cable            |
| 2. Eyepiece          | 8. Information cable      |
| 3. Measuring screw   | 9. Power Supply           |
| 4. Reading device    | 10. Electronics switch    |
| 5. Light switch      | 11. Battery 12v; 2,3 A/h  |
| 6. Electronics block | 12. Multimeter APPA 109 N |

*Figure 1. Appearance of the gravimeter ГАГ-3М*

To illustrate the operation of the modernized ГАГ-3М gravimeter, examples of its use at various objects are given below (tables 2, 3, figures 2,3)

Table 2 shows the results of measurements of the gravity acceleration gradient by gravimeters accompanying repeated measurements by absolute gravimeters at the international gravimetric station IGSN-71 No. 5035 "Ledovo".

**Table 2.**

*The results of measuring the gradient of the acceleration of gravity at the international gravimetric station IGSN No. 5035 "Ledovo"*

Devices	Measured values of gravity gradient, $\mu\text{Gal/m}$				Average values of gravity gradient, $\mu\text{Gal/m}$
LCR (USA)	307,2	306,4	309,6	307,0	307,6
ВИРГ (Russia)	309,0	311,0			310,0
Sodin №162 (Canada)	306,2	305,6			305,9
	Average over measurements				307,8
ГАГ-3М №8 (Russia)	307,4				307,4

The result of measurements with the ГАГ-3М gravimeter coincides within the error with the average value of the gravity gradient obtained by a group of instruments from different countries.

Table 3 shows an example of measuring the gravity acceleration gradient at a construction site during the laying and strengthening of an underground collector under conditions of a high level of vibration and seismic interference from the operation of building mechanisms and equipment, and gusty winds. The work was carried out using a geodetic tripod. The height difference between the lower and upper platforms for installing the gravimeter was 1417 mm. Zero offset corrections were not introduced.

**Table 3.**

*Example of Gravity Acceleration Gradient Measurement at the construction site*

Position	Time, hour	$\Delta g, \mu\text{Gal}$
bottom	13,38	724.5
top	13,45	1133.9
bottom	13,52	695.1
top	13,58	1111.5
bottom	13,70	674.9
top	13,82	1090.6
bottom	13,87	654.0

$$\Delta g \text{ bottom} - \Delta g \text{ top} = 426,55 \pm 0,9 \mu\text{Gal} \text{ or } W_{zz} = 301,0 \pm 0,6E$$

The measurement error of  $\Delta g$  is about  $1 \mu\text{Gal}$  under conditions of a high level of man-made interference.

Figure 2 shows gravimetric maps of the construction site of a critical structure, obtained from the results of measurements by two independent groups of  $\Gamma\text{A}\Gamma\text{-3M}$  gravimeters. On the gravimetric maps constructed from the measured increments of the acceleration of gravity, the isoanomalies are drawn through  $50 \mu\text{Gal}$ , the isoanomalies on the Bouguer anomaly maps with the regional component removed are drawn through  $10 \mu\text{Gal}$ .

Figure 2 demonstrates the high convergence of the measurement results of two independent groups of  $\Gamma\text{A}\Gamma\text{-3M}$  gravimeters and the high resolution of the gravimetric survey.

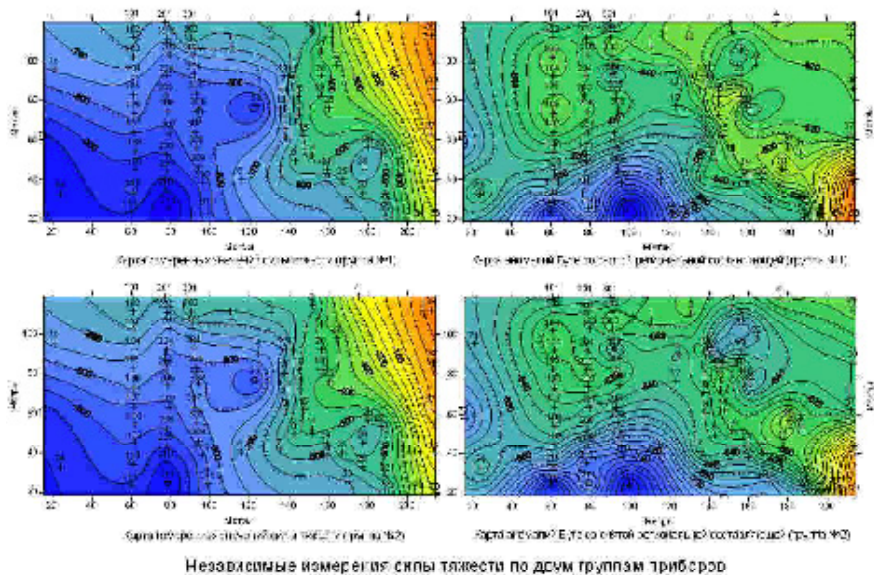


**Figure 2.** Gravimetric maps obtained from the results of measurements with  $\Gamma\text{A}\Gamma\text{-3M}$  gravimeters

High-resolution gravimetric survey makes it possible to predict the density section of the soil at the construction site without a lot of drilling and reduces the cost of construction work.

Figure 3 shows a fragment of registration of lunisolar tides by the ГАГ-3M gravimeter in laboratory conditions

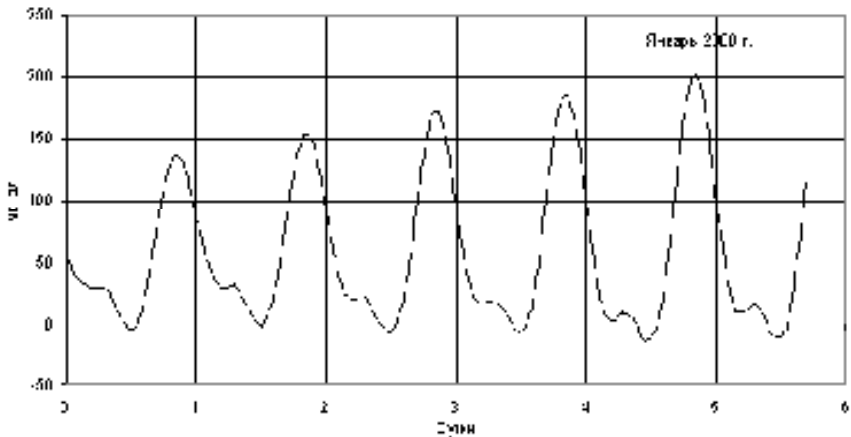


**Figure 3.** An example of recording lunisolar tides

The issues of metrology of ГАГ-3 sensitive elements have been worked out in publications and do not need special consideration.

Thus, the automation of the standard optical-mechanical gravimeter ГАГ-3 made it possible to use it at a higher technical level. The use of a number of know-hows that provide a significant reduction in destabilizing factors (barometric effect, temperature, dynamic, inelastic effects) made it possible in real field conditions to make measurements at the level of Brownian noise, i.e. actually at the level of physical prohibition.

Such a significant advance in the quality of measurements makes it possible to pose a number of new fundamental and applied problems. In fact, a new direction of microgravimetry is being opened, which makes it possible to detect anomalies in the acceleration of gravity in time and space of the order of  $10^{-10}$  g and to measure the gradient of the acceleration of gravity of the order of 1 Eotvos.

## References

1. Aki K., Richards P. *Quantitative seismology. Theory and methods, volume 1.* – Moscow: Mir, 1983. – p. 475.
2. V. B. Dubovskoy, V. I. Leontiev, A.V. Sbitnev, V.G. Zhilnikov. *Possibilities for improving gravity-inertial geophysical equipment // Scientific Instrumentation. – 2017. - Volume 27. - No. 1. - pp. 29-34.*

科学出版物

上合组织国家的科学研究：协同和一体化

国际科学大会的材料

2022年4月20日，中国北京

编辑A. A. Siliverstova

校正A. I. 尼古拉耶夫

2022年4月26日，中国北京

USL。沸点：98.7。 订单253. 流通500份。

在编辑和出版中心印制

无限出版社



